# Diacylglycerol Kinase α is a Pharmacologically Targetable Immune Regulator with a Newly Identified Role in Macrophage Activation

Laryssa Carmelle Manigat
Newton, Massachusetts

Bachelor of Science, Northeastern University, 2012

A Dissertation Presented to the Graduate Faculty of the University of Virginia in Candidacy for the Degree of Doctor of Philosophy

Department of Pathology

University of Virginia
December 2021

## Dedication

I dedicate this work to my parents, Marie Lourdes and Ernst Manigat, who have made great sacrifices in the name of my education. I will forever be grateful for their love and support, and the role that has played in my success.

**Acknowledgements**

I would first like to thank my mentor, Dr. Benjamin Purow, for his unwavering support and encouragement during the course of my graduate studies. His passion for research and compassion for his patients has always been an inspiration and driving force for myself and others in our lab. I will always appreciate his thoughtfulness, creativity, and determination, and will use those as guides for my own endeavors in the future.

My experience in Dr. Purow's lab would not have been the same if not for the kind and supportive colleagues I had the privilege of working with. Current and former members of the lab have shared a similar commitment to quality research, and to maintaining the positive environment we have built in the lab. I'm thankful for having spent these last several years learning with and from my fellow lab members.

I would also like to thank Dr. Thurl Harris and Mitch Granade for their substantial efforts in advancing both of the projects described within this dissertation. Their careful consideration in improving study design, as well as their generosity in sharing their time and resources, were instrumental to the success of this work, and I'm truly grateful for their collaboration.

Many of these experiments would not have been possible without the help of Dr. Norbert Leitinger and Scott Yeudall, who offered technical demonstrations, reagents, and protocols which were applied regularly and enabled the generation of considerable data.

I am grateful to members of the Advanced Microscopy Facility, the Research Histology Core, and the Biorepository and Tissue Research Facility for their reliability, flexibility, and quality of assistance.

I must also thank the members of my dissertation committee: Dr. James Mandell, Dr. Janet Cross, Dr. Daniel Gioeli, and Dr. Richard Price. They were consistently thoughtful and encouraging through all of our meetings, and I could always rely on them to challenge me to think more critically and with strong focus. I appreciate their guidance and the discussions we had which led to the completion of this dissertation.

**Abstract**

The diacylglycerol kinases (DGKs) are a family of lipid kinases whose primary function is the conversion of diacylglycerol (DAG) to phosphatidic acid (PA). There has been mounting evidence indicating that DGK enzymes are implicated in other physiologic processes, ranging from immune cell regulation to cancer progression. DGKα in particular is a known promoter of T-cell anergy, and has been demonstrated as a promising therapeutic target in multiple cancers including glioblastoma (GBM) and melanoma. Prior to these following studies, the only significant phenotype observed in DGKα knockout (KO) mice has been enhanced T-cell activity. Herein we reveal a novel, macrophage-specific, immune-regulatory function of DGKα. In bone marrow-derived macrophages (BMDMs) cultured from wild-type (WT) and KO mice, we observed increased responsiveness of KO macrophages to activating stimuli. Knockdown (KD) of *Dgka* in a murine macrophage cell line resulted in similar increased responsiveness. Demonstrating *in vivo* relevance, we observed significantly smaller wounds in *Dgka*$^{-/-}$ mice with full-thickness cutaneous burns, a complex wound healing process in which macrophages play a key role. The burned area also had increased numbers of macrophages. In a cortical stab wound model, *Dgka*$^{-/-}$ brains show increased Iba1$^{+}$ cell numbers at the needle track versus that in WT brains.

Targeting DGKα in order to stimulate T-cell function or to combat its tumorigenic effects in cancer is feasible due to the existence of several small-molecule inhibitors. R59949 and R59022 are tool compounds which limit the DGKα conversion of DAG to PA. The compound ritanserin was originally implicated clinically as a serotonin receptor antagonist used for the treatment of schizophrenia and has been used in clinical trial

settings with no demonstrated adverse effects. Likely due to ritanserin's structural similarity to R59949 and R59022, it is also capable of inhibiting DGKα, with the added benefits of safety and being clinically actionable. In the following studies, we have identified several additional and potentially clinically relevant small molecule compounds from a library of ritanserin analogs which are more potent and specific for DGKα than those identified previously. Effective targeting of DGKα has promising therapeutic implications, and our newly identified immune regulatory role of DGKα is further support for the appeal of developing these compounds. Taken together, these studies present a novel immune-regulatory function of DGKα in macrophages with potential implications for wound healing, cancer therapy, and other settings, and the identification of inhibitory compounds to translate these findings therapeutically.

# Table of Contents

# Chapter 1
# Introduction

*Overview of diacylglycerol kinases*

The diacylglycerol kinase (DGK) family of lipid kinases is responsible for the conversion of diacylglycerol (DAG) to phosphatidic acid (PA). Both DAG and PA are lipid signaling molecules with key roles in regulating numerous critical enzymes and in recruitment of cytosolic proteins to the cell membrane. DAG is largely responsible for the activation of protein kinase C (PKC), which itself regulates a wide range of cellular processes that include proliferation, cell survival, and migration (1). Of the three subfamilies of PKC enzymes, the conventional (cPKC) and novel (nPKC) PKCs require DAG for activation (2). PKCs are important cytoplasmic signal transducers and are involved in regulating signaling pathways in both the innate and adaptive immune systems through Toll-like receptor (TLR), T-cell receptor (TCR) and B-cell receptor (BCR) signaling (3). In addition to mediating immune responses, PKCs also regulate gene transcription, and may lead to the increased expression of oncogenes and promote cell dysregulation. However, they are generally considered tumor-suppressive due to the loss-of-function mutations and low PKC protein levels found in cancer (4). PA is an important regulator of cytosolic proteins, recruiting them to their appropriate membranes—as with sphingosine kinase 1—and can regulate processes such as cell proliferation through binding of the FKBP12-rapamycin binding region of mTOR (5). As membrane-bound lipids, DAG and PA also affect membrane structure and curvature. Due to the presence of two acyl chains connected to a smaller headgroup, these lipids promote a negative membrane curvature, which can induce or enhance membrane fusion (6–8). The processes of bilayer fission and fusion have hugely important roles, as they are the mechanisms by which many eukaryotic functions are carried out, including lipid transport, oocyte

fertilization, and the formation of phagosomes in macrophages and other phagocytic cells. As the molecular switches responsible for maintaining the balance of both of these important second messengers, the importance of proper DGK regulation is evident.

The majority of signaling DAG is made by the hydrolysis of phosphatidylinositol 4,5-bisphosphate ($PIP_2$) by phospholipase C (PLC), with an inositol triphosphate co-product (9). PA is made by phospholipase D (PLD) hydrolysis of PC, producing PA and choline. DAG and PA are interconvertible in that, much like DGK enzymes convert DAG to PA, phosphatidic acid phosphatases (PAPs) convert PA to DAG. Despite this ability, DAG and PA do not act in the same pathways. This is exemplified in the observation of differential downstream products following unidirectional targeting. The addition of PLD to synaptosomal plasma membranes resulted in the production of [32P]-labeled PA and [32P]-labeled phosphoinositides. When the DGKα inhibitor R59949 was incubated with PLD, the [32P]-labeled PA product was eliminated, but not phosphoinositides (10).

*Mammalian DGK isoforms*

There are ten known isoforms of mammalian DGK. They are grouped into five subfamilies based on common structural elements (Figure 1.1). All DGKs possess a catalytic domain and at least two cysteine-rich C1 domains. These N-terminal C1 domains are DAG binding sites, much like the C1 domains present in PKC enzymes (9). While C1 motifs were previously considered to be DNA-binding regions due to their resemblance with the DNA-binding regions of transcription factors, this is not the case. Instead, they are protein binding sites and their role in promoting anchoring or activation is yet to be determined (11). Differences between the different DGK subtypes begin with the

distinction that only type I DGKs are found to have EF hand motifs. These calcium-binding motifs make DGKα, β, and γ more active in the presence of calcium. Evidence suggests that this is due to conformational changes resulting from calcium binding which allow for membrane association and enzyme activation (12). Type II DGKs are unique in that they contain a pleckstrin homology (PH) domain, although these binding sites do not significantly impact enzyme activity. While type III DGKε doesn't have a unique identifying motif outside of its C1 and catalytic domains, type IV DGKs ζ and ι possess a nuclear localization signal (NLS) which is a substrate for cPKCs. They also contain ankyrin repeats and a PDZ binding motif at the C-terminus that are likely sites for protein-protein interactions. The type V DGKθ is the only DGK with a third C1 domain and a PH domain with an embedded Ras-association domain (9). The unique features present in each type of DGK suggest their each having specific functional niches beyond the shared conversion of DAG to PA.

This enzyme family is not only diverse in structure, but in subcellular and organ localization as well. While DGKs α and ζ are among the most commonly expressed isoforms, most tissues express several DGK family members—with some demonstrating particular importance to specific tissues. For example, DGKβ is expressed predominantly in the nerves and the brain, despite being expressed at overall lower levels compared to other isoforms (13). When multiple DGKs are expressed within a tissue, they are generally from different subtypes, suggesting that each DGK subtype is responsible for a unique biological function. Also, the type I DGKs, the only $Ca^{2+}$-dependent isoforms, may have particular relevance in physiological contexts where calcium levels are elevated.

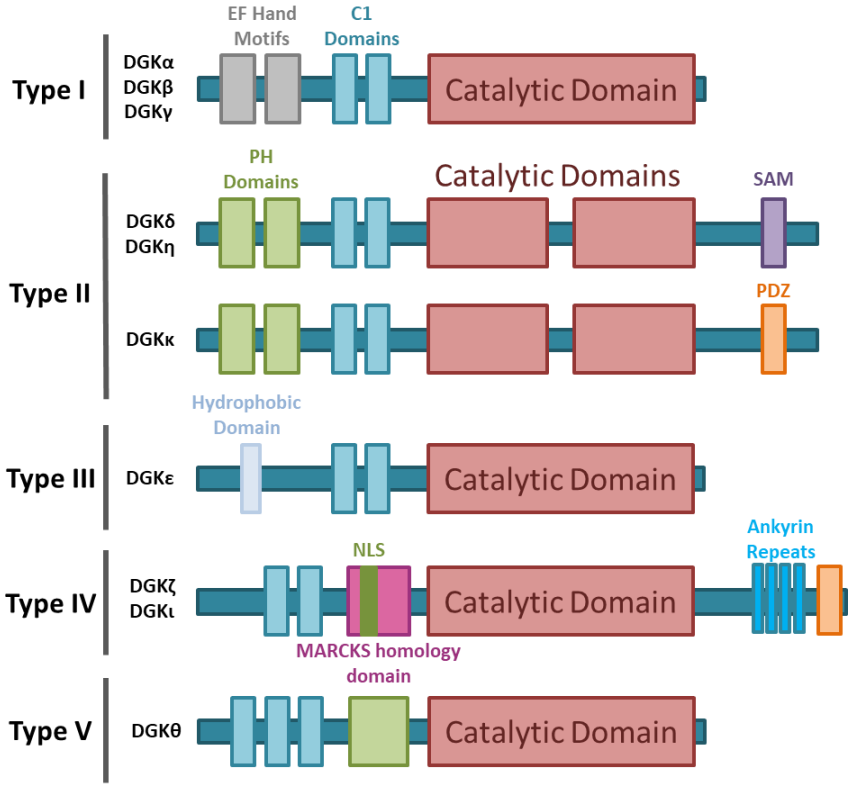


**Figure 1.1. Structure of DGK family isoenzymes.** Schematic diagram of 10 mammalian DGK enzymes divided into five subtypes. All mammalian DGKs have at least two cysteine-rich C1 domains and a catalytic domain. Type I DGKs, including DGKα, are the only isotypes to possess EF hand motifs, making them more active in the presence of calcium. Adapted from figure by Y. Shulga et al (9).

In unstimulated cells, most DGKs exist in the cytosol, translocating to relevant membranes upon activation. The unique motifs of the DGK subtypes allow these isoforms to be recruited to specific subcellular regions. The NLS of type IV DGKs result in their frequent translocation to nuclear membranes. The MARCKS domain also present within this subtype provides a PLC-dependent membrane-targeting. An N-terminal hydrophobic domain in DGKε is responsible for this isoform's endoplasmic reticulum (ER) localization. DGKγ is mainly colocalized with the Golgi, while DGKβ colocalizes with actin filaments, and DGKs α, ζ, and ι are known to shuttle in and out of the nucleus (9,14). Most DGKs are at least partly localized at the plasma membrane following agonist stimulation, as when DGKα is translocated following engagement of the T-cell receptor or Src activation (15,16).

*DGKα*

Of the ten DGK enzymes, DGKα has received a fair amount of attention in recent years as a result of its roles in immune regulation and the cytotoxic efficacy of DGKα inhibition in multiple cancers (Figure 1.2). Our lab has previously demonstrated the role of DGKα as a potential therapeutic target in melanoma and glioblastoma (GBM), while others have shown correlations with poor outcomes in diseases such as ovarian and gastric cancer (17,18). Our lab demonstrated the cytotoxic effect of DGKα inhibition through multiple targeting strategies, from small molecule and small interfering RNA (siRNA) inhibition (19), to microRNA (miRNA) inhibition with miR-297 (20), Promotion of tumor growth was also demonstrated; in the U87 and U251 GBM cell lines, overexpression of DGKα resulted in increased cell proliferation *in vitro* (19). The same was also true for the A375

human melanoma line, which when injected subcutaneously in nude mice presented with smaller tumor sizes in those mice treated with the DGKα inhibitor R59022. There are few small molecule inhibitors known to have great potency or specificity for DGKα. R59022 and R59949 have demonstrated and selective inhibition against DGKα and are structurally similar (21). Our lab identified the drug ritanserin, which had been tested in multiple clinical trials as a serotonin (5-HT) receptor antagonist, as a potential DGKα inhibitor due to its structural similarity to those previously mentioned. We were able to show that the typically treatment-resistant mesenchymal GBM subtype is particularly susceptible to ritanserin-induced DGKα inhibition *in vitro* and *in vivo* (22).

The importance of DGKα has been demonstrated in numerous cancers, and it has been shown in this context to function through key oncogenic pathways. In hepatocellular carcinoma (HCC), disease progression was shown to be enhanced by DGKα through activation of the Ras-Raf-MEK-ERK pathway (23). Knockdown of DGKα in HCC impairs MEK and ERK phosphorylation, and as has been observed in several other cancers, results in reduced tumor cell proliferation and invasion. In MDA-MB-231 breast cancer cells, the c-Met ligand HGF was found to induce DGKα activation and promote cell invasion and anchorage-independent growth (24). Furthermore, human melanoma cells are able to evade TNFα-induced apoptosis through DGKα activation of NF-κB (25). Given this, as well as what we know about the role it plays in immune regulation, DGKα has demonstrated potential as a therapeutic target in cancer.

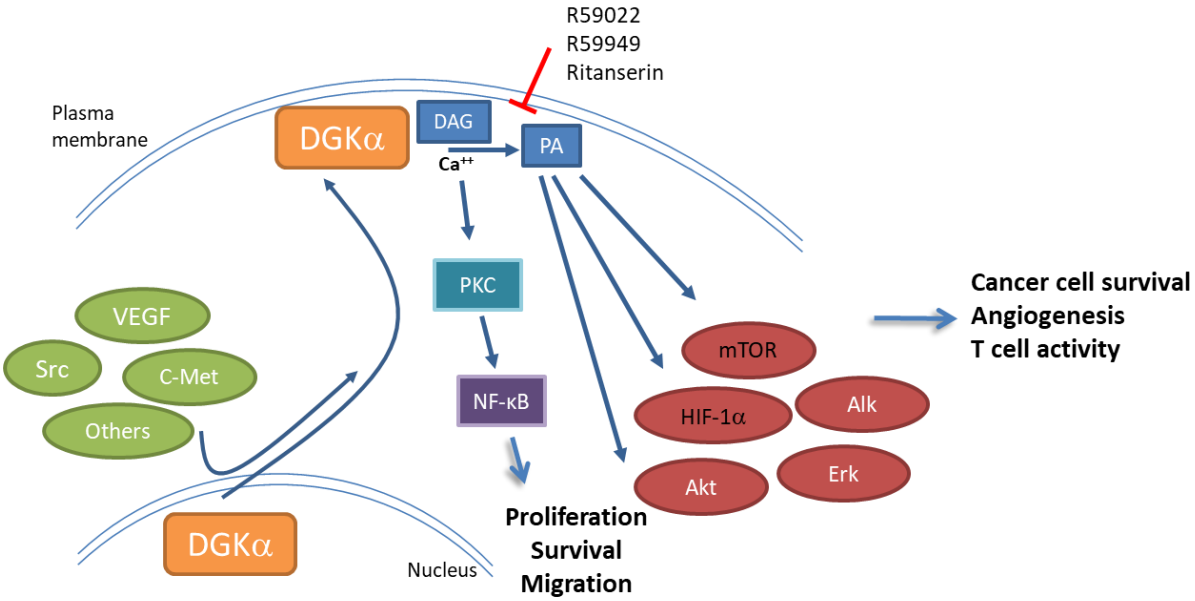


**Figure 1.2. DGKα regulation and activity.** Depiction of DGKα activation and function within the cell. Conversion of DAG to PA influences numerous oncogenic pathways, while small-molecule inhibition of DGKα blocks this conversion and promotes downstream activation of PKC, NF-κB, and influences cellular processes including proliferation, survival and migration. Adapted from figure by B. Purow (16).

*DGKα-mediated immune regulation*

Another important function of DGKα is its role in the promotion of T-cell anergy, a process in which T-cells are rendered unresponsive. *In vivo,* anergy induction is impaired in DGKα-deficient mice (26,27), and DGKα-deficient T-cells demonstrate increased DAG-dependent T-cell receptor signaling. DGKα, along with the Type IV DGKζ, are the abundant DGK isoforms in T-cells (28) and have both been identified as immune checkpoints in cancer. More recently, DGKα has also been linked to T-cell exhaustion, a distinct process in which T-cells become more inert after excessive receptor stimulation (29). DGKα overexpression is associated with defective translocation of RasGRP1 to the plasma membrane in T cells (30). The RasGRP/ERK pathway, which is mediated by DAG, is crucial in regulating T-cell development, homeostasis, and differentiation, and DGKα and ζ limit the activation of the PLCγ/Ras/ERK axis (28,31), *In vitro,* overexpression of DGKα and DGKζ resulted in decreased expression of the T-cell activation marker CD69 following T-cell receptor (TCR) complex signaling (32). Inhibition of DGKα has also been proposed as an approach for improving chimeric antigen receptor-modified T (CAR-T) cell therapy performance (33), and in addition DGKα inhibition has been found to synergize with anti-PD1 checkpoint inhibition in a mouse cancer model (29).

While immune cell regulation by DGKα has been predominantly limited to T-cell activation, there has also been evidence of potential regulation of NK cells. DGKα-mediated dampening of the ERK pathway, resulting in NK cell dysfunction, has been identified as an important immune escape mechanism in renal cell carcinoma (RCC) (34). Despite these key roles in T-cells and possibly NK cells, a role for DGKα in myeloid cells has not yet been tested; the relevance of DGKα in macrophage activation is thus a novel

area for investigation. DGKα regulation of macrophages could have many implications in areas such as wound healing, immunotherapy, and more. This dissertation provides the first assessment of a role for DGKα in macrophage activation.

*Macrophage function and activation*

Macrophages are prominent effector cells of the innate immune system with broadly ranging functions. From tissue-resident macrophages to tumor-associated macrophages (TAM), the responsiveness of these cells as well as their effects in different pathologies varies. The ontogeny of tissue-resident macrophages is an area which highlights the diversity of macrophage development and function. It had until recent years been the long-held belief that tissue-resident macrophages were derived and continuously replenished solely from adult blood circulating monocytes (35,36). Newer insights, however, have demonstrated that several tissue-resident populations are seeded sequentially during embryonic hematopoiesis. These cells are also self-maintained without bone marrow derived monocyte repopulation in adulthood. They are instead generated in the yolk sac during embryonic development from early erythro-myeloid progenitors (EMPs), and by fetal monocytes generated by EMPs seeded in the fetal liver (36). These aforementioned yolk sac macrophages give rise to the microglia in the brain, meaning that the adult brain is populated and sustained by tissue-resident macrophages derived during embryonic development. Interestingly, tissue-resident macrophages in several other organs are initially derived from yolk sac macrophages, then repopulated and sustained by fetal liver monocytes after E10.5 (35); this includes the Langerhans cells of the epidermis, the Kupffer cells of the liver, and the alveolar macrophages of the lungs. However, in the

intestines and the dermis, it is the bone marrow-derived monocytes (BMDMs) which are the source for tissue repopulation, being recruited and differentiated into macrophages, therefore enabling the use of BMDMs as model for investigation of dermal macrophage phenotypes.

The activation states of macrophages have also been a major area of insight and investigation. In this context, macrophages have been extensively studied due to their polarization states demonstrating pro- and anti-inflammatory function, often referred to as M1 and M2, respectively. The classically activated M1 macrophages have the traditionally activating stimuli of interferon-gamma (IFNγ) and lipopolysaccharide (LPS). These classically stimulated macrophages undergo polarization resulting in increased inflammation, tumor resistance, and graft rejection, while upregulating the secretion of pro-inflammatory cytokines such a TNFα and IL-1β, and exhibit increased phagocytic activity (37). Alternatively activated M2 macrophages are associated with matrix deposition, tissue remodeling, and graft acceptance, as well as upregulation of TGF-β and VEGF. M2 polarization is typically achieved through exposure to IL-4 or IL-13 (38). While this has been a traditional classification scheme for the range of macrophage activation states, it's important to note that macrophage activation is a spectrum with the M1 and M2 designations best used as reference points for activation at the extremes of a continuum of intermediate cells (39).

Macrophage activation can drive several diverse phenotypes which are regulated by several key pathways. Among these are Akt, Ras, and PKC, three pathways also known to be regulated by the DGK family of enzymes, including DGKα (19,21,40). The PI3K/Akt/mTOR pathway is an important regulator of macrophage survival, migration,

and proliferation, and also coordinates the response of macrophages to different metabolic and inflammatory signals (41). It is activated by TLR4 and other pathogen recognition receptors, as well as cytokine and chemokine receptors. Activated PI3K type I phosphorylates $PIP_2$, a crucial substrate in DAG production, to form phosphatidylinositol 3,4,5-triphosphate ($PIP_3$) at the plasma membrane (42). This results in the recruitment and activation of Akt by the mechanistic target of rapamycin complex (mTORC) 2. Activation of Akt in turn promotes the activation of mTORC1, mediating feedback inhibition to suppress mTORC2 and Akt activity (43,44). DGKα and PA have also been linked to several oncogenic pathways including mTOR and Akt (45,46). Knockdown of DGKα demonstrates a significant decrease in total mTOR and phos-$mTOR_{ser2448}$ in GBM cells, as well as reduced phosphorylation of $Akt_{ser473}$ (19). The role of PKC has also been demonstrated to be relevant in macrophage activation, and it has been suggested that the cPKC isoenzymes mediate the upregulation of iNOS expression and NO production in activated J774 macrophages in an NF-κB dependent manner. The inhibition of cPKC resulted in the inhibition of LPS-induced activation of STAT1, iNOS expression and NO production in inflammation, suggesting the inhibition of these isoenzymes may offer a novel target for the development of anti-inflammatory drugs (47). Further, it has been demonstrated that insulin-like growth factor (IGF)-1 is chemotactic to human THP-1 cell-derived macrophages, and activation of IGF-1R and the resultant Akt phosphorylation leads to PKC and subsequent p38 MAPK activation, suggesting a role for PKC in macrophage motility (48). The inhibition of DGKα results in the promotion of PKC activation as a result of the attenuation of DAG phosphorylation and conversion to PA, as

PKC is a downstream effector of DAG. This presents the potential for DGKα inhibition as a plausible strategy for the enhancement of macrophage migration due to PKC activation.

*Macrophages in wound healing*

Wound healing is a prime example of the diversity of functions performed by macrophages, in that each stage of the wound healing process has its own set of distinct needs able to be addressed by these cells. In early healing, when functions such as bacterial clearance and apoptosis are necessary for host defense, pro-inflammatory macrophages recruited to the wound site are the abundant macrophage type present (49). Late-stage healing necessitates an influx of fibroblasts to the wound site, angiogenesis, and extracellular matrix (ECM) deposition which are achieved by anti-inflammatory macrophages. Given its importance, wound healing is already a very well regulated and efficient process, making it difficult to develop treatments that substantially improve outcomes from patients suffering from traumatic injuries. Concurrent with local wound repair, the effects of large burn wounds have the potential to also stimulate a persistent pathophysiological stress response, which can affect the pharmacokinetics and pharmacodynamics of treatment drugs (50). The excisional wound splinting model and cutaneous burn models are both commonly employed methods for assessing wound healing (51,52), and both are used to assess potential benefits resulting from therapeutic intervention.

In considering strategies which may modulate the well-regulated and conserved process of wound healing, it is important to consider the mechanisms through which this process occurs. Continuing with the example of skin wounds, the role of macrophages is

layered, going beyond their previously described host defense-to-tissue remodeling functions. It is, in fact, tissue-resident macrophages which are among the first to respond to the site of a dermal wound and serve as early indicators of injury or invading pathogens (53). They do this by recognizing damage-associated molecular patterns (DAMPs) and initiating a pro-inflammatory cascade through the release of hydrogen peroxide (54). The subsequent macrophage response to injury is largely undertaken by differentiated blood circulating monocytes recruited by DAMP or pathogen-associated molecular pattern (PAMP) signals. These cells are stimulated by cytokines such as IL-4, IL-10, IFNγ, and the PAMP LPS, to differentiate into macrophages. While other cell types such as neutrophils are among the first to populate the wound bed a time of injury, within three to five days, macrophages are the most prominent cells in healing tissue (55) and depletion of macrophages at this time results in significantly delayed wound repair (56). Macrophage clearance of apoptotic neutrophils can induce their phenotypic switch from M1 to M2 (57,58), leading to the resolution of inflammation phase, and onset of the proliferative wound healing phase, where the formation of granulation tissue consisting of endothelial cells, fibroblasts, myofibroblasts, and keratinocytes (53). TGF-β, platelet-derived growth factor (PDGF), fibroblast growth factor 2 (FGF2) and insulin-like growth factor 1 (IGF-1) secreted by macrophages contribute to collagen production by fibroblasts. Macrophages in this vascularized ECM are a continued source of pro-inflammatory cytokines such as IL-1α, IL-1β, IL-6, and TNFα, which are crucial for the stimulation of fibroblast and keratinocyte proliferation (59). While little has previously been demonstrated regarding the potential role for DGKα in wound healing, one study has shown that its inhibition may prove useful as a preventive antifibrotic therapy for radiation-induced fibrosis (60).

Isolated fibroblasts taken prior to breast cancer radiotherapy treatment showed DNA methylation differences which were associated with fibrosis development after radiation, particularly in the *DGKA* locus which was less methylated in patients developing fibrosis.

As the resident macrophage cells of the brain, microglia perform similar surveillance and reparative functions as normal macrophages. These cells originate from the mesodermal cells of the yolk sac during embryonic development and are self-renewing (61,62). While macrophages and microglia express many similar surface markers such as Iba1, F4/80, CD45, CD68, and CD11b, often making them difficult to distinguish from one another, some distinctions may be made from peripheral macrophages. For instance, microglia are Mac-1/CD11b$^{+}$ CD45$^{low}$-expressing cells, while macrophages are Mac-1/CD11b$^{+}$ CD45$^{high}$ (63). Also, more recently-described markers such as TMEM119 serve to specifically identify subsets of microglia (64). Macrophages and microglia are also similar in their cytokine secretion profile, with activated microglia shown to secrete IL-1, IL-6, and TNF-α, with secretion of cytokines such as TNF-α and IL-1β serving to help activate other immune cells to engage in wound healing processes. In the brain these inflammatory cytokines may play harmful roles in various neuropathologic states, but are also important for limiting damage to the brain (65). Brain injury acts to not only activate microglia and induce their migration and proliferation, but also to cause hemorrhage and blood-brain barrier (BBB) disruption that can allow macrophages and monocytes in the blood to enter the injured brain region.

Activation of microglia also presents substantial overlap with mechanisms of macrophage activation. IFNγ and LPS typically convert resting microglia to a pro-inflammatory state, while IL-4, IL-10 , and IL-13 will convert them to an anti-

inflammatory state (66), both of which may play roles in the brain responses to wound healing. Signaling pathways linked to microglial function include PKC, ERK, and PI3K/Akt, with PKC having been shown to mediate microglial activation through pathways such as NF-κB/STAT1 and PLC-γ1/ERK (67,68).

*Currently available DGKα small molecule inhibitors*

The landscape of DGK inhibitors has not improved substantially since the discovery of the first DGKα inhibitor, R59022 (69). This is not surprising, given that the average time to approval for new drugs and devices in the United States by the FDA is about 12 years (70). This extended timeframe creates additional hurdles on the path to therapeutic development alongside the immense costs associated with getting a drug to market, as well as the frequency of drug failure (71,72). Drug failure is often the result of poor efficacy or safety risks; therefore, improved approaches for target identification and validation are needed for the drug development process to better reach and serve patients in need (73,74). In many cases however, the need to produce an entirely new drug is circumvented by repurposing an existing drug. Drug repurposing has emerged as an attractive model for therapeutic development, and in some cases a potential path toward expanded treatment options (75). While there is typically a pre-existing track record of safety and knowledge of side effects with existing drugs, repurposing drugs for novel applications also provides challenges not necessarily present when developing new agents. By the very nature of these agents being repurposed, these drugs are often nonspecific and have multiple targets, and may also demonstrate poor potency against the new target for which they are repurposed. Additionally, funding trials of repurposed drugs for new

applications can be extremely challenging, with large pharmaceutical companies typically not supporting such expensive efforts (76).

The compounds R59949 and R59022, identified as specific DGKα inhibitor tool compounds for research, had long been the sole small-molecule tools available for understanding the functional biological roles of DGKs (21,69,77). This has had a limiting effect on the study of small molecule inhibition of DGKα due to the poor potency of these drugs for DGKα and their potent inhibition of other targets. More recently, compound screening identified the drug CU-3 as a potent inhibitor for DGKα (78,79), adding to the small but growing list of therapeutics aimed at targeting the enzyme. The serotonin (5-$HT_2$) receptor antagonist ritanserin was initially developed as a treatment for schizophrenia (80,81), but has since been identified by us and collaborators as an inhibitor of DGKα as well—initially based on its structural similarity to R59022 and R59949 (Figure 1.3) (21). The potency of these drugs for serotonin receptors is yet another limitation of these compounds and present the potential for drug side effects, including somnolence, and they also have weaker activity against dopamine receptors (82). Interest in DGKα as a target for cancer immunotherapy has gained traction in recent years (17,83,84) and new inhibitors are currently in development at pharmaceutical companies. Given the druggable nature of DGKα and the numerous therapeutic indications for its inhibition, there is great potential in the continued search for novel compounds with greater potency and specificity, many of which may already exist in the compound libraries of pharmaceutical laboratories. We seek to demonstrate the potential for expanded immunologic effects of DGKα inhibition, showing for the first time activity in a myeloid cell type. The growing list of immunologic

benefits with DGKα inhibition is driving the search for novel DGKα inhibitors, with a growing pool of compounds being identified.

The rationale for the following projects is motivated by the increasing interest attracted by DGKα as a target in cancer, with DGKα inhibition having the potential to act directly against certain cancer cells, but also to boost activity of T-cells and possibly NK cells against cancer. The role of DGKα in myeloid cells of the immune system such as macrophages has not previously been assessed, and with DGKα inhibitors on their way to the clinic, it is vital that this be assessed. Chapter 2 is the first demonstration of a role for DGKα in macrophages, potentially broadening the immune benefits of DGKα inhibition/knockdown. Given the pressing need for more potent DGKα inhibitors, Chapter 3 studies a library of ritanserin analogs and identifies compounds with increased potency against DGKα and with limited activity against other DGK family members. This work should have an impact on the field of DGKα inhibition, with potential implications for cancer therapy and potentially other applications as well.

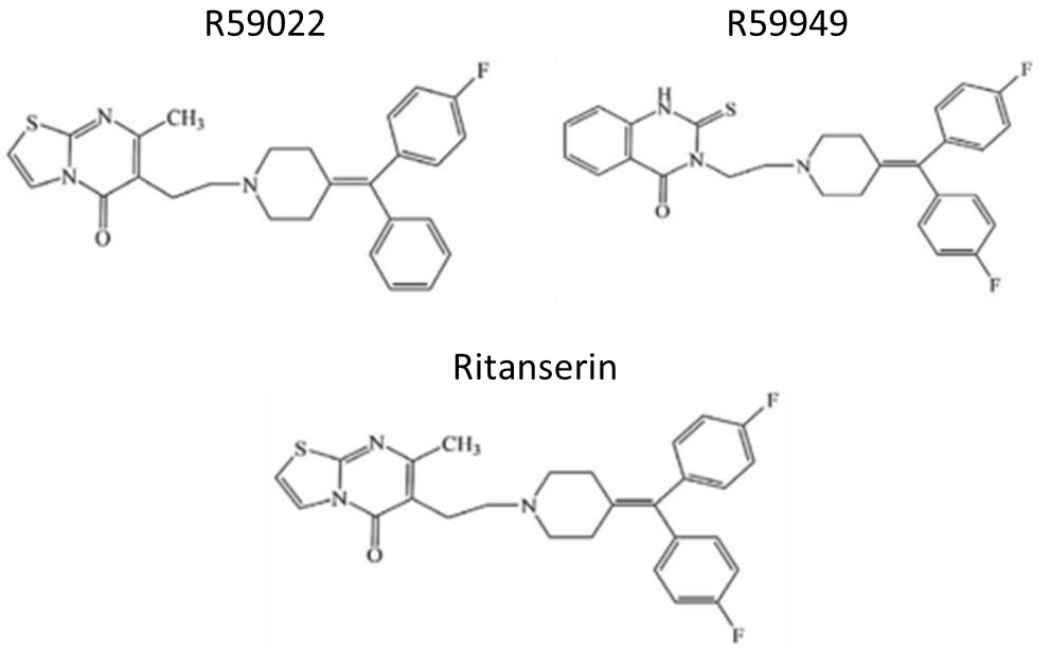


**Figure 1.3. Compound structures of known DGKα inhibitors.** Serotonin receptor antagonist ritanserin has been identified as an inhibitor of DGKα, initially based on its structural similarity to R59022 and R59949.

# Chapter 2

## Loss of Diacylglycerol Kinase α Enhances Macrophage Responsiveness

Laryssa C. Manigat[1], Mitchell E. Granade[2], Suchet Taori[3], Charlotte Anne Miller[3], Luke R. Vass[1], Xiao-Ping Zhong[4], Thurl E. Harris[2], Benjamin W. Purow[3]

Departments of [1]Pathology, [2]Pharmacology, [3]Neurology, Division of Neuro-Oncology, at the School of Medicine, University of Virginia, Charlottesville, VA, United States; [4]Duke University Medical Center, Division of Allergy and Immunology, Durham, NC, United States

(Adapted from manuscript published in *Frontiers in Immunology*, 5th November 2021)

**Abstract**

The diacylglycerol kinases (DGKs) are a family of enzymes responsible for the conversion of diacylglycerol (DAG) to phosphatidic acid (PA). In addition to their primary function in lipid metabolism, DGKs have recently been identified as potential therapeutic targets in multiple cancers, including glioblastoma (GBM) and melanoma. Aside from its tumorigenic properties, DGKα is also a known promoter of T-cell anergy, supporting a role as a recently-recognized T cell checkpoint. In fact, the only significant phenotype previously observed in *Dgka* knockout (KO) mice is the enhancement of T-cell activity. Herein we reveal a novel, macrophage-specific, immune-regulatory function of DGKα. In bone marrow-derived macrophages (BMDMs) cultured from wild-type (WT) and KO mice, we observed increased responsiveness of KO macrophages to diverse stimuli that yield different phenotypes, including LPS, IL-4, and the chemoattractant MCP-1. Knockdown (KD) of *Dgka* in a murine macrophage cell line resulted in similar increased responsiveness. Demonstrating *in vivo* relevance, we observed significantly smaller wounds in *Dgka*$^{-/-}$ mice with full-thickness cutaneous burns, a complex wound healing process in which macrophages play a key role. The burned area also demonstrated increased numbers of macrophages. In a cortical stab wound model, *Dgka*$^{-/-}$ brains show increased Iba1$^{+}$ cell numbers at the needle track versus that in WT brains. Taken together, these findings identify a novel immune-regulatory checkpoint function of DGKα in macrophages with potential implications for wound healing, cancer therapy, and other settings.

## Introduction

The diacylglycerol kinases (DGKs) are the molecular switches regulating diacylglycerol (DAG) conversion to phosphatidic acid (PA). These enzymes have essential roles in lipid synthesis, cell proliferation, and survival, with DAG and PA playing key roles in regulating numerous critical enzymes and in recruitment of cytosolic proteins to the cell membrane. The protein kinase C (PKC) family of enzymes are key mediators of DAG effects, and are known to regulate cellular functions including proliferation, cell survival, and migration (1). In addition to being important regulators of a diverse set of cellular processes, PKCs have also been linked to tumorigenesis (85,86). PA is also able to influence processes such as cell proliferation through its binding of the FKBP12-rapamycin binding region of mTOR (87,88). Therefore, proper regulation of DGK enzymes is crucial for maintaining homeostasis of DAG, PA, and their downstream effectors.

The ten mammalian DGKs are divided into five subtypes based on shared functional domains. All ten DGKs possess both a C1 and a catalytic domain, with variations existing in the N- and C-terminal regions. Even within subtypes, the DGKs may differ in abundance and in organ/subcellular distribution. For instance, Type I DGKs α and β differ markedly in tissue distribution; DGKα is one of the most commonly expressed DGKs and particularly enriched in the brain, lungs, and white blood cells, while DGKβ is found at lower levels and predominantly in nerves and the brain (5,6). This suggests potential specificity of certain DGKs for different cell types, and the occurrence of individual DGKs from different subtypes within a single tissue suggests their having specific functions. One known and recently identified function of DGKα – along with its other family member DGKζ – is its promotion of T-cell anergy (11,90,91). The ability to

limit T-cell activation in the tumor microenvironment, along with the promotion of tumor survival resulting from PA generation (45), are a tandem that underlie the challenges of therapeutic development in cancer, and present an opportunity for targeting DGKα in this context. The notion of DGKα as an immune regulator has become firmly established, with it now being described as an immune checkpoint (28), and its inhibition has been proposed as an approach for improving CAR-T cell performance (92). A role in regulating NK cell function has also been shown, with restoration of disabled MAPK pathway function in NK cells from human renal cell carcinoma following DGKα inhibition (34). However, a role for DGKα in macrophage function and the myeloid cells of the immune system has never been demonstrated.

Macrophages are important effector cells of the innate immune system and perform many varied and context-dependent functions. They are crucial to the maintenance of tissue homeostasis, and are among the first cells to respond in the event of injury (53). In addition to their important role in host defense, they also are necessary for tissue remodeling and repair. Pro-inflammatory macrophages are known to exhibit increased secretion of pro-inflammatory cytokines, and sometimes increased phagocytosis, aiding in the removal of pathogens and damaged tissue. Anti-inflammatory macrophages secrete high levels of anti-inflammatory cytokines and fibrogenic and angiogenic factors that promote tissue remodeling and repair (93). These polarization states have relatively well-defined stimuli and markers, which promote the state of activation best suited for the current environmental condition. Lipopolysaccharide (LPS) typically induces a pro-inflammatory phenotype, promoting upregulation of genes associated with inflammation, tumor resistance, and graft rejection, while IL-4 promotes matrix deposition necessary for tissue remodeling and

repair, characteristic of an anti-inflammatory phenotype (38). iNOS and Arginase-1 are two commonly referenced markers of pro- and anti-inflammatory activation, respectively. They play important roles in promoting the conditions which give rise to their respective polarization states (39). In the tightly regulated process of wound healing, pro-inflammatory macrophages are particularly important during the first inflammatory phase, while anti-inflammatory macrophages can be found during the proliferative and remodeling phases.

While DGKα has not been firmly linked to the myeloid arm of the immune system, we came to suspect such a connection following the observation that there were dramatically fewer skin ulcers over subcutaneous melanoma tumors in *Dgka*$^{-/-}$ versus wild-type (WT) mice. Given that DGKα had been shown to regulate other immune cells and that macrophages are known to play key roles in wound healing (94). including in the context of chronic wounds such as skin ulcers (53), we hypothesized that DGKα regulates macrophage activity as well. This prompted us to specifically investigate macrophage function in the setting of *Dgka* knockout and knockdown. Through these experiments, we have identified a novel role for DGKα in macrophage responsiveness and activation, using bone marrow-derived macrophages (BMDMs), a murine macrophage line, and two *in vivo* injury models.

## Materials & Methods

### *BMDM harvest*

BMDMs were derived from bone marrow harvested from 12-week old WT and *Dgka*$^{-/-}$ C57BL/6 mice. Mice were euthanized, hind limbs excised, and then skin, muscle,

and connective tissue removed. Bare femur was carefully separated from tibia/fibula, then both ends of each bone clipped to expose bone marrow. Using a 19G needle, a small hole was poked through the bottom of a 0.5mL Eppendorf tube which was then placed inside a 1.5mL Eppendorf tube. Clipped bones were inserted into the 0.5mL tube and the nested tubes spun for 10-20 seconds in a mini centrifuge, drawing marrow through the needle hole into the 1.5mL tube. Red blood cell progenitor lysis was accomplished with 0.83% (w/v) $NH_4Cl$ for 5 minutes at room temperature. Pelleted marrow cells were resuspended in BMDM culture medium.

*Macrophage differentiation and activation*

BMDM culture medium was prepared with RPMI 1640 with 2mM L-glutamine, 10% FBS, 2% HEPES, and 2% antibiotic-antimycotic. Differentiation medium was prepared as 90% BMDM culture medium and 10% L929 conditioned medium (LCCM) containing macrophage colony stimulating factor (M-CSF). BMDMs were cultured for four days in differentiation medium, which was replaced on days four and six. Differentiated macrophages were plated on day seven in BMDM culture medium without LCCM and incubated overnight followed by treatment with BMDM medium supplemented with 500ng/mL LPS (Invitrogen, #00-4976-93) or 2ng/mL IL4 (BioLegend, #574302). Cells were lysed for western blot and qPCR analysis.

*Migration assay*

Following differentiation of BMDMs, cells were starved in FBS-free media for 24h. After trypsinization and counting, $3x10^5$ cells were plated into 8μm transwell inserts

purchased from Abcam (#235694). The wells below transwells contained 600μL of culture media with 50ng/mL of monocyte chemoattractant protein-1 (MCP-1). Eighteen hours after the start of the assay, migrated cells were dissociated from the underside of the transwell and quantified per the manufacturer's instructions.

*Immunoblot*

Western blots were done on BMDM lysates using Cell Signaling Technology Cell Lysis Buffer 10x (#9803) supplemented with 0.5% SDS and protease inhibitor tablet (Roche, #04693124001). ~5μg protein was loaded and PVDF membranes were probed with antibodies specific to iNOS (Novus Biologicals, #NB300-605), Arginase-1 (Proteintech, #16001-1-AP), β-tubulin (Proteintech, #10094-1-AP), β-actin (Thermo Fisher Scientific, # PA5-85291), DGKα (Proteintech, #11547-1-AP), and Phospho-(Ser) PKC Substrate (Cell Signaling, #2261). Quantification of immunoblots was performed by first normalizing band intensities to β-tubulin or β-actin to control for loading variability. Relative intensities were then calculated by normalizing to PBS control conditions.

*Real-Time qPCR*

RNA isolation was performed using Qiagen RNeasy Mini Kit (#74104), and cDNA synthesis done with Qiagen QuantiTect Reverse Transcription kit (#205311) according to manufacturer's instructions. Real-time qPCR was performed using Applied Biosystems PowerSYBR Green PCR Master Mix (#4367659). Expression of target mRNA was normalized to ribosomal 18s RNA and quantified using the $2^{-\Delta\Delta CT}$ method. Primer pairs were sourced from the PrimerBank of the Center for Computational and Integrative

Biology of Massachusetts General Hospital and Harvard University.(95–97) Sequences used were Mouse 18s Forward: GTAACCCGTTGAACCCCATT, Reverse: CCATCCAATCGGTAGTAGCG; iNOS (PrimerBank ID 146134510c1) Forward: GTTCTCAGCCCAACAATACAAGA, Reverse: GTGGACGGGTCGATGTCAC; Arginase-1 (PrimerBank ID 158966684c1) Forward: CTCCAAGCCAAAGTCCTTAGAG, Reverse: GGAGCTGTCATTAGGGACATCA; SOCS1 (PrimerBank ID 6753424a1) Forward: CTGCGGCTTCTATTGGGGAC, Reverse: AAAAGGCAGTCGAAGGTCTCG; SOCS3 (PrimerBank ID 6671758a1) Forward: ATGGTCACCCACAGCAAGTTT, Reverse: TCCAGTAGAATCCGCTCTCCT. Ki67 (PrimerBank ID 1177528a1) Forward: ATCATTGACCGCTCCTTTAGGT, Reverse: GCTCGCCTTGATGGTTCCT. DGKα (PrimerBank ID 31560473c1) Forward: GTGATGTGTACTGCTACTTCACC, Reverse: CACTTCCGTGCTATCCAGGA. DGKβ (PrimerBank ID 26336555a1) Forward: ATGAAGACCTTTCTGGAAGCTG, Reverse: TTTACATTTGGGCTAGAATGGGG. DGKγ (PrimerBank ID 26354382a1) Forward: ATGAGCGAAGAACAATGGGTC, Reverse: GGGCTTGTGTGGGTCATACTG. DGKζ (PrimerBank ID 30794244a1) Forward: CTCTTTGGGCACAGGAAAGC, Reverse: TGCTGACTCACTCCAGTCCA.

*Cell culture and transfection*

J774 macrophages were cultured in DMEM supplemented with 10% FBS and 1% penicillin-streptomycin. Cells were transfected using Lipofectamine RNAiMAX

(Invitrogen, #13778030) with control (Ambion #AM4611) and DGKα siRNA (Ambion, #AM16708 – 161793, 161794).

*Mouse and wound models*

The *Dgka*$^{-/-}$ mouse colonies used in these experiments were established in the lab of Dr. Xiao-Ping Zhong at Duke University, and were generated as previously described.(98) Cutaneous burn model mice were anesthetized using ketamine/xylazine. Hair was removed by shaving, followed by depilatory cream applied for 3 minutes. An 8mm-diameter metal rod set in boiling water was then applied for 10 seconds to bare skin raised from both flanks. Mice were then given buprenorphine slow-release analgesic, rehydrated, and returned to single housed cages. Burns were photographed daily using isoflurane anesthesia and imaged by microscope equipped with an Amscope MD200 camera. Measurements were taken using ImageJ image processing software.

Cortical stab wounds were performed by stereotactic alignment and immersion of a 30G needle 2mm lateral and 1mm anterior to the bregma, advancing 3mm into the brain. Brains were saline-perfused and harvested four days post-injury, then formalin-fixed in 10% formalin for 24h at room temperature, then transferred to 70% ethanol prior to paraffin-embedding. All *in vivo* experiments were performed under IACUC-approved protocol 3833.

*Immunohistochemistry*

Mouse skin and brains were fixed in 10% formalin for 24h at room temperature, then transferred to 70% ethanol prior to paraffin embedding. Immunohistochemistry was

performed on a robotic platform (Ventana discover Ultra Staining Module, Ventana Co., Tucson, AZ, USA). Tissue sections (4 µm) were deparaffinized using EZ Prep solution (Ventana). A heat-induced antigen retrieval protocol set for 64 min was carried out using Cell Conditioner 1 (Ventana). Endogenous peroxidases were blocked with peroxidase inhibitor (CM1) for 8 min before incubating the section with Iba1 antibody (Invitrogen, Cat#PA5-21274) at 1:1,250 dilution for 60 min at room temperature. Antigen-antibody complex was then detected using DISCOVERY OmniMap anti-rabbit multimer RUO detection system and DISCOVERY ChromoMap DAB Kit (Ventana Co.). All slides were counterstained with hematoxylin subsequently; they were then dehydrated, cleared and mounted for assessment.

*Image analysis*

Whole slide images of immunohistochemical slides were obtained on the Aperio ScanScope slide scanner at 20x magnification. All images were analyzed using the open source digital pathology software, QuPath (v0.2.3).(99) In the software, stained cells were quantified as number positive/$mm^2$ and segmented by size and shape, with a range of 50-500$\mu m^2$ to capture cells of varying depths within the plane.

*Immunofluorescence*

Manual immunofluorescent (IF) staining was done on mouse brain and skin slides blocked for one hour at room temperature (RT) in a humidity chamber with 5% mouse serum, 5% donkey serum, and 0.3% Triton X-100. Primary antibody solutions were prepared in PBS with 0.3% Triton X-100. Primary antibodies used were specific to F4/80

(Novus Biologicals, #NB800-404), Iba1 (Novus Biologicals, #NB100-1028), and DGKα (Bioss Antibodies, #BS-14294R). Tissue was incubated overnight at 4°C in humidity chamber. Fluorescent antibodies (Abcam) used were donkey anti-rat AF647 (#ab150155), donkey anti-rat AF488 (#ab150153), donkey anti-rabbit AF647 (#ab150075), and donkey anti-goat AF488 (#ab150133). Secondary solutions were prepared in PBS with 0.3% Triton X-100 and incubated on slides for three hours at RT in humidity chamber protected from light. Stained slides were mounted using mounting medium with DAPI (Abcam, #ab104139). Slides were imaged using the Leica Thunder Imager at 10x magnification, and analyzed on the Leica Application Suite X (LAS X) software platform.

*Statistics*

Statistical analysis was performed using GraphPad Prism 8 software. Student's t test (two-tailed) was used for analysis of differences between two groups. One or two-way ANOVA with Tukey or Sidak post-hoc test was used for multiple comparisons. Data are presented as mean ± SD. $P < 0.05$ was considered statistically significant.

## Results

### Dgka$^{-/-}$ *BMDMs are more responsive to LPS and IL-4 stimulation*

To test whether DGKα regulates macrophage activity and responsiveness, we isolated and cultured BMDMs from *Dgka*$^{-/-}$ and WT mice and tested the expression of activation markers upon stimulation with LPS or IL-4. qPCR analysis demonstrated that *Nos2* (gene encoding iNOS) expression was significantly increased 24h after LPS stimulation, as was *Arg1* (gene encoding arginase) expression following IL-4 stimulation

(Figure 2.1A). Differences are evident both as a direct contrast between *Dgka*$^{-/-}$ and WT, and also in the degree of upregulation from baseline with PBS control-treated cells. These differences were also evident in the immunoblot analysis of WT and *Dgka*$^{-/-}$ BMDM lysates at 24h post stimulation (Figure 2.1B, C). We additionally tested the expression of two members of the SOCS family, which are intracellular cytokine-inducible proteins known to regulate macrophage activation and polarization (100). While SOCS1 is reported to promote both pro- and anti-inflammatory activation, SOCS3 has been found to have a key role in pro-inflammatory polarization alone (101,102). Consistent with these roles, we have found in BMDMs that *Socs1* expression responds strongly to LPS and IL-4 stimulation, and that *Socs3*, expression is enhanced only by LPS stimulation – with both showing greater increases in *Dgka*$^{-/-}$ BMDMs than in WT BMDMs (Figure 2.1D). To confirm the genotype of study mice used, BMDM lysates were also probed for DGKα protein expression (Figure 2.1E). Interestingly, we observed that DGKα expression is affected by both LPS and IL-4 in WT BMDMs (Figure 2.2A, B). An increase in DGKα protein expression was evident in LPS-treated WT BMDMs, while IL-4 treatment resulted in reduced protein levels (Figure 2.2C). Given that there are ten DGK family members including DGKα, we considered whether other DGKs compensate for its absence in treated and untreated conditions (Figure 2.2D); we found that loss of DGKα caused no change in mRNA expression levels of the remaining type I DGKs, nor type IV DGKζ. It was not surprising to observe the presence of DGKα transcript within the *Dgka*$^{-/-}$ samples given the KO strategy, as this KO does still yield a modified *Dgka* transcript, but not the protein.

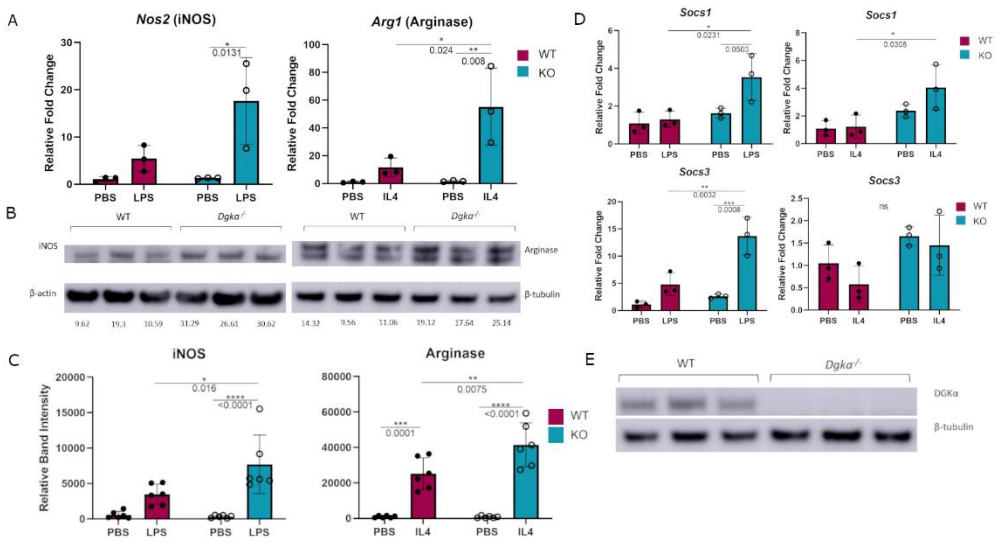


**Figure 2.1. Increased expression of macrophage activation markers in *Dgka*$^{-/-}$ BMDM following LPS or IL4 stimulation. (A)** WT and *Dgka*$^{-/-}$ BMDMs were treated with 500ng/mL LPS or 2ng/mL IL-4 for 24h and assessed by qPCR for changes in *Nos2* and *Arg1* expression, respectively. **(B)** Immunoblot depicting protein expression of iNOS in lysates of LPS treated WT and *Dgka*$^{-/-}$ BMDMs (left) and arginase expression of IL-4 treated BMDMs. Quantification of band intensity normalized to PBS treated WT mice (not shown) are indicated in text below bands. **(C)** Summary plot depicting quantification of immunoblot band intensity of two independent experiments as in **(B)** for n=6 per group. **(D)** WT and *Dgka*$^{-/-}$ BMDMs treated with LPS and IL-4 were assessed by qPCR for expression of SOCS1 and SOCS3. In **(A)** and **(D)** samples were normalized to the PBS treated WT control. **(E)** immunoblot of WT and *Dgka*$^{-/-}$ BMDM whole cell lysates with anti-DGKα antibody. Each data point represents an individual mouse for n=3 per group. Error bars: SD. *p<0.05, **p<0.01, ***p<0.001, ****p<0.0001; ns, not significant; Two-way ANOVA with Tukey post-hoc test.

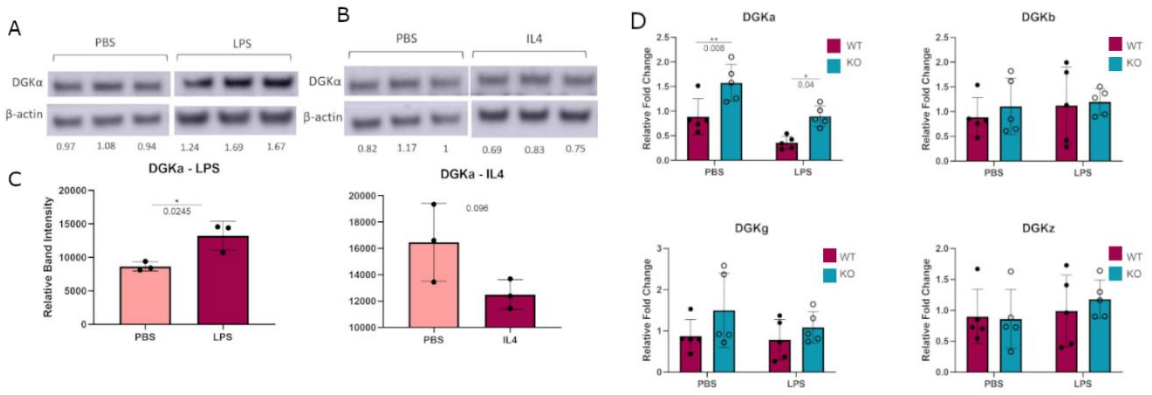


**Figure 2.2. DGKα expression may be slightly altered by treatment with LPS and IL4, but expression of DGK family members is generally unaffected by knockout of *Dgka* or LPS treatment.** WT BMDMs were treated with PBS and LPS **(A)**, or PBS and IL4 **(B)** and DGKα protein expression was measured by immunoblot. Band intensities normalized to PBS treated group are indicated in the text below the bands. **(C)** Quantification of immunoblot band intensity. Error bars: SD. *p<0.05; student's t-test. **(D)** WT and *Dgka*$^{-/-}$ BMDMs treated with PBS or LPS for 24h were assessed by qPCR for expression levels of type I DGKs α, β, and γ, and type IV DGKζ. DGKα KO was caused by a deletion between exon 9 to the intron between exons 16 and 17. The primer pair used to assess DGKα mRNA expression is prior to this deletion. Error bars: SD. *p<0.05, *p<0.01; Two-way ANOVA with Tukey post-hoc test.

*Increased responsiveness of J774 macrophages to LPS and IL-4 stimulation and increased PKC activity following* Dgka *knockdown*

We tested whether *Dgka* knockdown would similarly increase responsiveness to cytokine stimulation in a widely-used murine macrophage line. In the J774 line, transient transfection with two different *Dgka* specific siRNAs indeed resulted in similar patterns of macrophage marker upregulation by qPCR. Following LPS and IL-4 stimulation, J774 cell expression of *Nos2* and *Arg1*, respectively, was increased in cells that had been transfected with *Dgka* siRNA significantly more than in cells transfected with negative control siRNA (Figure 2.3A). In the absence of LPS or IL-4 stimulation, mRNA expression levels are the same across groups. Western blot analysis of whole cell lysates further supported this increased stimulation (Figure 2.3B). Quantification of increases in iNOS and Arginase protein expression are also shown (Figure 2.3C). We also noted more prolonged iNOS protein expression in LPS-treated *Dgka* KD cells over a time course of 24h compared to control siRNA-transfected cells (Figure 2.4A, B).

As previously noted, PKC is a key effector of the DGKα substrate DAG. To determine if downstream DAG signaling in the absence of DGKα influences PKC, and therefore implicate PKC as a potential mediator of increased *Dgka* KD macrophage responsiveness, an immunoblot of the *Dgka* siRNA transfected J774 lysates was probed for phosphorylated PKC substrates (Figure 2.3D, E). 48h after siRNA transfection, and 24h after PBS or LPS treatment, PBS-treated J774 cells with *Dgka* KD exhibit increased levels of phospho-PKC substrates versus control siRNA-transfected J774. While LPS treatment did not demonstrate an increase in PKC activation, LPS-treated cells that were transfected with *Dgka* siRNA exhibited modestly higher levels of phospho-PKC substrates than

control siRNA-transfected cells. Successful *Dgka* knockdown was confirmed by western blot (Figure 2.5A, B).

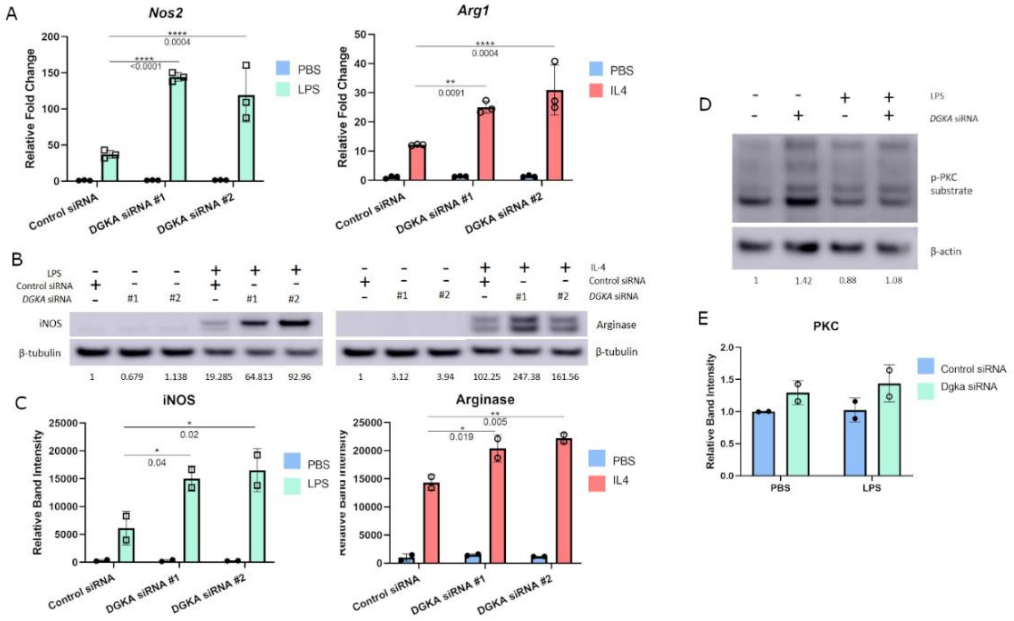


**Figure 2.3. Knockdown of *Dgka* from J774 murine macrophage cell line shows increased amplification of macrophage activation markers following LPS or IL4 stimulation. (A)** J774 murine macrophages were stimulated with 500ng/mL LPS or 2ng/mL IL-4 following control or *Dgka* siRNA transfection and assessed by qPCR for *Nos2* and *Arg1*, respectively. Samples were normalized to the PBS treated control siRNA transfected cells. **(B)** Immunoblot analysis of whole cell J774 lysates probing for iNOS in LPS-treated cells and Arginase in IL4-treated cells. Relative band intensities normalized to PBS-treated control are indicated as text below the immunoblots. Representative data shown. **(C)** Summary plot depicting quantification of immunoblot band intensity from two independent experiments as in **(B)**. **(D)** J774 macrophages transfected with either control siRNA or *Dgka* siRNA were treated with LPS for 24h, and the protein expression of phospho-PKC substrates is shown by immunoblot. Relative band intensities normalized to PBS treated control are indicated below the immunoblots. **(E)** Summary plot depicting quantification of immunoblot band intensity of two independent experiments as in **(D)**.

Error bars: SD. *p<0.05, **p<0.01, ****p<0.0001; Two-way ANOVA with Tukey post-hoc test.

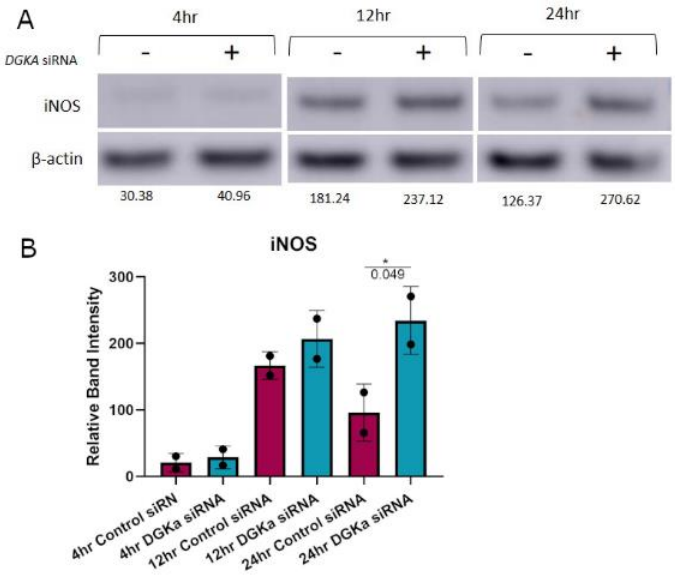


**Figure 2.4. iNOS protein expression is not evident at early time points following LPS treatment of J774 macrophages. (A)** J774 cells transfected with control or *Dgka*$^{-/-}$ siRNA were treated with LPS for 4, 12, and 24h. Subsequent immunoblots probed for iNOS were quantified with band intensities relative to PBS treated controls (not shown) indicated in text below bands. **(B)** Quantification of immunoblot iNOS band intensity from two independent experiments. Error bars: SD. *p<0.05; Ordinary One-way ANOVA with Tukey post-hoc test.

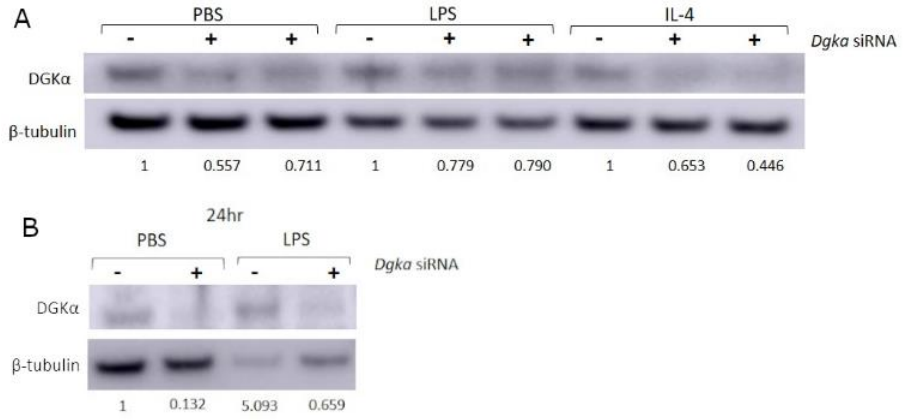


**Figure 2.5. *Dgka* knockdown by transient siRNA transfection reduces DGKα protein expression. (A, B)** Immunoblot of whole cell lysates from transfected J774 cells probed for DGKα and β-tubulin. Relative band intensity normalized to respective control siRNA transfected cells per treatment group indicated in text below bands.

*Increased sensitivity to regulation of cell cycling with* Dgka *knockout/knockdown*

Macrophages also respond to some stimuli with increased cell cycling, and proliferation of tissue-resident macrophages has been identified as a response to local inflammation and injury (103,104). We therefore tested whether BMDMs and J774 would have increased expression of a widely-used marker of cell cycling in response to LPS stimulation with *Dgka* knockout and knockdown, respectively. Ki67 expression, which has long been used in immunohistochemical staining as a marker of cell proliferation, has also been measured by qPCR to measure cell cycling (105–107). In differentiated and minimally proliferative BMDMs, only *Dgka*$^{-/-}$ cells had an increase in *Mki67* expression by qPCR in response to LPS stimulation (Figure 2.6A). *Mki67* expression levels were unchanged in WT BMDMs following addition of LPS, and there was a significant increase in *Dgka*$^{-/-}$ LPS treated BMDMs compared to WT LPS. This may suggest that loss of *Dgka* results in increased sensitivity to proliferative stimuli. In contrast, it has been reported that LPS treatment of J774 cells inhibits their proliferation (108,109). We indeed observed this in J774 cells, as indicated by a decrease in *Mki67* expression by qPCR, and found that *Dgka* knockdown increased sensitivity to this inhibition – supporting our hypothesis of increased macrophage responsiveness, albeit in this case with a negative response (Figure 2.6B). In the interest of assessing the proliferative potential of LPS-treated BMDMs, WT macrophages were treated for 48h with PBS or 500ng/mL of LPS and counted (Figure 2.7). We found that there was indeed a significant increase in cell number in the LPS-treated condition. BMDMs have a tendency to be more proliferative than macrophages derived from other sources (110), and may thus be at the proliferative end of the spectrum of variable macrophage responses to LPS.

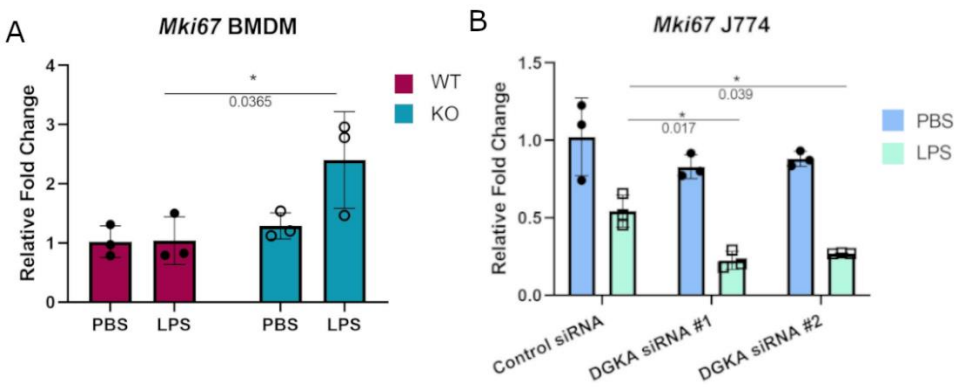


**Figure 2.6. Increased sensitivity to regulation of cell cycling with *Dgka* knockout/knockdown. (A)** qPCR analysis of *Mki67* expression in WT and *Dgkα*$^{-/-}$ BMDMs treated for 24h with 500ng/mL LPS. **(B)** J774 macrophages transfected with two different *Dgka* siRNAs were similarly assessed by qPCR for *Mki67* following LPS stimulation. Each data point in **(A)** represents an individual mouse for n=3 per group. Representative data are shown in **(B)**. Samples were normalized to PBS-treated WT or control siRNA cells. Error bars: SD. *p<0.05; Two-way ANOVA with Tukey post-hoc test.

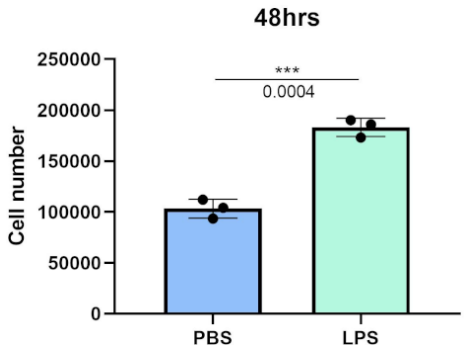


**Figure 2.7. Increased cell numbers in LPS treated BMDMs after 48h.** WT BMDMs were treated with LPS for 48 hours and show increased cell numbers compared to PBS treated controls. Error bars: SD. ***p<0.001; Student's t-test.

*Increased migration of* Dgka$^{-/-}$ *BMDMs* in vitro

In considering the potential physiological effects of increased macrophage responsiveness resulting from DGKα loss, a transwell migration assay was performed to compare the responsiveness of WT versus *Dgka*$^{-/-}$ BMDMs to a chemoattractant. When FBS-starved cells were plated on an 8μm pore membrane transwell across from 50ng/mL MCP-1, a significant increase in cell migration was observed after 18h in *Dgka*$^{-/-}$ BMDMs compared to WT (Figure 2.8).

*Smaller wounds from full-thickness cutaneous burns in* Dgka$^{-/-}$ *skin*

To investigate whether an *in vivo* pathologic process dependent on macrophages would show differences in *Dgka*$^{-/-}$ mice, we assessed differences in wound healing with a full-thickness cutaneous burn model. When cutaneous burns were induced in the flanks of study mice, *Dgka*$^{-/-}$ mouse wounds were found to be smaller than those from WT mice at 24 and 72 hours (Figure 2.9A). Blinded wound area measurements were taken at specified time-points, and initial wound sizes were comparable across all mice (Figure 2.9B). Wound area differences at day seven are not significantly different by two-way ANOVA statistical analysis. However, when we examined the ratio of wound size at day seven to initial size using the Student t-test, we observed significantly smaller wounds in the *Dgka*$^{-/-}$ mice (Figure 2.9C). No difference was observed between the ratio of wound size at day eleven to initial size when wounds were largely closed. The difference of ratios to initial size at day seven between control and the *Dgka*$^{-/-}$ mice may be due to that time frame reflecting the proliferative phase of healing (55,111) and may be related to increased macrophage responsiveness in the healing skin of *Dgka*$^{-/-}$ mice. Wound area at 24 hours post injury

increased from the initial area measurements due to expected and rapid tissue inflammation, but interestingly this increase in size was less pronounced in *Dgka*$^{-/-}$ mouse wounds.

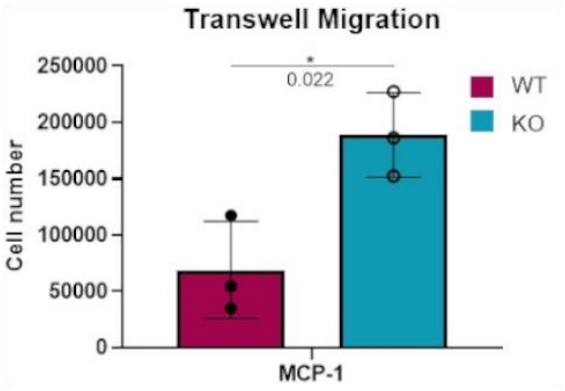


**Figure 2.8. Increased transwell migration toward MCP-1 in *Dgka*$^{-/-}$ BMDMs.** 3x10$^5$ WT and *Dgka*$^{-/-}$ BMDMs were FBS-starved for 24h, then plated into 8μm pore transwells over media containing 50ng/mL MCP-1. After 18 hours, transwells were removed and cells were counted per the manufacturer's instructions. Error bars: SD. *p<0.05; Student's t-test.

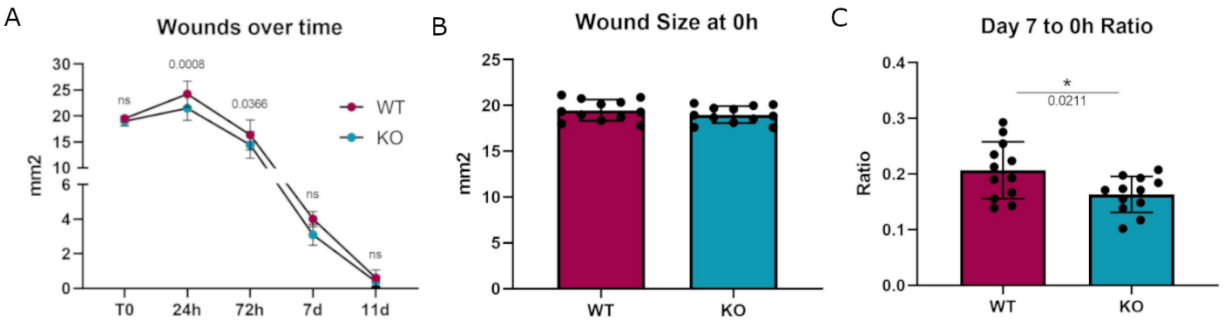


**Figure 2.9. Decreased wound size over time in *Dgka*$^{-/-}$ mice compared to WT. (A)** Area measurement of burn wounds in KO and WT mice compared over time. **(B)** Sizes of wounds from both groups are comparable at time zero. **(C)** One week post injury, wound sizes in KO mice are smaller relative to those at T0. Each data point represents a single burn, with two burns on the each of n=6 mice per group. Error bars: SD. *p<0.05; ns, not significant; Two-way ANOVA with Sidak post-hoc test **(A)**, Student's t-test **(B, C)**.

*Increased macrophage numbers at site of skin burn injury in* Dgka$^{-/-}$ *mice*

We hypothesized that the more responsive macrophages in *Dgka*$^{-/-}$ mice might be present in greater numbers at a site of tissue injury and inflammation. Flank skin was harvested from study mice from the experiments in Figure 5 at days three, seven, and fourteen and processed for immunological staining for the macrophage marker Iba1 (Figure 2.10A). Additionally, skin from the flanks of unburned mice was also collected and similarly processed for comparison. Tissue images were annotated to analyze regions of the burn, defined as the full thickness of skin below eschar or open wound, epi/dermis (consisting of both the epidermis and dermis above the panniculus carnosus), and the hypodermis (the region below the panniculus carnosus). The number of Iba1$^{+}$ stained cells in each region was compared between groups (Figure 2.11). Iba1$^{+}$ cell numbers remained higher in the epidermis and dermis of *Dgka*$^{-/-}$ mice at all three time points, yet normalized from higher cell counts at day three down to WT levels by day fourteen in the hypodermis (Figure 2.11A). Comparisons between unburned and burned skin at day three above and below the panniculus carnosus showed a significant increase in Iba1$^{+}$ cell counts in the hypodermis of *Dgka*$^{-/-}$ mice (Figure 2.11B). The hypodermis consists largely of adipose tissue that has been found to promote macrophage infiltration through secretion of macrophage migration inhibitor factor (MIF) (112). PKC has been implicated in the regulation of MIF (113,114), suggesting that DGKα inhibition leading to increased DAG signaling and subsequent PKC activation may help explain the increased number of cells positive for the macrophage marker Iba1 observed in *Dgka*$^{-/-}$ mouse hypodermis. We found a significant increase in macrophage numbers in *Dgka*$^{-/-}$ burns at day three (Figure 2.10B). This included increased Iba1$^{+}$ cells compared to both unburned *Dgka*$^{-/-}$ skin and burned

WT skin. There was no significant difference in the number of Iba1$^{+}$ cells between unburned and burned WT mice at day three. This changes by days seven and fourteen, when we observed the number of Iba1$^{+}$ cells increase in WT skin over time and catch up to numbers in the *Dgka*$^{-/-}$ skin burn area (which remained stable). This may correlate with the prominent role of macrophages in early wound healing (94). Supporting the validity of Iba1 as a macrophage marker for skin, as well as confirming expression of DGKα in macrophages, we performed immunofluorescence showing colocalization of Iba1 plus the mouse macrophage marker F4/80 or DGKα plus F4/80 in mouse skin (Figure 2.12A, B). While colocalization was not quantified, the majority of cells positive for each marker also expressed the other, and given macrophage heterogeneity, we would not expect all macrophages to express both at high levels (115).

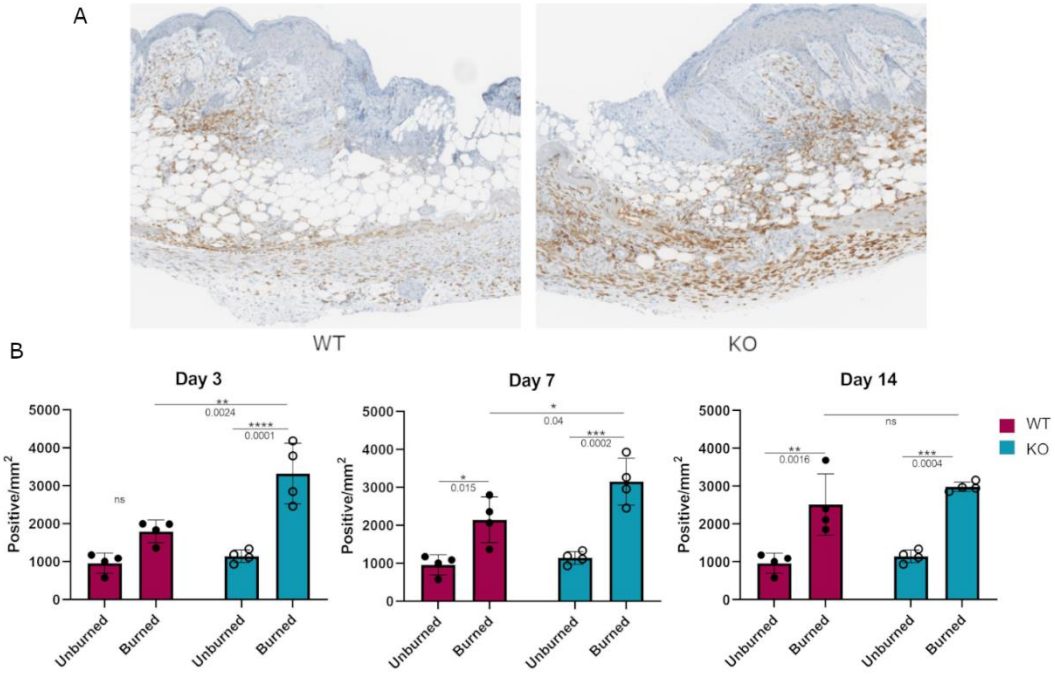


**Figure 2.10. Increased numbers of Iba1$^{+}$ macrophages in burned skin of *Dgka*$^{-/-}$ mice.** **(A)** IHC staining of Iba1$^{+}$ macrophages from excised and bisected day 3 wounds of WT and *Dgka*$^{-/-}$ mice show increased number of cells at the site of the burn. **(B)** Quantification of Iba1$^{+}$ stained cells in burned skin at three time-points in comparison to unburned skin. Each data point represents a single burn (or unburned skin region), with two burns per mouse per time-point for n=2 mice per time point. Unburned skin represent single time point used for comparison of all three burn time points. Error bars: SD. *p<0.05, **p<0.01, ***p<0.001, ****p<0.0001; ns, not significant; Two-way ANOVA.

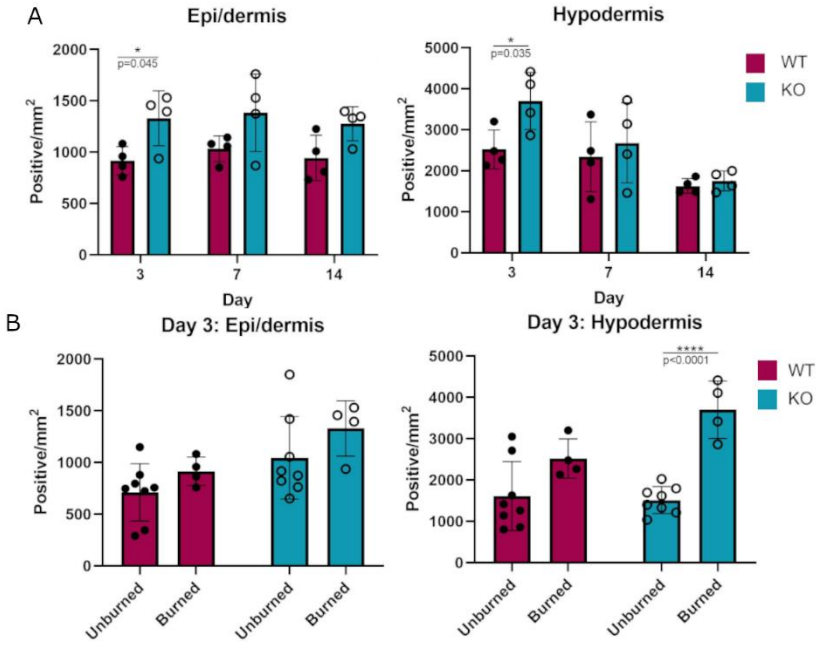


**Figure 2.11. Iba1 staining in regions of burned/unburned skin of *Dgka*$^{-/-}$ versus WT mice over time demonstrate increased macrophage numbers in *Dgka*$^{-/-}$ *mice*. (A)** In the epidermis/dermis of burned mice, the number of macrophages remains steady over time, while there is a spike in hypodermal macrophage infiltration at day 3. Which diminishes over time. **(B)** Comparison of burned vs. unburned skin do not show significant changes in macrophage numbers either in WT or KO mice at day 3. A significant increase over unburned macrophage counts is observed in the hypodermis of KO mice, not observed in WT. Each data point represents a single burn, with two burns per mouse per time-point for n=6 mice per group. Error bars: SD. *p<0.05, ****p<0.0001. Two-way ANOVA.

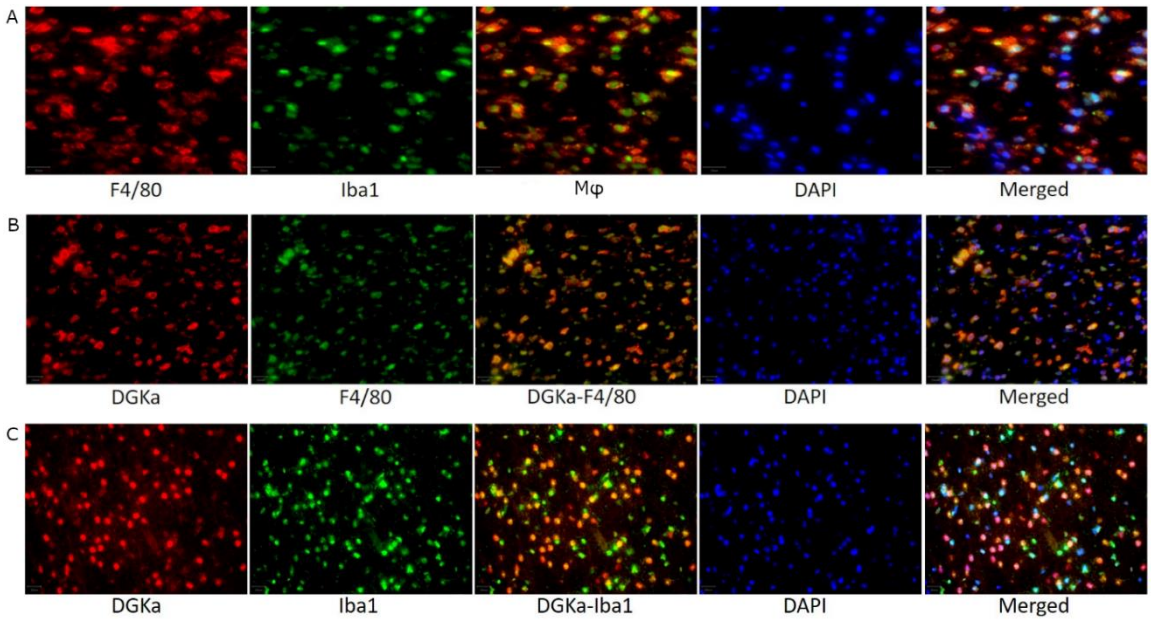


**Figure 2.12. Colocalization of F4/80 and Iba1 in skin macrophages, and DGKa colocalization with macrophages/microglia. (A)** Immunofluorescence (IF) staining and colocalization of F4/80 and Iba1 in mouse skin. **(B)** IF staining and colocalization of DGKa and F4/80 in mouse skin. **(C)** IF and colocalization of DGKa and Iba1 in mouse brain.

*Increased Iba1$^{+}$ cell numbers at the site of cortical stab injury in* Dgka$^{-/-}$ *brains*

To assess if the phenomenon of DGKα loss resulting in increased macrophage responsiveness extended to other *in vivo* injuries as well, we tested a cortical stab wound model in *Dgka*$^{-/-}$ versus WT mice. Microglia are resident macrophage analogs in the brain, and are the predominant Iba1$^{+}$ cell population at this site other than in rare pathologies such as brain tumors. Activated microglia, which are induced in situations such as brain injury and inflammation, have higher expression of Iba1 than do resting microglia. Four days after a surgical brain injury with a needle, mouse brains were collected and subsequently sectioned and stained for Iba1$^{+}$ cells. When each was compared to the uninjured contralateral brain, *Dgka*$^{-/-}$ wound areas showed significantly more Iba1$^{+}$ cells in the region than in equal wound areas from WT mouse brains, as evident in representative brain slices (Figure 2.13A) and with quantification (Figure 2.13B). Immunofluorescence confirmed colocalization of DGKα and Iba1 in brain microglia (Figure 2.12C).

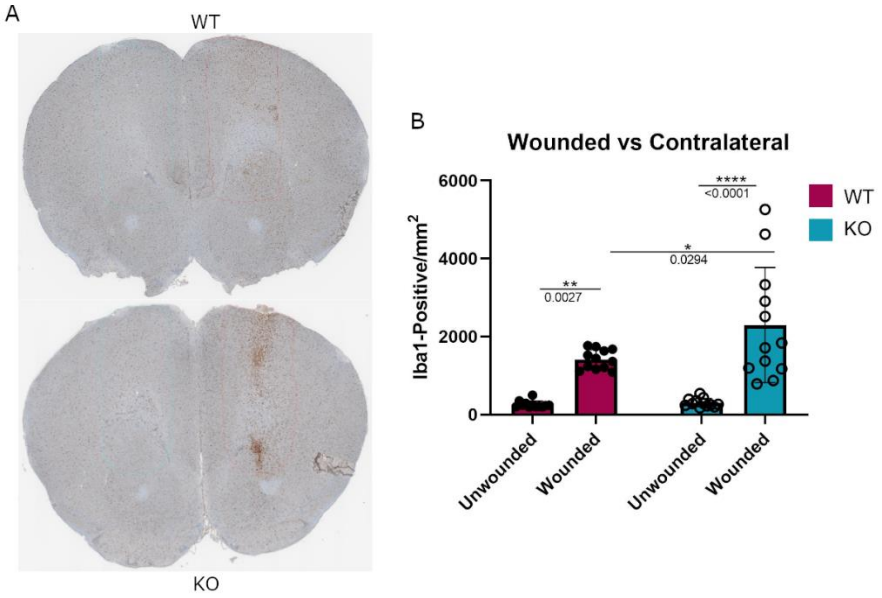


**Figure 2.13. Increased Iba1$^{+}$ cell numbers at needle track of surgically wounded *Dgka*$^{-/-}$ and WT mice in acute brain injury model. (A)** Representative cross sections highlighting needle track and unwounded contralateral cortex. **(B)** Quantification of Iba1$^{+}$ cells in the needle track demonstrates an increase in Iba1$^{+}$ cell number in wounded *Dgka*$^{-/-}$ brains versus that in the contralateral, unwounded side. Each data point represents one of four brain sections cut from the site of needle injection, from each of n=3 mice per group. Error bars: SD. *p<0.05, **p<0.01, ****p<0.0001; Two-way ANOVA with Tukey post-hoc test.

**Discussion**

With these studies, we have identified a novel mechanism by which DGKα regulates the immune system. Stimulation of BMDMs derived from WT and *Dgka*$^{-/-}$ mice with either LPS or IL-4 upregulated expression of macrophage activation markers in both groups, but consistently did so to a greater extent in the *Dgka*$^{-/-}$ mice. Baseline expression of activation markers was not enhanced by DGKα loss, but the macrophage response to stimulation was enhanced. Notably, this was not simply a shift in polarization, as the responses to both pro- and anti-inflammatory promoting stimuli were enhanced and expression of classic pro- and anti-inflammatory markers were each increased. Sensitivity of macrophages to diverse stimuli including LPS, IL-4, and the chemoattractant MCP-1 was increased in each case. Elevated expression of iNOS and arginase in response to stimuli could itself have significant implications, as each plays an important role in macrophage function. iNOS is implicated in pathogen scavenging through its production of NO and citrulline from arginine. By converting arginine to polyamine and collagen precursor ornithine, the enzyme arginase contributes to extracellular matrix production. Increasing expression of both in macrophages with the use of a DGKα inhibitor might promote host defense and tissue repair, in keeping with our results in the wound models. Confirming our findings in *Dgka* knockout mouse macrophages, transient knockdown of *Dgka* in a murine macrophage line yielded similar results. We were also able to observe an increase in PKC activation with *Dgka* knockdown, providing a potential mechanism for elevated macrophage responsiveness. We hypothesize that the increase in some DAG species with *Dgka* knockout/knockdown and the resulting increase in PKC activation boosts macrophage responsiveness to numerous stimuli, with PKC activity acting as a

rheostat controlling macrophage stimulation. In support of this, PKC has been reported as a key element in macrophage cell signaling in response to diverse inputs (48,116,117).

The promotion of macrophage cell cycling in these same stimulatory conditions, as evidenced by increased Ki67 mRNA expression in *Dgka*$^{-/-}$-derived BMDMs, presents further support for enhanced cell responsiveness; this was evident even in terminally differentiated and minimally proliferative cells. In cells with suppressed proliferation, as is the case with LPS-treated J774 macrophages, *Dgka* knockdown led to further downregulation of *Mki67* than that observed in controls. These results are the first demonstration of increased responsiveness of macrophages with *Dgka* knockout and inhibition, as previous interactions between DGKα and immune activation have been limited to T-cells and NK cells (34). Importantly, increased responsiveness was demonstrated with pure macrophage cultures such as a cell line, indicating it was not a secondary effect due to increased activity of neighboring immune cells such as T or NK cells.

Enhancements in the proliferation and migration of *Dgka* KD macrophages and KO mouse macrophages was also demonstrated through *in vitro* proliferation and migration assays. As implicated in Chapter 1, the signaling effects of increased DAG availability resulting from inhibition of DGKα may serve a role in enhanced macrophage migration due to possible downstream PKC activation. A role for PKC in macrophage motility has been demonstrated (1,48) as well as in macrophage proliferation (1). Other pathways that were considered candidates in mediating DGKα effects on proliferation (shown by *Mki67* expression in qPCR and cell count assay), are Akt, Ras, and NF-κB. Akt and Ras have both been linked to DGKα signaling through both DAG/PKC signaling (21), and in the influence

over T-cell anergic and active states (28) and therefore were considered potential mechanisms for these effects. NF-κB is a well-known regulator of cell proliferation (118–120) and DGKα has been shown to play a role in its regulation in melanoma (25). However, when IκBα and phospho-IκBα expression levels following LPS stimulation were probed by immunoblot of WT and *Dgka*$^{-/-}$ BMDM lysates, there were no observable differences between groups at 30 minutes, two, four, and twenty-four hour time points (Figure 2.14A, B). Immunoblots for phospho-Akt and phospho-Erk at sites indicating pathway activity also did not show differences in DGKα knockout/knockdown (Figure 2.14 C). Additional studies will be necessary to better assess the mechanisms underlying these observed phenotypes, and whether PKC is the primary mediator.

The brain injury model also indicated higher numbers of Iba1$^{+}$ cells in the wound area of *Dgka*$^{-/-}$ mice. While not confirmed as activated microglia, this is likely given their predominance in the region of brain injury; the result therefore suggests that the effects of *Dgka* knockout may extend to tissue-resident macrophage analogs. Our burn model sought to highlight any differences this knockout might have in the wound healing process, and to identify the cells being regulated. Our initial observation of decreased skin ulceration over subcutaneous tumors in *Dgka*$^{-/-}$ mice not only prompted us to investigate macrophage involvement, but also suggested that the response to injury might be altered in *Dgka*$^{-/-}$ mice. Our findings in the burn model supported this, with smaller burn wounds and locally increased macrophage numbers in *Dgka*$^{-/-}$ mice. Our *in vitro* findings of increased cell cycling and increased migration of *Dgka* knockout/knockdown macrophages suggest that either increased proliferation or influx of these macrophages could explain their higher numbers at wound sites. Notably, our results relied on the use of Iba1 as a well-validated

specific marker for macrophages and local macrophage analogs (121,122), The specificity of Iba1 to the microglia in the brain has also been reported (123), and evidence that phenotypic Iba1 expression is comparable to that of CD68 and F4/80 was included in establishing this macrophage/microglia marker (124). The process of healing in mouse skin is extremely efficient, making it difficult to identify anything that improves wound healing or wound size. Macrophages are at the forefront of this rapid wound closure and healing in mouse skin, and increasing their numbers and responsiveness at wound sites could have substantial implications for healing. Both our wound models support the *in vivo* relevance of this work and its potential implications for tissue injury and healing.

There was noticeable variability in the number of $Iba1^{+}$ cells in the wounded brain *Dgka*$^{-/-}$ cohort of mice, in direct contrast to the consistent staining levels in WT brains (Figure 2.13B). Though some of this may reflect a larger cell count in the KO versus WT mice, the spread of the data suggests there may be other sources of increased variability in the KO mice results. This may be the result of one or more phenomena. Genetic drift in the KO mice may have occurred, resulting from spontaneous changes in genomic DNA over generations. This has the potential to introduce phenotypic consequences such as changes in immunity (125), which in the context of this cortical stab wound variability may present itself as changes in the BBB resulting in increased permeability to immune cells in select mice. Additionally, KO mice housed in different areas might have possessed dissimilar gut microbiota as a result of being caged near other mice. This may have had an impact on brain physiology given the influence of the microbiota-gut-axis. The microbiome of the gut may influence inflammatory reactions in the brain by modulating microglia activation (126,127). There might also have been a threshold effect resulting in

either the presence or absence of a phenotypic change, as is evident in those mice with $Iba1^+$ cell numbers comparable to WT. The potential of DGKα as a therapeutic target in several cancers has been demonstrated by us and others, and more potent and specific DGKα inhibitors are in development at large pharmaceutical companies. While they are being developed as immunotherapy adjuncts to promote T and NK cell activity, our results suggest it will be critical to also determine the effects of these inhibitors on macrophages. Given that tumor-associated macrophages (TAMs) have powerful tumor-promoting effects (128,129), it must be assessed whether DGKα inhibition promotes or suppresses this pro-tumor macrophage activity; these studies are ongoing. DGKα inhibition would be especially appealing if it were able to not only directly attack cancer cells and boost T and NK cell activity, but also improve macrophage activity against cancer cells.

While these findings extend the role of DGKα in the immune system, with potential clinical implications, we acknowledge significant limitations in this study. We have not definitively identified the molecular mechanism by which *Dgka* knockout/knockdown increases responsiveness of macrophages, though this is a subject of active investigation, and our current study has suggested elevated PKC activity as a potential mediator. The relevant signaling appears to differ from the primary reported mechanism for the T cell regulation by DGKα, which has been reported to include increased Ras activity (91), given that our phosphor-Erk immunoblots did not show differences between our WT DGKα inhibited conditions, suggesting that Ras is not a significant mediator. This study is also limited to murine macrophages and mice, and it is important to extend these findings to human macrophages. Further, the WT and $Dgka^{-/-}$ mice used in this study were not derived from a single colony. The use of litter mates is valuable for ensuring both a comparable

genetic background and similar environments between treatment groups. As an example, there was a lack of segmented filamentous bacteria (SFB) noted in the Jackson Laboratory vivarium compared with those at other facilities, which was found to dramatically affect an IL-17-associated phenotype in specific pathogen-free mice (130). Potential variability introduced through differentially produced and raised mice should be eliminated in future experiments.

Taken together, these data present a novel immunologic function for DGKα as a regulator of macrophage activation. This is the first demonstration of a DGK family member suppressing macrophage function; one prior report linked DGKζ to macrophage activity in juvenile arthritis and cytokine storm mouse models (131), but it showed a stimulatory role for DGKζ opposite that we observed for DGKα. If DGKα plays a similar role in human macrophages and related cells, this extends its recently-identified role as an immune checkpoint to the innate immune system and may also have therapeutic implications. As noted above, more potent and specific DGKα inhibitors are in development as adjuncts for cancer immunotherapy, and these findings could extend their utility beyond the cancer setting. Given the role of macrophages in healing injury and combating infectious disease, DGKα inhibitors might find clinical applications in treating these pathologies as well. However, it remains to be seen how the effects of small-molecule DGKα inhibitors on macrophages will compare to those from DGKα knockdown/knockout. Furthermore, our results suggest that DGKα knockdown/knockout enhances responses to either pro-M1 or pro-M2 stimuli; in settings such as cancer where the goal is typically to enhance the M1 phenotype, it may therefore be necessary to combine DGKα inhibition with a pro-M1 agent.

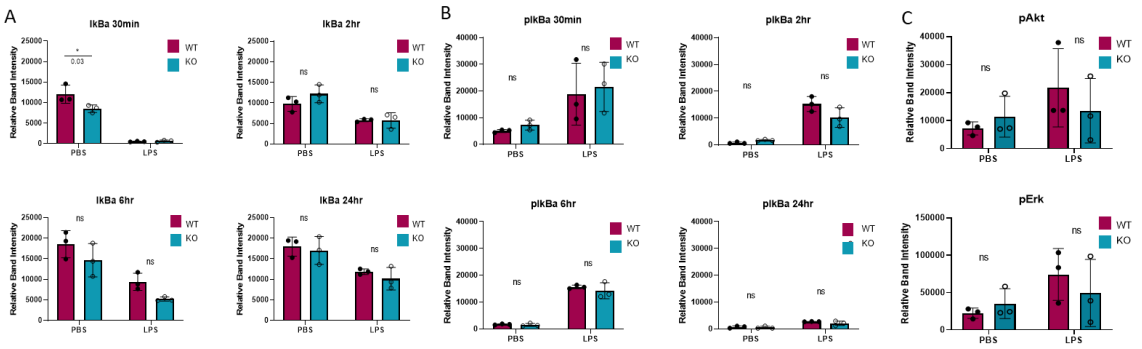


**Figure 2.14. WT and *Dgka*$^{-/-}$ BMDMs do not differ in NF-κB, Erk, and Akt activation following LPS stimulation. (A, B)** Densitometry plots depicting relative band intensities from immunoblots of IκBα, p-IκBα at thirty minutes, two hours, six hours, and 24 hours following LPS treatment of WT and *Dgka*$^{-/-}$ BMDMs. **(C)** Quantification of relative band intensities of pAkt and pErk 24 hours following LPS treatment of WT and *Dgka*$^{-/-}$ BMDMs.

# Chapter 3

## Identification of ritanserin analogs that display DGK isoform specificity

Mitchell E. Granade[1†], Laryssa C. Manigat[2†], Benjamin W. Purow[3], Thurl E. Harris[1]

Departments of [1]Pharmacology, [2]Pathology, [3]Neurology, Division of Neuro-Oncology, at the School of Medicine, University of Virginia, Charlottesville, VA, United States

**Abstract**

The diacylglycerol kinase (DGK) family of lipid enzymes catalyzes the conversion of diacylglycerol (DAG) to phosphatidic acid (PA). Both DAG and PA are lipid signaling molecules that are of notable importance in regulating cell processes such as proliferation, apoptosis, and migration. There are ten mammalian DGK enzymes that appear to have distinct biological functions. DGKα has emerged as a promising therapeutic target in numerous cancers including glioblastoma (GBM) and melanoma as treatment with small molecule DGKα inhibitors results in reduced tumor sizes and prolonged survival. Importantly, DGKα has also been identified as an immune checkpoint due to its promotion of T cell anergy, and its inhibition has been shown to improve T cell activation. There are few small molecule DGKα inhibitors currently available, and the application of existing compounds to clinical settings is hindered by species-dependent variability in potency, as well as concerns regarding isotype specificity particularly amongst other type I DGKs. In order to resolve these issues, we have screened a library of compounds structurally analogous to the DGKα inhibitor, ritanserin, in an effort to identify more potent and specific alternatives. We identified two compounds that more potently and selectively inhibit DGKα, one of which (JNJ-3790339) demonstrates similar cytotoxicity in GBM cells and safety in normal cells as ritanserin. Consistent with its inhibitor profile towards DGKα, JNJ-3790339 also demonstrated improved activation of T cells compared with ritanserin. Together our data support efforts to identify DGK isoform selective inhibitors as a mechanism to produce pharmacologically relevant cancer therapies.

## Introduction

Diacylglycerol kinases (DGKs) are a family of enzymes that phosphorylate diacylglycerol (DAG) to form phosphatidic acid (PA) (132). Both DAG and PA are active signaling molecules that are tightly regulated to influence central cell signals such as Protein Kinase C/D, Ras, mTOR, SHP1, and many others (9,89,133,134). Importantly, the elimination of DAGs via DGKs is considered the main pathway by which DAG-related signaling is attenuated (89). The mammalian family of DGK enzymes is characterized into 5 classes based on the presence of different functional domains and is comprised of 10 unique isoforms (9). While this large number of isoforms has made characterizing the biological function of these enzymes challenging, there is now mounting evidence for involvement of several of these isoforms in a variety of pathological states.

Recently, DGKα has become of particular interest in the cancer field for its dual role in both promoting cancer growth and metastasis and simultaneously suppressing T-cell activation (135). DGKα is a member of the type I isoform group that has been implicated in the progression of many types of cancers, including melanoma and glioblastoma (GBM) (19,25). DGKα has also been identified as an important checkpoint in T-cell activation, and overactive DGKα leads to the induction of T-cell anergy (15,26,30,136,137). DGKα inhibition can rescue T-cell activation, and *Dgka* knockout mice have hyperactive T-cells that are resistant to anergy (27,137). In keeping with this, there is now mounting evidence that DGKα inhibition may improve immunotherapies such as CAR-T cells (28,33,138). It is important to note that there is substantial evidence to suggest that DGKζ may be stronger than DGKα in modulating T-cells, and the use of

CRIPSR/Cas9 to knock out both DGKα and DGKζ resulted in significant improvements to antitumor activity by human CAR-T cells (33). However, DGKζ has also been shown to be important for restraining immunosuppressive regulatory T- (Treg) cells, as well as suppressing NF-κB activation, thus creating potential complications in targeting it for cancer therapy (139,140).

Interestingly, the inhibition of DGKα in cancer cells and T-cells has differential effects on the Ras pathway, decreasing and increasing its activity, respectively (141,142). Additionally, DGKα has been shown to have different substrate specificity depending on membrane morphology (143). This suggests that DGKα has context-dependent effects that vary across cells and tissues and even intracellular conditions. Further, there is evidence for specific DAG species being converted into PA in certain cell types that appears to depend on which DGK family member is predominantly expressed (144–146). It is therefore likely that the biological roles of the various DGK members are distinguished by expression profiles, context of activation, and subcellular localization. This highlights the importance of developing inhibitors with a high degree of specificity for the purposes of cancer treatment.

There are two long-established inhibitors of DGKα that have been used extensively *in vitro* in the laboratory, R59022 and R59949. While they have been important tool compounds for studying the role of DGKα in cells, they have relatively poor potency against DGKα and are more potent against serotonin receptors – likely limiting their clinical potential. With the goal of identifying other DGKα inhibitors with higher clinical potential, as well as understanding the chemical features to enable the design of superior inhibitors, we recently characterized the structurally-similar serotonin receptor antagonist

ritanserin as a DGKα inhibitor (21). The primary advantage ritanserin holds over other DGKα inhibitors lies in its characterization in clinical trials, studying it as a serotonin receptor antagonist, which have already demonstrated its safety and beneficial pharmacological properties in human patients (81). The small molecule ketanserin is a related serotonin receptor antagonist, that does not demonstrate any ability to inhibit DGKα, and is therefore used as a negative control in the following studies. The serotonin receptor inhibition of ritanserin may complicate its effects as a DGKα inhibitor. While the DGKα inhibitor R59949 has been shown to boost T-cell activity in both human and mouse T-cells, a recent report indicates that ritanserin has a similar promoting effect in human but not mouse T-cells (147). This context-dependent inconsistency may be better understood and addressed by the identification of novel and more potent and specific inhibitors for DGKα. Velnati and colleagues recently published AMB639752 as a minimal pharmacophoric structure for DGKα inhibition that lacks anti-serotonergic activity and demonstrated its selectivity over other DGK isoform types, yet its selectivity over the other type I isoforms has not been explored (148), Additionally, Liu et al. reported on their compound CU-3, which displays a high degree of potency against DGKα and significant selectivity over other isoforms (78). However, the *in vivo* safety and toxicity for this compound and related structures remains unknown. Meanwhile, some studies have begun to localize the critical features required of ritanserin and related compounds for DGK inhibition and identify the mechanism of action, however thus far no new ritanserin analogs have been identified (149,150). In this study, we screened a compound library generated by Janssen Pharmaceuticals containing compounds structurally similar to ritanserin. We sought to identify ritanserin analogs that provide higher potency against DGKα, as well as

selectivity versus other type I DGK isoforms, working toward the ultimate goal of improved DGKα inhibitors for immunotherapy and cancer treatment.

## Materials and Methods

### *Materials*

[$\gamma^{32}$P]-ATP (6000Ci/mmol) was from Perkin Elmer (Boston, MA). The lipid species used in the preparation of liposomes included: 1,2-dioleoyl-sn-glycerol (dioleoyl; 18:1, 18:1), 1,2-dioleoyl-sn-glycero-3-[phospho-L-serine] (PS), and 1,2-dioleoyl-sn-glycero-3-phosphocholine (PC). All lipids and other materials for the preparation of liposomes were from Avanti Polar Lipids (Alabaster, AL). FLAG M2 and HA antibodies, rabbit and mouse alkaline-phosphatase conjugated secondary antibodies, and ritanserin were from Sigma-Aldrich (St. Louis, MO). The β-tubulin antibody was from Cell Signaling Technology (Danvers, MA). Ketanserin was from Tocris Bioscience (Avonmouth, Bristol, UK). Anti-Human CD3, clone HIT3a and Anti-Human CD28, clone CD28.2 were obtained from BD Biosciences (San Jose, CA). All other commonly used reagents were from Sigma-Aldrich, unless otherwise indicated. All cell lines were obtained from ATCC (Rockville, MD).

### *Construction of expression plasmids*

The expression plasmids, pcDNA3-FLAG-rat-DGKα(151), pcDNA3-FLAG-rat-DGKβ(152), and pcDNA3-FLAG-rat-DGKγ were gifted to Dr. Kevin Lynch (University of Virginia, School of Medicine) by Dr. Kaoru Goto (Yamagata University, School of

Medicine) and were kindly shared with us by Dr. Lynch. The expression plasmid pCMV-rat-DGKζ-HA was a gift from Dr. Matthew Topham (University of Utah, School of Medicine).

*Overexpression of DGK isoenzymes*

To study the inhibitory activity of compounds against type I DGK isoenzymes (α, β, γ) and DGKζ, human embryonic kidney (HEK 293T) cells (ATCC, Manassas, VA) were cultured in DMEM with 5% fetal bovine serum (FBS) (Gemini Bio-Products, Foundation FBS, West Sacramento, CA) and 1% antibiotic/antimycotic (Fisher Scientific, Waltham, MA). Ten-cm plates of cells were transiently transfected with 5 µg of plasmid DNA for the appropriate plasmid expressing DGK or GFP as a control using polyethyleneimine, 25 kDa linear (Polysciences, Warrington, PA). Cells were fed with fresh media 24 hours after transfection, and 48 hours following the transfection, the cells were harvested and homogenized with a 22 G needle using 300 µL/plate of buffer A (20 mM HEPES, pH 7.2, 150 mM NaCl, 0.5 mM DTT, 0.1% Brij-35, and the protease inhibitors phenylmethylsulfonyl fluoride (PMSF), leupeptin, and pepstatin). The cell lysates were cleared by centrifugation at 16,000 g for 10 min at 4°C. The supernatant was collected and immediately stored at -80°C. For normalizing protein loading in enzyme activity assays, total protein concentration was measured using a BCA protein assay (Thermo Scientific, Waltham, MA).

*Western immunoblot analysis*

To verify the expression of the DGK isotypes, 50 µg of total protein from cell

lysates was separated by 8.75% SDS-PAGE under reducing conditions and transferred onto a polyvinylidene difluoride (PVDF) membrane (Immobilon, Darmstadt, Germany). The membrane was blocked by incubation in Tris-buffered saline with detergent Tween 20 (TBST) containing 10% (w/v) dried milk for 1 hour at room temperature. The TBST contained the following: 50 mM Tris, 150 mM NaCl, and 0.05% (w:v) Tween 20, pH 7.4. The membrane was incubated with monoclonal M2 anti-FLAG antibody (Sigma, F1804) or monoclonal anti-HA (Sigma, H6908) antibody (1:1000) in TBST, at room temperature for 2 hours with gentle agitation. The membranes were then washed with three 5-minute washes with TBST and gentle agitation, and incubated with alkaline phosphatase-conjugated mouse (Sigma, A3562) or rabbit (Sigma, A3687) secondary antibody (1:10,000) diluted in TBST with 2% (w/v) dried milk, for 1 h at room temperature. After three 15 min washes with TBST, the membrane was briefly incubated in chemiluminescent alkaline phosphatase substrate, Applied Biosystems (Poster City, CA). The immunoreactivity was detected using a Fuji LAS 4000. For a loading control, the membranes were stripped using a mild stripping buffer (1.5% (w/v) glycine, pH 2.2, 1% (v/v) Tween 20, and 0.1% (w/v) SDS), blocked again for 1 hour, and incubated with anti-β-tubulin followed by rabbit secondary antibody and chemiluminescent detection as above.

*Preparation of liposomes*

The preparation of liposomes was modified from our previously reported methods.(21,153) Briefly, PC and DAG were dissolved in $CHCl_3$, and PC was dissolved in 10% isopropyl alcohol in $CHCl_3$; all lipids were combined, and dried under $N_2$ gas to remove all solvent. The total liposomal concentration of lipids was 10 mol% DAG, 20

mol% PS, and 70 mol% PC. The lipids were hydrated to 10 mM in buffer B (50 mM (3-(N-morpholino)propanesulfonic acid) (MOPS), pH 7.5, 100 mM NaCl, and 5 mM $MgCl_2$). The lipids were then subjected to five freeze-thaw cycles in liquid nitrogen, followed by extrusion through a 100 nm polycarbonate filter 11 times to generate liposomes with an average diameter of 100 nm.

*Kinase assays*

The protocol for measurement of DGK activity was modified from our previously reported methods.(21,153) Briefly, the reactions contained buffer B, 0.1 mM $CaCl_2$, 1 mM dithiothreitol (DTT), cell lysate expressing the appropriate DGK or GFP control, and 2 mM lipids. Because enzyme activity can vary between separate preparations due to differences in transfection efficiency, the total protein amount of cell lysate used in each assay was always confirmed to exhibit DGK activity that falls within the linear range. For primary screening of DGKα, 2.8 µg of total protein was used. Five µg of total protein was used for all other corresponding DGK assays. Total protein amount for GFP control was always matched for each DGK. The reactions were initiated by the addition of 10 µL of 10 mM ATP spiked with [$\gamma^{32}$P]-ATP to a final volume of 100 µL, and allowed to proceed for 20 min at 30°C. All reactions were terminated with the addition of 0.5 ml of methanol with 0.1 N HCl, followed by 1 ml of ethyl acetate. To facilitate separation of the organic phase, 1 mL of 1 M $MgCl_2$ was added and the solution thoroughly vortexed. To measure the incorporation of [$^{32}$P] into DAG, 0.5 ml of the organic phase was removed, and the radioactivity was measured using a scintillation counter. The activities of lysates overexpressing DGKs (signal) were normalized to activities of lysates expressing only GFP

(background). The specific activities of lysates with GFP represented less than 10% of the signal for all DGKs and were not detectably altered by the presence of inhibitors or DMSO. The specific activity for each assay was calculated as nmol of product formed per minute per mg of total protein. All kinase assays were performed in triplicate or as indicated for inhibitor screening.

*Inhibitor Screening*

For primary screening of potential inhibitor compounds against DGKα, compounds were dissolved in DMSO, diluted in buffer B, and added directly to kinase assays for a final concentration of 50 μM. The final concentration of DMSO in the reactions was 0.5% (v/v) and did not affect the enzyme activity; DMSO was used as a vehicle control for all screening runs. Screening assays were allowed to equilibrate for 5 min at room temperature following the addition of compound before being initiated with ATP. All compounds were screened in duplicate, and 50 μM ritanserin was used as an internal positive control for all screening runs. All hits were rescreened using the same protocol with a minimum of three biological replicates for confirmation. Inhibitory activity of compounds against other DGKs was similarly tested by diluting the compounds and adding directly to kinase assays for the appropriate $IC_{50}$ concentration, with 5 min for equilibration.

*Dose Response for $IC_{50}$ Determination*

To determine the IC50 value for ritanserin and all candidate compounds, a 5-point dose response curve was performed with each compound ranging in concentration from 100 nM to 500 μM. Measurements for each dose with all compounds were made with three

independent experiments containing two technical replicates each.

*Cell culture and cytotoxicity assay*

Human Jurkat T-cells, A375 melanoma cell line, and U251 GBM cell line were cultured in DMEM with 10% FBS and 1% penicillin-streptomycin. Cells were plated in 96-well plates and treated in triplicate with 5, 15, 25, and 40 μM of analog compounds or equivalent amounts of DMSO vehicle control. After 48 h, alamarBlue assay was performed to measure cell viability (Bio-Rad, #BUF012B).

*Primary T-cell harvest and activation assay*

Complete RPMI (cRPMI) was prepared with 500 mL RPMI 1640 (Gibco, #11875093), 10% FBS, 1% non-essential amino acids, 1% pen/strep, 1% pyruvate, and 0.1% 2-ME. Spleens from two C57BL/6J and two *DGKα*$^{-/-}$ mice (10-week) were harvested into 2 mL cRPMI, then dissociated through a 40 μm cell strainer. The cell suspension was centrifuged at 1200 rpm for 5 min, then treated with RBC lysis buffer (0.83% [w/v] $NH_4Cl$). Cells were pelleted once more and suspended in cRPMI for further T cell isolation with Invitrogen Dynabeads Untouched Mouse T-Cells Kit (#11413D) according to the manufacturer's protocols. Isolated T-cells were stimulated with 1 μg/mL functional antibodies against CD3/CD28 and simultaneously incubated with 5 μM analogs for 6 hours prior to harvest for subsequent qPCR analysis. Human Jurkat T cells were also similarly stimulated and treated with ritanserin analogs for downstream processing.

*Real-Time qPCR*

RNA preparation was performed using Qiagen RNeasy Mini Kit, and cDNA synthesis accomplished with Qiagen QuantiTect Reverse Transcription kit according to the manufacturer's instructions. Real-time qPCR was performed using Applied Biosystems Power SYBR Green PCR Master Mix. Expression of target mRNA was normalized to ribosomal 18S RNA and calculated using the $2^{-\Delta\Delta CT}$ method. Primers used were Mouse 18S Forward: GTAACCCGTTGAACCCCATT, Reverse: CCATCCAATCGGTAGTAGCG; CD69 (PrimerBank ID 221554485c1) Forward: CCCTTGGGCTGTGTTAATAGTG, Reverse: AACTTCTCGTACAAGCCTGGG. CD69 primer was sourced from the PrimerBank of the Center for Computational and Integrative Biology of Massachusetts General Hospital and Harvard University.(95–97) Quantification of target amplification was quantified as the relative fold change above DMSO-treated WT controls.

*Statistical Analyses*

Comparisons between groups were analyzed by multiple Student's t-tests without correction for multiple comparisons when appropriate, and by one-way Analysis of Variance (ANOVA) with Dunnett's multiple comparisons test as appropriate and as indicated in the figure legends. After performing dose response experiments, a GraphPad Prism function called log [inhibitor] vs. response -- Variable slope (four parameters) was used to calculate $IC_{50}$ values. All values are reported as the mean of triplicate values ± SD. Data shown are representative of at least three independent experiments, except Figure 13 where independent values are shown. Significance was set to $p < 0.05$, and p-values are reported as indicated in the figure legends.

For selection of hits from our primary screen, strictly standardized mean difference

(SSMD) was calculated as an estimate of unpaired replicates with unequal variance. Hits were selected based on the criteria of SSMD ≤ -5 and $Log_{10}$ (Fold-change) < -0.6.

## Results

*Ritanserin lacks specificity for DGKα over other type I DGK isoforms*

The serotonin receptor antagonist ritanserin and the analogs R59022 and R59949 have shown antitumor efficacy both *in vitro* and *in vivo* in multiple cancers, with demonstrated mediation through DGKα (19,22,154). In characterizing the inhibitory activity of ritanserin against the other type I DGK isoforms, DGKβ and DGKγ, we overexpressed FLAG-tagged DGK isoform constructs and confirmed their expression in HEK 293T cell lysates (Figure 3.1A). To validate subsequent kinase assays, the linear range of activity was identified for each enzyme (Figure 3.1B), alongside a GFP control, to ensure that the intensity of enzyme activity would be proportional to the concentration of enzyme assayed.

At the chosen 5 µg of total protein, we determined the relative incorporation of [$^{32}$P] into our DAG liposomes with each DGK type I isoform (Figure 3.1C), with DGKα/γ showing the highest enzyme activity. With the introduction of ritanserin to determine level of inhibition, we found that at 27.4 µM, ritanserin significantly inhibits the activity of all three isoforms, relative to DMSO control treatment (Figure 3.1D). The greatest inhibitory efficacy was seen with DGKα (>60%), but substantial inhibition was also observed in DGKγ (~48%), and modest inhibition in DGKβ (~21%). This lack of specificity amongst the individual type I isoforms is contrasted by near-total inactivity against other DGK

isoforms such as δ, θ, and ι, and suggests that structural features shared between the isoforms may contribute to their potential for inhibition by ritanserin (21).

*Screen of ritanserin analog library points to novel DGKα small-molecule inhibitors*

To identify additional compounds with improved selectivity for DGKα over other type I isoforms, we screened a selected library of 188 compounds with a potential for inhibition of DGKα. The structure of ritanserin consists of two -4-fluoro-benzene rings, a thiazolopyrimidine group, and a protonatable nitrogen which is contained within a piperidine (Figure 3.2A). Having been developed as a serotonin receptor antagonist, the central nitrogen of ritanserin is known to be key for its anti-serotonergic function, but has also been found to be necessary for inhibitory activity towards DGKα (148). The library of compounds was provided to us by Janssen Pharmaceuticals and was built based on their structural similarity to ritanserin.

Using our radiolabeled kinase assay, we screened all 188 ritanserin analogs for inhibitory effects against DGKα enzyme activity, normalized to vehicle. To identify compounds of greatest interest, we established criteria based on the strictly standardized mean difference (SSMD, < -5) and log fold change (< -0.6), and identified 30 compounds that met these thresholds for all three criteria (Figure 3.2B, Table 1). When select hits were rescreened alongside ritanserin, nine compounds demonstrated comparable or improved inhibition of DGKα; however, only seven of these compounds had available structural information and were thus chosen for further testing (Figure 3.2C, E-K). Notably, two of these compounds were more similar in structure to the DGKα inhibitor R59949 than ritanserin (Figure 3.2D, H, K).

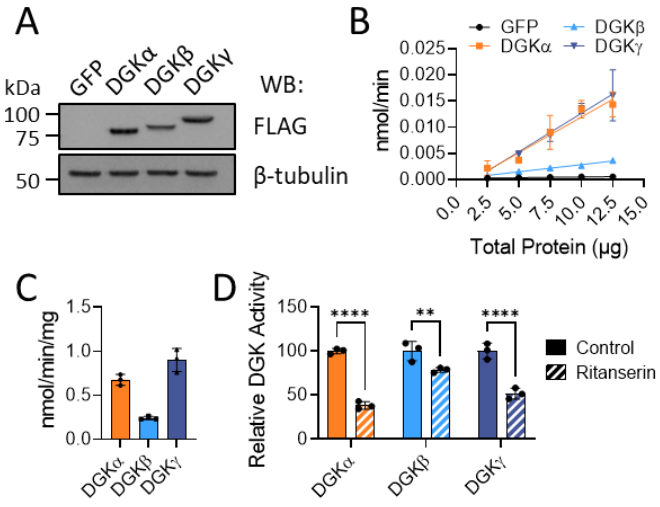


**Figure 3.1. Ritanserin exhibits significant inhibition of all type I DGK isoforms. (A)** GFP control or indicated FLAG-tagged DGK constructs were expressed in HEK-293T cells, harvested 48 hours after transfection, and expression checked by immunoblot for the FLAG tag at the appropriate molecular weight. **(B)** Enzyme activity as a function of the protein concentration in cell lysates expressing GFP or indicated DGK and measured as nmol of ATP incorporation into PA per minute. **(C)** Enzyme activity of type I DGKs when assayed with 5 µg total protein of cell lysate. **(D)** Relative DGK activity with or without ritanserin for type I DGK isoforms. The concentration of ritanserin used in each assay was the IC50 of ritanserin for DGKα (27.4 µM) compared to DMSO control. *$p<0.05$, **$p<0.01$, ***$p<0.001$

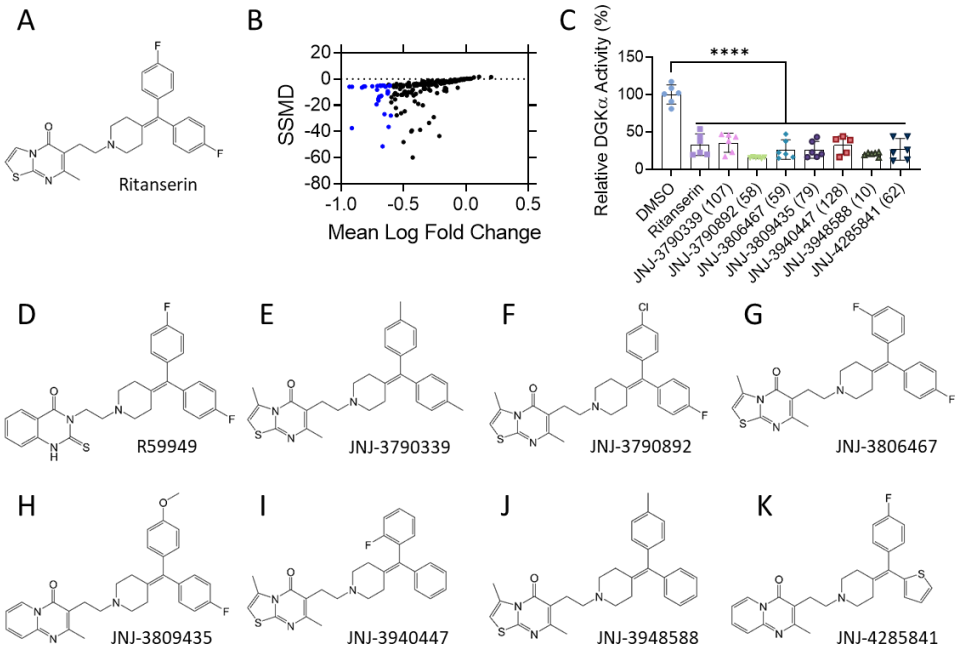


**Figure 3.2. Screening a library of ritanserin analogues reveals additional inhibitors against DGKα. (A)** Molecular structure of ritanserin. **(B)** Dual-flashlight plot for all compounds screened against DGKα. Blue points indicate compounds that met the selection criteria for strictly standardized mean difference (SSMD) and mean log fold change. **(C)** Relative DGKα activity in confirmation screen. FLAG-tagged DGKα was overexpressed in HEK-293T cells, and DGK activity in 5 µg of protein lysates was measured. DMSO concentration was 0.5% in all assays and all compounds at 50 µM. **(D)** Molecular structure of the DGK inhibitor R59949. (E-K) Molecular structures for all identified compounds as indicated. ****p<0.0001

| Compound (Library #) | SSMD | Log Fold Change |
|---|---|---|
| 3 | -13.47 | -0.70 |
| 10 | -15.15 | -0.70 |
| 29 | -13.24 | -0.68 |
| 32 | -11.19 | -0.63 |
| 33 | -10.17 | -0.63 |
| 34 | -12.81 | -0.68 |
| 38 | -8.30 | -0.71 |
| 39 | -9.41 | -0.63 |
| 52 | -5.12 | -0.66 |
| 53 | -5.59 | -0.75 |
| 54 | -5.04 | -0.69 |
| 55 | -5.38 | -0.68 |
| 56 | -5.99 | -0.93 |
| 58 | -5.75 | -0.82 |
| 59 | -5.73 | -0.81 |
| 61 | -5.03 | -0.61 |
| 62 | -5.96 | -0.91 |
| 63 | -5.38 | -0.71 |
| 79 | -5.01 | -0.67 |
| 106 | -28.00 | -0.60 |
| 107 | -16.45 | -0.70 |
| 110 | -26.87 | -0.65 |
| 120 | -37.52 | -0.92 |
| 125 | -51.47 | -0.67 |
| 126 | -36.56 | -0.62 |
| 128 | -19.41 | -0.72 |
| 136 | -5.20 | -0.61 |
| 139 | -6.61 | -0.83 |
| 140 | -5.18 | -0.61 |
| 141 | -5.97 | -0.64 |

**Table 1. Candidate compounds resulting from the primary screening campaign.**

*Specificity of ritanserin analogs for DGKα*

Based on our initial two screens assessing the ritanserin analogs for potency against DGKα, we next set out to determine the specificity of these compounds for DGKα over the other type I DGK isoforms. We first performed dose response experiments to determine the $IC_{50}$ and $IC_{90}$ values for the seven candidate compounds towards DGKα resulting from the screen (Table 2). We tested these compounds on DGKβ and DGKγ at their determined $IC_{50}$ and $IC_{90}$ values towards DGKα. Two were identified to have very limited inhibitory activity against the DGK type I isoforms β and γ. Thus, while ritanserin demonstrated a degree of inhibition of DGKβ/γ, as seen in Figure 3.1D, compounds JNJ-3790339 and JNJ-3940447 at $IC_{50}$ did not affect DGKβ/γ activity (Figure 3.3), demonstrating greater specificity of these compounds towards DGKα.

We further sought to evaluate the specificity of these compounds by determining their inhibition of another DGK subtype. We chose the type IV DGKζ, due to its known role in the suppression of Treg cells and NF-κB activation. Type IV DGKs are distinct from type I in that they lack the N-terminal RVH and EF Hand motifs which cooperate to control calcium-dependent enzyme activation (155). They additionally have PDZ-binding and ankyrin domains involved in protein-protein interactions, as well as a MARCKS domain. After confirming expression of DGKζ in our HEK-293T cell lysates, we identified a protein concentration within the linear range of activity (Figure 3.4A, B) and measured activity following treatment with ritanserin, compound JNJ-3790339, and compound JNJ-3940447. Neither ritanserin nor its analogs showed any inhibitory effect on DGKζ at $IC_{50}$ (Figure 3.4C).

We tested all of our candidate compounds to assess inhibitory activity against

DGKβ/γ/ζ, at the $IC_{50}$ as determined for DGKα (Table 3). Notably, ritanserin shows no activity against DGKζ at either concentration, suggesting type I specificity, favoring DGKα. These data indicate the potential to identify potent DGKα specific inhibitors from a catalog of ritanserin-like compounds. Additional structural information may be beneficial in characterizing structural motifs relevant to DGK inhibition.

| Compound | $IC_{50}$ (μM) | $IC_{90}$ (μM) |
|---|---|---|
| Ritanserin | 27.4 | 123.3 |
| Ketanserin | - | - |
| JNJ-3790339 (107) | 9.6 | 429.8 |
| JNJ-3790892 (58) | 25.5 | 260.2 |
| JNJ-3806467 (59) | 32.9 | 223.9 |
| JNJ-3809435 (79) | 142 | >1 mM |
| JNJ-3940447 (128) | 17.5 | 387.2 |
| JNJ-3948588 (10) | 33.0 | 262.3 |
| JNJ-4285841 (62) | 88.4 | >1 mM |

**Table 2. DGKα $IC_{50}$ and $IC_{90}$ values for candidate compounds.**

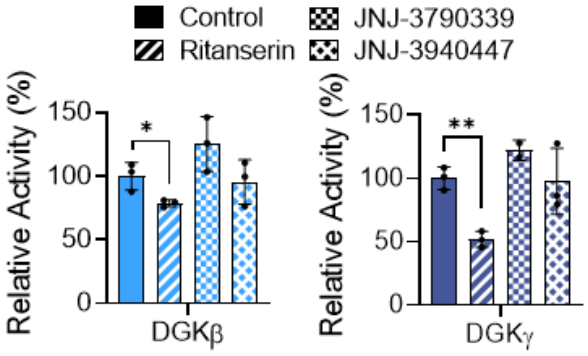


**Figure 3.3. Screening candidates do not exhibit inhibition against other type I DGK isoforms.** Inhibitory activity for ritanserin and top candidate compounds against DGKβ and DGKγ at their DGKα $IC_{50}$ as indicated in Table 2. *p<0.05, **p<0.01

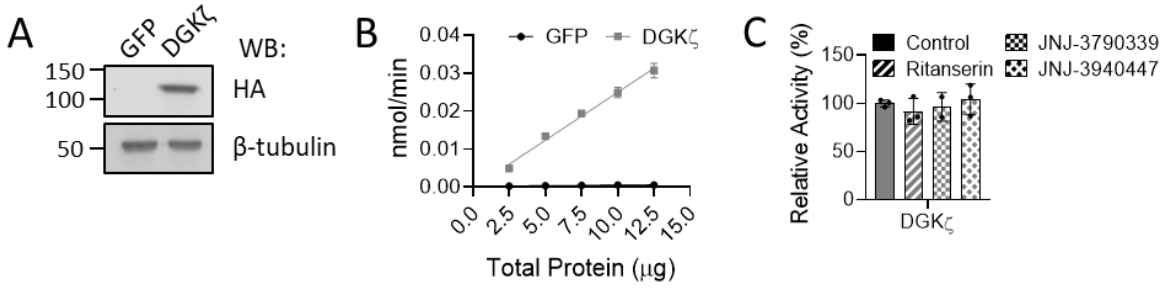


**Figure 3.4. Ritanserin analogues do not significantly inhibit DGKζ. (A)** GFP control or HA-tagged DGKζ constructs were expressed in HEK-293T cells, harvested 48 hours after transfection, and expression checked by immunoblot for the HA tag at the appropriate molecular weight. **(B)** Enzyme activity for cell lysate with overexpressed DGKζ was tested for the range of linearity prior to subsequent experiments. **(C)** Inhibitory activity for ritanserin and lead candidate compounds against DGKζ.

| | DGKβ | | DGKγ | | DGKζ | |
|---|---|---|---|---|---|---|
| Compound | Relative Activity | p-value | Relative Activity | p-value | Relative Activity | p-value |
| Ritanserin | 0.79 | 0.6721 | 0.52 | 0.0404 | 0.92 | 0.9994 |
| Ketanserin | 1.08 | 0.9972 | 0.91 | 0.9939 | 0.93 | 0.9996 |
| JNJ-3790339 | 1.25 | 0.5073 | 1.42 | 0.0915 | 1.38 | 0.491 |
| JNJ-3790892 | 0.93 | 0.9994 | 0.56 | 0.0699 | 1.00 | >0.9999 |
| JNJ-3806467 | 1.09 | 0.9936 | 0.71 | 0.3568 | 0.81 | 0.9579 |
| JNJ-3809435 | 1.14 | 0.9488 | 0.52 | 0.0461 | 0.75 | 0.8425 |
| JNJ-3940447 | 0.95 | 0.9996 | 0.98 | 0.9998 | 1.04 | 0.9997 |
| JNJ-3948588 | 1.05 | 0.9996 | 0.75 | 0.5154 | 0.91 | 0.9994 |
| JNJ-4285841 | 0.62 | 0.139 | 0.33 | 0.0037 | 0.73 | 0.7975 |

**Table 3. Specificity at the $IC_{50}$ for all screening candidates.**

*Induction of apoptosis in cancer cells by ritanserin analogs*

One of the promising uses for DGKα small-molecule inhibition is in the treatment of various cancers for which targeting DGKα has demonstrated cytotoxicity. To determine if our newly identified inhibitors show the same cytotoxic effects against cancer cells *in vitro* and *in vivo* as DGKα inhibition has previously shown (19), we performed dose response assays with the human melanoma cell line A375 and the GBM cell line U251 using ritanserin, ketanserin, JNJ-3790339, JNJ-3940447, and vehicle (Figure 3.5A). We also tested them with the human-derived Jurkat T-cell leukemia line. Ritanserin and JNJ-3790339 treatment resulted in significant loss in cell viability at 15 μM of compound in both the A375 and U251 cell lines (Figure 3.5B), and at 25 μM both ritanserin and JNJ-3790339 had largely ablated survival in both cancer cell lines with limited cytotoxicity in the Jurkat T-cells. JNJ-3940447 did not achieve similar levels of cytotoxicity in A375 and U251 until 40 μM. Even at 40 μM, both JNJ-3940447 and ritanserin showed limited cytotoxicity in Jurkat cells, while JNJ-3790339 showed no more cytotoxicity than vehicle control.

*Activation of primary WT and* DGKα$^{-/-}$ *T-cells*

Given the demonstrated ability of the small molecule DGKα inhibitors to promote T-cell activation (147) we investigated whether the inhibitors identified by this screen might also possess this immune-stimulating ability. Human Jurkat T-cells were costimulated with functional CD3/CD28 antibodies alongside ritanserin, ketanserin, or the analogs identified by our screen. The most potent inhibitor we identified, JNJ-3790339, displayed the highest activation response and was significantly higher than activation in

the presence of DMSO (Figure 3.6A). The negative control ketanserin was also included in the assay, as it is structurally similar to ritanserin and its analogs, and functions as a serotonin inhibitor but not as a DGKα inhibitor. As expected, ketanserin did not result in increased expression of CD69.

T-cells isolated from the spleens of WT and *DGKα*$^{-/-}$ mice were similarly costimulated alongside three analogs from our initial screen identified as the most potent inhibitors of DGKα (Figure 3.6B). JNJ-3790339 and JNJ-3790892 resulted in enhanced T-cell activation in Jurkat T-cell leukemia cells and primary murine T-cells, respectively. This effect was lost in treated *DGKα*$^{-/-}$ cells. JNJ-3790339 and JNJ-3790892 had among the lowest $IC_{50}$ demonstrated by enzyme activity assay, while compound JNJ-3940447 with the second-lowest $IC_{50}$ did not produce such an activating effect. The imperfect correlation between DGKα $IC_{50}$ and T-cell activation suggests that there may be additional specific properties of these drugs that modulate their T-cell activation, such as permeability and retention in T-cells. Ritanserin was not used in experiments with primary murine T-cells due to its previously demonstrated inability to activate murine T-cells, but the DGKα inhibitor R59949 was used instead (147). In these settings the two ritanserin analogs JNJ-3790339 and JNJ-3790892 possess greater potential to stimulate T-cells than ritanserin and R59949 (Figure 3.6A, B). Future experiments will introduce earlier time points to investigate the upregulation of CD69 mRNA expression, which plateaus and declines between four to six hours (156). It will also be important to determine what effect the higher cytotoxic concentrations of compound have on CD69 expression, as this may relate to whether single concentrations of drug may simultaneously stimulate T-cells and have cytotoxicity for cancer cells.

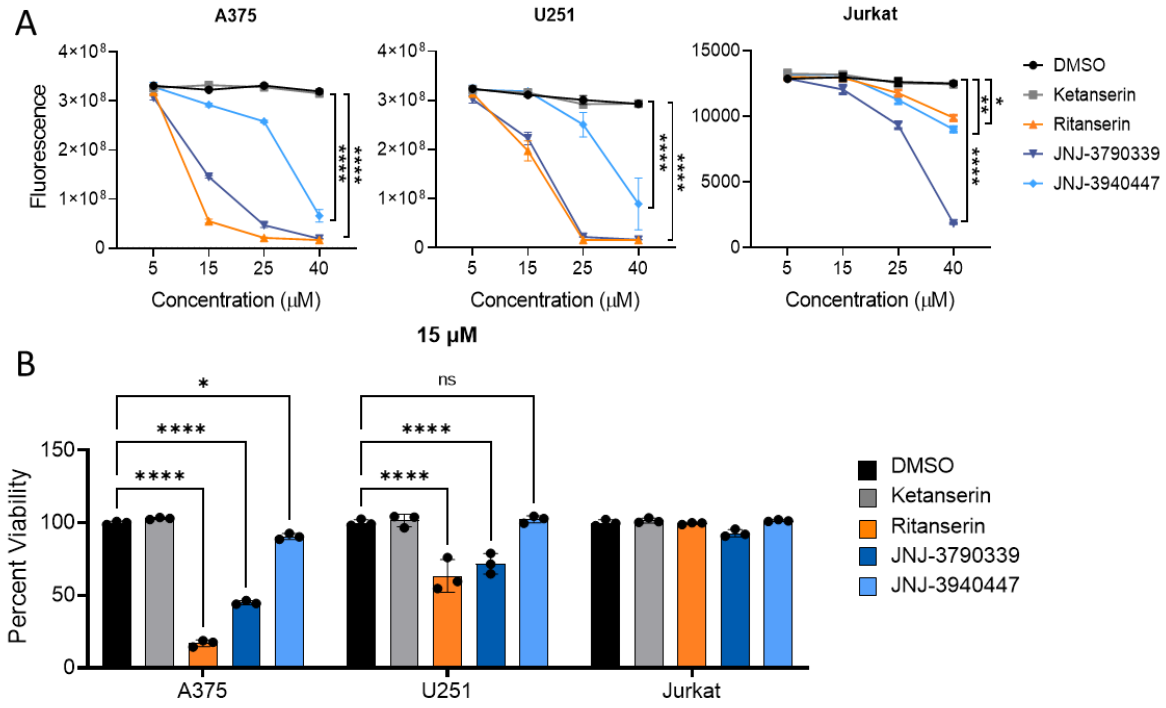


**Figure 3.5. Demonstrated cytotoxic efficacy of ritanserin and JNJ-3790339 and JNJ-3940447 against human melanoma, GBM, and T-cell leukemia cell lines. (A)** Dose response curve for cytotoxicity that measures alamarBlue fluorescence from A375, U251, and Jurkat cells treated with vehicle (DMSO), and the indicated concentrations of ketanserin, ritanserin, and analog compounds JNJ-3790339 and JNJ-3940447. **(B)** Percent viability of cells treated with the same compounds as in **(A)** at 15 μM shows high cell viability in Jurkat T-cells treated with ritanserin and JNJ-2790229. *p<0.05, **p<0.01, ****p<0.0001, ns, not significant

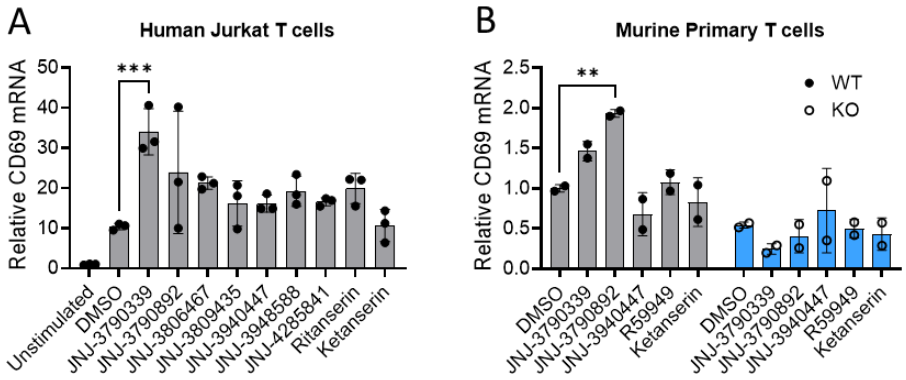


**Figure 3.6. Ritanserin analogs JNJ-3790339 and JNJ-3790892 promote activation of primary murine T-cells. (A)** Human-derived Jurkat T-cell line was unstimulated, or stimulated with 1 μg/mL functional antibodies against CD3/CD28 and treated for 6 hours with indicated ritanserin analogs at 5 μM. T-cell activation was assessed by qPCR measurement of CD69 mRNA levels. **(B)** Primary isolated murine T-cells from WT and *DGKα*$^{-/-}$ (KO) mice were stimulated and treated for 6 hours with indicated inhibitors and T-cell activation assessed by CD69 expression as described in **(A)**. **p<0.01, ***p<0.001

**Discussion**

The large number of mammalian DGK isoforms and apparent lack of substrate specificity has made deciphering the individual roles of the different isoforms into an immensely complex task. Having access to selective and specific pharmacological compounds that modulate the activity of individual DGK isoforms is crucial to interrogating the physiological roles of these enzymes. DGKα is a member of the type I isoform group of DGKs that has been implicated in a number of pathological conditions, including glioblastoma and melanoma, and represents a promising therapeutic target (135). The other type I DGKs, β and γ, possess the same structural domains as DGKα, most notably calcium-binding EF hand motifs which enhance their activity in the presence of calcium. Their structural and functional similarity highlight the importance of identifying specific and selective inhibitors for DGKα. Liu et al have reported on a DGKα inhibitor, CU-3, with a novel scaffold that proved to be both potent and highly selective over all other DGK isoforms and was efficacious in improving the activation of Jurkat T cells assayed for IL-2 production measured by cDNA PCR amplification (78). Velnati and colleagues recently identified a novel pharmacophoric structure for inhibiting DGKα with the compound AMB639752, which has improved selectivity for type I DGK isoforms and eliminates anti-serotonergic activity that is a significant potential limitation of the ritanserin analogues (148). However, the selectivity of AMB639752 for DGKα over other type I isoforms is unknown, and both scaffolds lack indications of *in vivo* activity.

The identification of ritanserin as a DGKα inhibitor demonstrates the value in repurposing therapeutics, as previous clinical trial data has already shown that it is safe and

well tolerated in human patients (81). Initially designed as a serotonin receptor antagonist, its ability to inhibit DGKα suggested its potential for use in the treatment of certain cancers such as glioblastoma and melanoma(21). While ritanserin was found to effectively inhibit DGKα and demonstrate cytotoxic effects in cancer cells, its potency was not a great improvement beyond those of the previously identified DGKα inhibitors R59022 and R59949. Furthermore, in this study we found that while ritanserin has a high degree of specificity for type I DGK isoforms (21), there is little specificity between the type I isoforms (Figure 3.1). By screening a library of 188 ritanserin analogs initially created by Janssen Pharmaceuticals, we were able to identify 15 additional compounds with significant inhibitory activity against DGKα (Figure 3.2, Table 1). We found that two of these compounds in particular, JNJ-3790339 and JNJ-3940447, demonstrated a high degree of selectivity for DGKα over the other type I DGKs (Figure 3.3). We also investigated the activity of these inhibitors on a DGK from an alternate subtype, the type IV DGKζ, due to its known role in promoting T-cell anergy, a function it shares with DGKα. We found that neither ritanserin nor the analogs JNJ-3970339 and JNJ-3940447 demonstrated any significant inhibitory activity with DGKζ (Figure 3.4). It is possible a compound with dual inhibitory functions against DGKα and DGKζ may have higher therapeutic potential and thus it may be worth further investigating the activity of these ritanserin analogs against DGKζ. Even when we tested these compounds at their $IC_{90}$, JNJ-3790339 maintained a high specificity for DGKα and JNJ-3940447 demonstrated only moderate activity against DGKζ and a downward trend in DGKγ activity that was not statistically significant (~68% inhibition against DGKα vs ~31% against DGKs γ and ζ, not shown). Unfortunately, it remains unclear how the minor differences in the structures

of these two compounds yield this higher selectivity. There are currently no crystal structures for any of the type I DGKs, and there was not enough accessible information on structures within this library to perform a structure-activity relationship analysis.

The enhanced potency and selectivity of JNJ-3790339 and JNJ-3940447, however, supported further investigation into their therapeutic potential. GBM is the most common primary cancer of the central nervous system and makes up >51% of all gliomas (157). It is the most aggressive primary brain tumor with a median survival of 15 months and a 5-year survival rate of less than 5% (158). GBM is extremely resistant to treatment, even with surgical resection followed by concurrent radiation and chemotherapy, highlighting the need for novel therapeutics. We have previously shown that the overexpression of DGKα found in GBM cells suppresses cAMP levels to drive the key oncogenic pathways mTOR and HIF-1α (19). Melanoma is another notoriously aggressive and invasive cancer, and while the advent of immunotherapy has resulted in improved patient outcomes over the past decade, there has been demonstrated potential for the efficacy of adjuvant DGKα inhibition (19). Inhibition of DGKα with ritanserin or its analog R59022 results in toxicity to GBM cell lines that does not occur in non-cancer derived cell lines (19,22). We tested JNJ-3790339 and JNJ-3940447 for their ability to induce cell death within the melanoma cell line A375 and GBM cell line U251 (Figure 3.5). We found that JNJ-3790339 was similar to ritanserin in inducing cancer cell death across all tested concentrations, while compound JNJ-3940447 induced relatively little cytotoxicity in both the cancer cells and Jurkat T-cells. The lack of direct correlation between DGKα inhibition and cytotoxicity within cancer cells suggests that there may be additional specific properties of these drugs affecting their action in cells, such as cell permeability, retention, or off-target effects.

In addition to their direct effects on cancer cells, novel inhibitors to DGKα have potential to become valuable as adjuncts to cancer immunotherapies. The ability of ritanserin to upregulate T-cell activation is an attractive benefit of DGKα inhibition, since immunotherapies have emerged as very effective treatments for some cancer patients. Treatment of immunogenic malignancies such as melanoma have yielded major improvements in patient survival with the advent of immune checkpoint inhibitors. These treatments reverse the immunosuppressive effects of PD-1/PD-L1 and CTLA4, enabling T-cells to combat tumor progression. Combining these drugs with an agent such as ritanserin could prove valuable in the clinic, with possible synergistic effects; notably, DGKα has been shown to mediate resistance to PD-1 inhibitors (84), We sought to determine if JNJ-3790339 and JNJ-3940447 could also promote T-cell activation, using a human T-cell line and primary T-cells isolated from WT and *DGKα*$^{-/-}$ mice. The range of analogs we tested enabled us to get a preliminary sense of correlations between DGKα inhibitory potency and T-cell activation. We observed in the Jurkat human T-cell line that JNJ-3790339 enhanced the upregulation of CD69 gene expression, an early marker for T-cell activation, and exhibited an improved response over ritanserin (Figure 3.6). Interestingly, JNJ-3790892 also displayed a significant increase in CD69 expression above DMSO in primary T-cells but no improvement in potency or selectivity over ritanserin. The differential effects of the two compounds across different cell types might be due to differences in drug permeability and retention, or slight modification by inhibition of other target. These may stem from species-specificity differences, similar to how ritanserin is able to promote CD25 and CD69 expression in human T-cells, but not in mouse T-cells (147). Importantly, we confirm that these effects are DGKα-mediated, as primary T-cells

harvested from the spleens of *DGKα*$^{-/-}$ mice do not show enhanced T-cell activation upon treatment with DGKα inhibitors (Figure 3.6). It will be important in the future to include normal cell controls to confirm that our compounds at their tested concentrations are not cytotoxic to cell populations we wish to preserve in a clinical setting. These can include primary mouse and human T-cells, as well as lines such as those from human fibroblasts. Controls for GBM lines can include normal human neural stem cells that propagate indefinitely in their undifferentiated state, or which can be differentiated into astrocyte control cells.

In summary, through these experiments we have identified compounds that more potently and selectively inhibit the promising immunotherapy and cancer target DGKα. In particular, we have identified JNJ-3790339 as a compound with superior selectivity for DGKα, similar induction of cytotoxicity in cancer cells, and improved ability to upregulate T-cell activation. JNJ-3790339 shares a high degree of structural similarity to ritanserin and would likely behave similarly *in vivo*. We recognize that there is some inconsistency between potency of DGKα inhibition and promotion of T-cell activity with our newly identified compounds. Reasons for this may include variable penetration of the different compounds across cell membranes, as well as different susceptibility to cellular efflux pumps, which are mechanisms demonstrated to influence resistance to chemotherapy (159,160). Activity against other targets including serotonin and possibly dopamine receptors may also modulate these drugs' ability to influence T-cell activation. Further investigation is needed to determine a complete structure-activity relationship for this class of drugs, as well as cell permeability and retention, their activity against serotonin receptors, and their *in vivo* pharmacokinetic profile. The potential clinical benefit of these

drugs alone and in combinations with available immunotherapies underscores the importance of further pursuit of these repurposed analogs.

# Chapter 4

## Discussion & Future Directions

*Therapeutic potential and considerations with DGKα inhibition*

The studies presented in Chapters 2 and 3 reintroduce DGKα as a druggable target but add a novel role in macrophage activation. With its previously described function as an immune checkpoint due to its effects on T-cell modulation (28), this evidence provides new insight into a broader role as an important immune regulator. These effects were demonstrated in the physiological setting of wound healing, with *DGKα*$^{-/-}$ mice having greater numbers of macrophages present at wound sites in response to injuries (Figures 2.10, 2.11). The therapeutic potential in this area alone is broad, ranging from ischemic stroke, to burn healing, and the advent of a possible new treatment option could have far-reaching clinical effects. Modest improvements in healing time may be a challenging yet plausible outcome of DGKα inhibition, as suggested by the above study (Figure 2.9). Macrophage plasticity is an important characteristic of these cells that may fail in certain settings; for example, failure to transition between pro- and anti-inflammatory phases can result in chronic, unresolving inflammation as in diabetic wound healing(49). This sort of pathology may substantially benefit from a therapy modulating the activation of these cells. These experiments were performed in whole organism KO of DGKα with the enzyme absent in all cells, so it will be important to determine if this treatment option would be viable with systemic administration of an inhibitor or through local administration of a topical formulation of an inhibitor.

In addition to wound healing, there are a great number of pathologies that are directly influenced by macrophage function. In type 1 diabetes, pro-inflammatory macrophages trigger inflammatory responses initiating insulitis and pancreatic β cell death, while anti-inflammatory macrophages negatively regulate the disease by decreasing

hyperglycemia, insulitis, and inflammation in the pancreas (161). In type 2 diabetes, pro-inflammatory macrophages are implicated in insulin resistance and the activation of inflammatory signals during disease progression, while anti-inflammatory macrophages attenuate the inflammation of adipose tissue. It is evident that this cell type is associated with many of the complications that emerge in diabetes (162,163), so DGKα inhibition may function as a tool to regulate those effects and further elucidate their roles. Our results suggest that DGKα knockout/knockdown increases macrophage responsiveness, and this might worsen some pathologies, but help others.

*Effects of DGKα inhibition in cancer*

Macrophages play a vital role in cancer development and progression. Cancers have sometimes been referred to as wounds that don't heal (164–166). This is due in part to the similarities between the remodeling of the ECM, which occurs during both wound healing and during metastasis. During normal wound healing, negative feedback mechanisms terminate reparative responses once healing is complete, an event that goes unregulated during metastasis. During tumor progression, tumor-associated macrophages (TAMs) promote many of the processes which support tumor growth and local invasion. These cells can promote angiogenesis, inhibit T-cell-mediated cytotoxicity, and contribute to ECM remodeling to facilitate cell extravasation (167). While studies have shown that TAMs are able to exhibit polarization in both pro- and anti-inflammatory directions, they are largely considered to have acquired the M2-like anti-inflammatory phenotype and commonly express biomarkers such as MMP2/9, and activated STAT-3 (168). Signaling ligands secreted by macrophages – including TGF-β, VEGF, PDGF, M-CSF, and IL-10 – promote

tumor initiation and growth, fostering conditions that contribute to therapeutic failure (169). More understanding regarding the regulatory mechanisms of macrophages, including TAMs, has great potential to improve therapeutic strategies for disease management. Tumor cell cytotoxicity as a result of DGKα inhibition has been previously demonstrated (19), but it will be very important for the feasibility of this treatment strategy to investigate the role DGKα plays in the setting of the tumor microenvironment, where TAM activation may exacerbate disease progression.

*DGKα as an immunotherapeutic target*

In the realm of immunotherapy, DGKα has emerged as a potential target for combination therapy, as it has been demonstrated that DGKα inhibition enhances the efficacy of anti-PD-1 therapy (84). There is a need for more potent and specific DGKα inhibitors, and the main interest in developing them has been as boosters of T-cells alongside other therapies such as anti-PD-1 checkpoint inhibitors. A recent study demonstrated anti-cancer synergy in combining anti-PD-1 inhibition and DGKα inhibition (29). Acquired treatment resistance is a problem frequently encountered, despite the unprecedented clinical success of immune checkpoint inhibitors (170). The mechanisms of tumor immune resistance are complex, involving changes in the antitumor immune response pathways as well as in the signaling pathways within tumor cells themselves, with both leading to the formation of an inhibitory immunosuppressive microenvironment (171). Intrinsic or primary drug resistance, wherein a malignancy is totally unresponsive to immunotherapy from first dose, is another avenue of immunotherapy resistance. One proposed mechanism for the development of primary resistance is the blockade of immune

checkpoints leading to the polarization of immunosuppressive cells, such as M2 macrophages (171). Primary resistance also presents with upregulated expression of chemokines with immunosuppressive potential, such as IL-10 or VEGFA, and macrophage chemotaxis genes, including CCL2 and CCL13 (172). DGKα is also implicated in facilitating treatment resistance by promoting T-cell exhaustion as well as anergy, and DGKα inhibition has been found to restore cytotoxic function of CAR-T and $CD8^+$ T-cells (29). The combination of DGKα inhibition with anti-PD-1 treatment resulted in a synergistic effect promoting induction of AP-1, an important regulator of the Ras/ERK pathway that is associated with T-cell activation. However, there is also new evidence to suggest that DGKζ inhibition may more strongly boost T-cell function than does DGKα inhibition (173). That being said, the effects of DGKα and DGKζ knockdown may have varying effects across cell types, and this observation on the relative potency of DGKα versus DGKζ may not hold true in other immune cell types. While our data indicate a macrophage-activating effect for DGKα knockout, one prior study has suggested that DGKζ knockout does the opposite and may suppress macrophages (131). Therefore, DGKα in combination with other immunotherapies might be a more effective treatment option than DGKζ inhibition in cancers where macrophages may be used to combat the tumor, as in human osteosarcoma (174).

Future experiments incorporating anti-PD-1 checkpoint inhibitors alone or in combination with DGKα inhibition can be used in cancer models to observe their effects on efficacy, with the hypothesis that DGKα inhibition will improve treatment outcomes. These studies using various mouse models, from nude mice lacking T-cells, to SCID mice lacking both T- and B-cells, can probe for the importance of various immune cell subsets

in DGKα's ability to enhance checkpoint inhibitor therapy. T-cell depletion using CD3, CD4 or CD8 antibody may similarly highlight the relevant subsets in combination treatment. It will be particularly important when following up the present studies with testing of DGKα inhibitors in cancer models to deplete macrophages with techniques such as clodronate liposomes, to determine their role in the activity of DGKα inhibitors alone or in combination regimens.

With new evidence that DGKα is also able to regulate macrophage activation, there may be an additional immunotherapeutic indication for combination DGKα treatment. Anti-CD47 therapy is a promising addition to the catalogue of immunotherapies for cancer treatment. While to date the majority of immunotherapies have been agents targeting CTLA-4 and PD-1/PD-L1, targeting macrophages presents the opportunity to abrogate myeloid-specific immune checkpoints as well – such as blockade of the CD-47/SIRPα interaction, which has proven efficacious in early studies in blood cancers as well as solid tumors (175,176). CD47 is a powerful "don't-eat-me" signal suppressing phagocytosis. It was shown with the transfusion of $CD47^{-/-}$ red blood cells (RBCs) into WT mice that the mutant RBCs were rapidly eliminated from circulation (177), but splenectomized mice and mice having undergone macrophage depletion showed impaired removal of $CD47^{-/-}$ RBCs. It has also been suggested that targeting the CD47/SIRPα axis may alter the polarization state of macrophages in the tumor (178). In glioblastoma, anti-CD47 treatment was found to enhance tumor cell phagocytosis by both M1 and M2 macrophages, and can shift macrophages toward an M1 phenotype *in vivo* (179). Given our findings that DGKα knockout enhances macrophage responsiveness, we hypothesize that adding DGKα inhibition to a pro-phagocytic therapy such as anti-CD47 antibodies will enhance its

efficacy. CD47 is highly expressed on many different types of cancer so therapies which block the CD-47/SIRPα interaction may be broadly applicable and amenable to combination with DGKα inhibition. This is among the future directions being pursued as an outcome of this project.

Among other possible therapeutics that have emerged resulting from their ability to regulate macrophage activation is niacin, a lipid-regulating agent used for treatment of high-grade inflammatory diseases, and which has been demonstrated to impair glioma tumor growth and stimulate myeloid cells (180–183). Niacin, or nicotinic acid (NA), is a member of the vitamin B family and known as one of the most effective agents helping to protect against cardiovascular risk factors by increasing high density lipoprotein (HDL) levels and simultaneously decreasing very low density lipoprotein (VLDL) and low density lipoprotein (LDL) (184). Well-known for its functions in the treatment and prevention of atherosclerosis, its newly uncovered ability to control brain tumor growth is suggested to be due to promotion of microglial anti-GBM activity. It was previously shown that while macrophages and microglia from healthy individuals were able to curb brain tumor-initiating cell (BITC) growth in culture, this effect was lost in cells from patients with GBM (185) – and NA has been proposed as a means to overcome such compromised immunity. NA treatment of mice bearing intracranial BTICs derived from GBM patients increased the macrophage and microglia representation within the tumor (183). NA is safely used in humans at high doses, and it is already being incorporated into a clinical trial in Alberta, Canada for patients with newly-diagnosed glioblastoma. There may be even stronger potential for combination treatment with an adjuvant such as ritanserin, and our laboratory will be investigating this combination as well. Such a combination could fulfill some of

the exciting potential that may arise from repurposing existing drugs. DGKα inhibition in combination with NA treatment has the potential to further boost the performance of anti-tumor microglia and macrophages in cancers such as GBM, a setting in which each has demonstrated single-agent efficacy (19,183).

Additionally, the CSF-1/CSF-1R axis is a key macrophage signaling pathway which has been linked to increased tumor cell survival, proliferation and enhanced motility, and its inhibition has shown potential for improving prognosis in breast and prostate cancers through modulating TAMs (186–189). TAMs in the tumor microenvironment are known to impose tumor-promoting functions, leading to tumor growth and treatment resistance. CSF-1R inhibition represents another strategy to modulate TAMs, which depletes macrophages and reduces tumor volume in several xenograft models (190). With the intended purpose of DGKα inhibition being to enhance the activity of macrophages or microglia in a given setting, promotion of TAM activation in a cancer setting could be an undesirable effect. However, there are data to suggest that after CSF-1R inhibition glioma TAMs lose M2 polarization and show enhanced phagocytosis (191). This therapeutic strategy might therefore also benefit from combination with DGKα inhibition, with the hope of increasing activation of these anti-tumor macrophages. Macrophage responsiveness to such therapies may be enhanced by the stimulatory effects from DGKα inhibition.

*Identification of mechanisms behind DGKα-loss mediated macrophage responsiveness*

An important area of investigation that must be addressed before implementing DGKα inhibition in the clinic is the identification of the key mechanisms responsible for

the increased responsiveness of macrophages with DGKα knockout/knockdown. While we have provided molecular evidence of enhanced macrophage activation (Figure 2.1), as well as *in vivo* support for an effect in two wound models, we have not yet dissected the mechanism of action responsible for this apparent activation. It has previously been shown that DGKα inhibition is associated with increased PKC activation (21). As a key mediator of the effects of DAG in cells, PKC is worthy of further study, as it also has been reported as a key element in macrophage cell signaling (48,116,117). In our research, we too observed a trend toward increased PKC activation following DGKα knockdown, and future experiments on DGKα in macrophages could test whether PKC antagonists block the effects of DGKα KO/KD or inhibition, and whether PKC agonists elicit similar cell responsiveness. PKC signaling in macrophage activation has been found to mediate the upregulation of iNOS expression and NO production in activated J774 macrophages in an NF-κB dependent manner (47), and this mechanism may be integral to our own observations with DGKα loss and knockdown. Early investigation into potential mechanisms included the assessment of the NF-κB transcription factor family. Immunoblots for IκBα and p-IκBα at multiple time points with and without LPS treatment showed predictable expression changes with the addition of LPS, but no differences were found across the WT and *Dgka*$^{-/-}$ BMDMs (data not shown). NF-κB and its upstream drivers therefore did not supplement PKC as potential mechanisms for *Dgka* loss-induced responsiveness.

Further research will also incorporate unbiased approaches to seeking potential mediators of the effects of DGKα knockout/inhibition on macrophages using profiling strategies such as RNA-seq and phosphoproteomics of *Dgka*$^{-/-}$ versus WT mouse

macrophages to identify transcriptomic and signaling differences. Our laboratory has previously demonstrated that the prenyltransferase geranylgeranyltransferase type 1 (GGTase-1) is a mediator of mesenchymal GBM cell sensitivity to ritanserin (22). We consider the possibility that GGTase-1 may also act as another potential mediator of DGKα effects on macrophages, as previous studies have demonstrated the ability of GGTase-1 to regulate macrophage activity (192,193).

Additional studies should also be performed to determine if DGKα loss promotes increased phagocytic activity and/or increased monocyte differentiation. Increased migration toward a chemoattractant was demonstrated in our work (Figure 2.8) and this provides some insight into the effect of DGKα on macrophage motility. However, insight into different functional mechanisms of these cells would provide a more thorough illumination of the exact function of DGKα as well as provide additional evidence to support DGKα as a mediator macrophage activation. Fluorescent bead internalization in conjunction with imaging at regular intervals could illustrate the rate and volume of macrophage phagocytosis in normal versus DGKα-deficient macrophages. And while the ontogeny of macrophages has been well studied and established, the potential for DGKα influence on macrophage differentiation remains unexplored; the observed increase of macrophage numbers at wound sites is also a phenomenon that is not fully understood and could also be related to the effects of DGKα on monocyte differentiation. The increase in local macrophage cell number may represent enhanced differentiation of blood circulating monocytes, proliferation of tissue-resident macrophages, or chemotaxis of nearby macrophages to the area, and in our brain injury model could also reflect monocytes and macrophages introduced into the brain through blood vessel rupture as a result of the injury

itself. Analysis by flow cytometry may be useful for determining the identity of myeloid cells in response to brain injury in *DGKα*$^{-/-}$ mice, with antibodies specific for F4/80, CD45, CD11b and TMEM119 providing insight into predominant cell type. Probing for Ki67 and DGKα expression *in vivo* may also shed light on whether the propensity for proliferation depends on DGKα status.

Additional testing will also incorporate the use of small-molecule DGKα inhibitors against macrophages in various settings. This includes investigating the role of such compounds in wound models such as the burn and cortical stab wound injury models. These studies should better determine the potential of DGKα inhibition as a wound healing treatment, versus our previous studies which relied on knockout of the enzyme. While testing the effects of small-molecule DGKα inhibitors on macrophages is vital for potential translation of our findings, it introduces additional levels of complexity. Factors such as dose and schedule of DGKα inhibitors may prove to be extremely important; unpublished data from our laboratory already suggests the importance of dosing schedule on the efficacy of DGKα inhibitors in treating GBM. Intermittent dosing has proven to be far more effective in enhancing microglia and macrophage infiltration into GBM in an immunocompetent mouse model, as well as with reducing tumor burden. It will be instructive to observe how effects of intermittent or continuous small-molecule DGKα inhibition compares with effects on macrophages in *Dgkα*$^{-/-}$ mice.

*Development of novel small-molecule DGKα inhibitors*

To maximize the potential benefits of DGKα inhibition, potent and specific inhibitor compounds must be available for therapeutic use. The identification and

development of DGK inhibitor compounds has been a research area of growing interest. Until fairly recently, R59022 and R59949 were the only available known DGKα inhibitors. Currently Bristol Myers Squibb is pursuing DGKα and DGKζ inhibitors, and other companies appear to be developing them as well. A successful method for uncovering novel inhibitors could stem from comparing the structures of similar inhibitory compounds to develop an understanding of shared chemical structures that may be necessary – or need to be eliminated – to develop potent and specific inhibitors for DGKα (148). With our own research as well, we began with a library of structural analogs to ritanserin as the basis of our search. While still able to discern novel data from the available compounds and data at our disposal, hurdles in the form of collaborator non-transparency prevented a full accounting of all the structural insights which exist in our compound library of interest. Others involved in the development of DGKα inhibitors are also utilizing a different approach. The identification of CU-3 contrasts those previously mentioned given its structural dissimilarity to the previously known inhibitors. CU-3 was found to selectively inhibit DGKα with the relatively low $IC_{50}$ value of 0.6μM and to competitively reduce the affinity of DGKα for ATP, but not DAG (78). Caspase-3/7 activity in a human hepatocellular carcinoma line in which DGKα is highly expressed was assessed following CU-3 treatment and found to be enhanced, indicating induction of apoptosis by the drug. IL-2 production was also enhanced with the addition of CU-3 in Jurkat T leukemia-cells, making it a more potent inhibitor of DGKα with similar ability to promote T-cell activation. Little is known, however, about the safety and efficacy of this compound as a potential therapeutic agent. Utilization of novel compound structures as opposed to structural analogs of R59022, R59949, and ritanserin are an attractive avenue for compound

discovery. These may avoid issues related to unwanted serotonin receptor interactions, which have known side effects including somnolence. It may be possible, however, to identify ritanserin analogs that lack the serotonin receptor inhibition but retain full or more potent DGKα inhibition. Novel compound structures based on the deconstruction of ritanserin are also the subject of closer investigation (150). These studies provide crucial insight into the structure-function relationships of compound components. Information regarding the cell permeability and retention of drugs will be an important next step for the compounds identified in the aforementioned study. This will enable the future development of safe, potent, and specific inhibitors to a target with increasingly-recognized therapeutic potential.

The studies presented herein support the continued study of DGKα as a promising target for immunotherapeutic consideration, with slowly growing availability of small molecule inhibitors for research use and, potentially in the future, clinical application. There remains very much to expand upon in the data presented, and some of this work is currently ongoing. DGKα presents unique immune-modulatory capabilities, in that *DGKα*$^{-/-}$ macrophages show enhanced responsiveness to divergent stimuli. This implies that DGKα inhibition may potentially act as an amplifier of macrophage responses, and heighten its potential in combination with other macrophage and microglia modifying agents, as described above. With a clearer understanding of the precise mechanisms underlying DGKα-mediated macrophage regulation, we may better establish a foundation for the future immunotherapeutic development of DGKα inhibitors – with the potential for improved patient outcomes.

# Chapter 5

# References

1. Fogh BS, Multhaupt HAB, Couchman JR. Protein Kinase C, Focal Adhesions and the Regulation of Cell Migration. J Histochem Cytochem. 2014 Mar;62(3):172.

2. Kolczynska K, Loza-Valdes A, Hawro I, Sumara G. Diacylglycerol-evoked activation of PKC and PKD isoforms in regulation of glucose and lipid metabolism: a review. Lipids in health and disease. 2020 Dec;19:1-5

3. Lim PS, Sutton CR, Rao S. Protein kinase C in the immune system: From signalling to chromatin regulation. Immunology. 2015 Dec 1;146(4):508–22.

4. Antal CE, Hudson AM, Kang E, Zanca C, Wirth C, Stephenson NL, et al. Cancer-Associated Protein Kinase C Mutations Reveal Kinase's Role as Tumor Suppressor. Cell. 2015 Jan 29;160(3):489.

5. Yoon MS, Sun Y, Arauz E, Jiang Y, Chen J. Phosphatidic Acid Activates Mammalian Target of Rapamycin Complex 1 (mTORC1) Kinase by Displacing FK506 Binding Protein 38 (FKBP38) and Exerting an Allosteric Effect. J Biol Chem. 2011 Aug 26;286(34):29568.

6. Kooijman EE, Chupin V, de Kruijff B, Burger KNJ. Modulation of membrane curvature by phosphatidic acid and lysophosphatidic acid. Traffic. 2003 Mar 1;4(3):162–74.

7. McMahon HT, Boucrot E. Membrane curvature at a glance. J Cell Sci. 2015;128(6):1065–70.

8. Campomanes P, Zoni V, Vanni S. Local accumulation of diacylglycerol alters membrane properties nonlinearly due to its transbilayer activity. Commun Chem. 2019 Dec 1;2(1):1–8.

9. Shulga Y V., Topham MK, Epand RM. Regulation and functions of diacylglycerol kinases. Chem Rev. 2011;111(10):6186–208.

10. Moritz A, De Graan PNE, Gispen WH, Wirtz KWA. Phosphatidic acid is a specific activator of phosphatidylinositol-4- phosphate kinase. J Biol Chem. 1992 Apr 15;267(11):7207–10.

11. Olenchock BA, Guo R, Carpenter JH, Jordan M, Topham MK, Koretzky GA, et al. Disruption of diacylglycerol metabolism impairs the induction of T cell anergy. Nat Immunol. 2006;7(11).

12. Topham MK. Signaling roles of diacylglycerol kinases. J Cell Biochem. 2006;97(3):474–84.

13. Shirai Y, Kouzuki T, Kakefuda K, Moriguchi S, Oyagi A, Horie K, et al. Essential Role of Neuron-Enriched Diacylglycerol Kinase (DGK), DGKβ in Neurite Spine Formation, Contributing to Cognitive Function. PLoS One. 2010 Jul 15;5(7):e11602.

14. Fazio A, Obeng EO, Rusciano I, Marvi MV, Zoli M, Mongiorgi S, et al.

Subcellular Localization Relevance and Cancer-Associated Mechanisms of Diacylglycerol Kinases. Int J Mol Sci 2020, Vol 21, Page 5297. 2020 Jul 26;21(15):5297.

15. Sanjuán MA, Pradet-Balade B, Jones DR, Martínez-A C, Stone JC, Garcia-Sanz JA, et al. T Cell Activation In Vivo Targets Diacylglycerol Kinase α to the Membrane: A Novel Mechanism for Ras Attenuation. J Immunol. 2003;170(6):2877–83.

16. Purow B. Molecular pathways: Targeting diacylglycerol kinase alpha in cancer. Clin Cancer Res. 2015;21(22):5008–12.

17. Li J, Pan C, Boese AC, Kang J, Umano AD, Magliocca KR, et al. DGKA Provides Platinum Resistance in Ovarian Cancer Through Activation of c-JUN–WEE1 Signaling. Clin Cancer Res. 2020 Jul 15;26(14):3843–55.

18. Kong Y, Zheng Y, Jia Y, Li P, Wang Y. Decreased LIPF expression is correlated with DGKA and predicts poor outcome of gastric cancer. Oncol Rep. 2016 Oct 1;36(4):1852–60.

19. Dominguez CL, Floyd DH, Xiao A, Mullins GR, Kefas B a., Xin W, et al. Diacylglycerol kinase α is a critical signaling node and novel therapeutic target in glioblastoma and other cancers. Cancer Discov. 2013;3(7):782–97.

20. Kefas B, Floyd DH, Comeau L, Frisbee A, Dominguez C, Dipierro CG, et al. A miR-297/hypoxia/DGK-a axis regulating glioblastoma survival.

21. Boroda S, Niccum M, Raje V, Purow BW, Harris TE. Dual activities of ritanserin and R59022 as DGKα inhibitors and serotonin receptor antagonists. Biochem Pharmacol. 2017;123:29–39.

22. Olmez I, Love S, Xiao A, Manigat L, Randolph P, McKenna BD, et al. Targeting the mesenchymal subtype in glioblastoma and other cancers via inhibition of diacylglycerol kinase alpha. Neuro Oncol. 2017;(January 2018):1–11.

23. Takeishi K, Taketomi A, Shirabe K, Toshima T, Motomura T, Ikegami T, et al. Diacylglycerol kinase alpha enhances hepatocellular carcinoma progression by activation of Ras-Raf-MEK-ERK pathway. Journal of hepatology. 2012 Jul 1;57(1):77-83

24. Filigheddu N, Cutrupi S, Porporato PE, Riboni F, Baldanzi G, Chianale F, et al. Diacylglycerol Kinase is Required for HGF-induced Invasiveness and Anchorage-independent Growth of MDA-MB-231 Breast Cancer Cells. Anticancer Res. 2007 May 1;27(3B):1489–92.

25. Yanagisawa K, Yasuda S, Kai M, Imai S ichi, Yamada K, Yamashita T, et al. Diacylglycerol kinase α suppresses tumor necrosis factor-α-induced apoptosis of human melanoma cells through NF-κB activation. Biochim Biophys Acta - Mol Cell Biol Lipids. 2007;1771(4):462–74.

26. Riese MJ, Moon EK, Johnson BD, Albelda SM. Diacylglycerol Kinases (DGKs): Novel Targets for Improving T Cell Activity in Cancer. Front Cell Dev Biol. 2016;

27. Olenchock BA, Guo R, Carpenter JH, Jordan M, Topham MK, Koretzky GA, et al. Disruption of diacylglycerol metabolism impairs the induction of T cell anergy. Nat Immunol. 2006;7(11):1174–81.

28. Noessner E. DGK-α: A checkpoint in cancer-mediated immuno-inhibition and target for immunotherapy. Front Cell Dev Biol. 2017;5(MAR).

29. Arranz-Nicolás J, Martin-Salgado M, Adán-Barrientos I, Liébana R, del Carmen Moreno-Ortíz M, Leitner J, et al. Diacylglycerol kinase α inhibition cooperates with PD-1-targeted therapies to restore the T cell activation program. Cancer Immunol Immunother. 2021 Nov 1;70(11):3277–89.

30. Zha Y, Marks R, Ho AW, Peterson AC, Janardhan S, Brown I, et al. T cell anergy is reversed by active Ras and is regulated by diacylglycerol kinase-α. Nat Immunol. 2006;7(11):1166–73.

31. Mérida I, Torres-Ayuso P, Ávila-Flores A, Arranz-Nicolás J, Andrada E, Tello-Lafoz M, et al. Diacylglycerol kinases in cancer. Vol. 63, Advances in Biological Regulation. 2017. p. 22–31.

32. Ávila-Flores A, Arranz-Nicolás J, Andrada E, Soutar D, Mérida I. Predominant contribution of DGKζ over DGKα in the control of PKC/PDK-1-regulated functions in T cells. Immunol Cell Biol. 2017 Jul 1;95(6):549–63.

33. Jung IY, Kim YY, Yu HS, Lee M, Kim S, Lee J. CRISPR/Cas9-Mediated Knockout of DGK Improves Antitumor Activities of Human T Cells. Cancer Res. 2018;78(16):4692–703.

34. Prinz PU, Mendler AN, Brech D, Masouris I, Oberneder R, Noessner E. NK-cell dysfunction in human renal carcinoma reveals diacylglycerol kinase as key regulator and target for therapeutic intervention. Int J Cancer. 2014 Oct 15;135(8):1832–41.

35. Ginhoux F, Guilliams M. Tissue-Resident Macrophage Ontogeny and Homeostasis. Immunity. 2016 Mar 15;44(3):439–49.

36. Hoeffel G, Ginhoux F. Ontogeny of tissue-resident macrophages. Front Immunol. 2015;6(SEP):486.

37. Lee KY. M1 and M2 polarization of macrophages: a mini-review. Rev Artic Med Biol Sci Eng. 2019;2(1):1–5.

38. Oneissi Martinez F, Sica A, Mantovani A, Locati M. Macrophage activation and polarization. Front Biosci. 2008;13:453.

39. Mosser DM, Edwards JP. Exploring the full spectrum of macrophage activation. Vol. 8, Nature Reviews Immunology. Nature Publishing Group; 2008. p. 958–69.

40. Rizzo MA, Shome K, Watkins SC, Romero G. The recruitment of Raf-1 to membranes is mediated by direct interaction with phosphatidic acid and is independent of association with Ras. J Biol Chem. 2000 Aug 4;275(31):23911–8.

41. Song G, Ouyang G, Bao S. The activation of Akt/PKB signaling pathway and cell survival. J Cell Mol Med. 2005 Jan 1;9(1):59–71.

42. Vergadi E, Ieronymaki E, Lyroni K, Vaporidi K, Tsatsanis C. Akt Signaling Pathway in Macrophage Activation and M1/M2 Polarization. J Immunol. 2017 Feb 1;198(3):1006–14.

43. Covarrubias AJ, Aksoylar HI, Horng T. Control of macrophage metabolism and activation by mTOR and Akt signaling. Semin Immunol. 2015 Aug 1;27(4):286–96.

44. Covarrubias AJ, Aksoylar HI, Yu J, Snyder NW, Worth AJ, Iyer SS, et al. Akt-mTORC1 signaling regulates Acly to integrate metabolic input to control of macrophage activation. Elife. 2016 Feb 19;5.

45. Foster DA. Phosphatidic acid signaling to mTOR: Signals for the survival of human cancer cells. Biochim Biophys Acta - Mol Cell Biol Lipids. 2009 Sep;1791(9):949–55.

46. Yalcin A, Clem B, Makoni S, Clem A, Nelson K, Thornburg J, et al. Selective inhibition of choline kinase simultaneously attenuates MAPK and PI3K/AKT signaling. Oncogene 2010 291. 2009 Oct 26;29(1):139–49.

47. Salonen T, Sareila O, Jalonen U, Kankaanranta H, Tuominen R, Moilanen E. Inhibition of classical PKC isoenzymes downregulates STAT1 activation and iNOS expression in LPS-treated murine J774 macrophages. Br J Pharmacol. 2006 Apr 1;147(7):790–9.

48. Furundzija V, Fritzsche J, Kaufmann J, Meyborg H, Fleck E, Kappert K, et al. IGF-1 increases macrophage motility via PKC/p38-dependent αvβ3-integrin inside-out signaling. Biochem Biophys Res Commun. 2010 Apr 9;394(3):786–91.

49. Boniakowski AE, Kimball AS, Jacobs BN, Kunkel SL, Gallagher KA. Macrophage-Mediated Inflammation in Normal and Diabetic Wound Healing. J Immunol. 2017 Jul 1;199(1):17–24.

50. Wang Y, Beekman J, Hew J, Jackson S, Issler-Fisher AC, Parungao R, et al. Burn injury: Challenges and advances in burn wound healing, infection, pain and scarring. Adv Drug Deliv Rev. 2018 Jan 1;123:3–17.

51. Wang X, Ge J, Tredget EE, Wu Y. The mouse excisional wound splinting model, including applications for stem cell transplantation. Nature Protocols. 2013 Feb;8(2):302-9.

52. Kaufman T, Lusthaus SN, Sagher U, Wexler MR. Deep partial skin thickness burns: A reproducible animal model to study burn wound healing. Burns. 1990 Feb

1;16(1):13–6.

53. Uygun BE, Christophe Helary B, Berthiaume F, Krzyszczyk P, Schloss R, Palmer A. The Role of Macrophages in Acute and Chronic Wound Healing and Interventions to Promote Pro-wound Healing Phenotypes. Front Physiol | 2018;1:419.

54. Minutti CM, Knipper JA, Allen JE, Zaiss DMW. Tissue-specific contribution of macrophages to wound healing. Semin Cell Dev Biol. 2017 Jan 1;61:3–11.

55. Delavary BM, Van Der Veer WM, Van Egmond M, Niessen FB, Beelen RHJ. Macrophages in skin injury and repair. Immunobiology. 2011;216:753–62.

56. Lucas T, Waisman A, Ranjan R, Roes J, Krieg T, Müller W, et al. Differential Roles of Macrophages in Diverse Phases of Skin Repair. J Immunol. 2010 Apr 1;184(7):3964–77.

57. Hesketh M, Sahin KB, West ZE, Murray RZ. Macrophage Phenotypes Regulate Scar Formation and Chronic Wound Healing. Int J Mol Sci 2017, Vol 18, Page 1545. 2017 Jul 17;18(7):1545.

58. Khallou-Laschet J, Varthaman A, Fornasa G, Compain C, Gaston AT, Clement M, et al. Macrophage Plasticity in Experimental Atherosclerosis. PLoS One. 2010 Jan 25;5(1):e8852.

59. Werner S, Grose R. Regulation of wound healing by growth factors and cytokines. Physiol Rev. 2003;83(3):835–70.

60. Weigel C, Veldwijk MR, Oakes CC, Seibold P, Slynko A, Liesenfeld DB, et al. Epigenetic regulation of diacylglycerol kinase alpha promotes radiation-induced fibrosis. Nat Commun. 2016 Mar 11;7(1):1-2.

61. Ginhoux F, Greter M, Leboeuf M, Nandi S, See P, Gokhan S, et al. Fate mapping analysis reveals that adult microglia derive from primitive macrophages. Science (80- ). 2010 Nov 5;330(6005):841–5.

62. Karve IP, Taylor JM, Crack PJ. The contribution of astrocytes and microglia to traumatic brain injury. Br J Pharmacol. 2016 Feb 1;173(4):692–702.

63. D'Mello C, Le T, Swain MG. Cerebral Microglia Recruit Monocytes into the Brain in Response to Tumor Necrosis Factorα Signaling during Peripheral Organ Inflammation. J Neurosci. 2009 Feb 18;29(7):2089–102.

64. Satoh J ichi, Kino Y, Asahina N, Takitani M, Miyoshi J, Ishida T, et al. TMEM119 marks a subset of microglia in the human brain. Neuropathology. 2016 Feb 1;36(1):39–49.

65. Smith JA, Das A, Ray SK, Banik NL. Role of pro-inflammatory cytokines released from microglia in neurodegenerative diseases. Brain Res Bull. 2012 Jan 4;87(1):10–20.

66. Fan Y, Xie L, Chung CY. Signaling Pathways Controlling Microglia Chemotaxis. Mol Cells. 2017 Mar 1;40(3):163.

67. Mohanraj M, Sekar P, Liou HH, Chang SF, Lin WW. The Mycobacterial Adjuvant Analogue TDB Attenuates Neuroinflammation via Mincle-Independent PLC-γ1/PKC/ERK Signaling and Microglial Polarization. Mol Neurobiol. 2019 Feb 1;56(2):1167–87.

68. van der Vorst EPC, Theodorou K, Wu Y, Hoeksema MA, Goossens P, Bursill CA, et al. High-Density Lipoproteins Exert Pro-inflammatory Effects on Macrophages via Passive Cholesterol Depletion and PKC-NF-κB/STAT1-IRF1 Signaling. Cell Metab. 2017 Jan 10;25(1):197–207.

69. De Chaffoy de Courcelles D, Roevens P, Van Belle H. R 59 022, a diacylglycerol kinase inhibitor. Its effect on diacylglycerol and thrombin-induced C kinase activation in the intact platelet. J Biol Chem. 1985 Dec 15;260(29):15762–70.

70. Van Norman GA. Drugs, Devices, and the FDA: Part 1: An Overview of Approval Processes for Drugs. JACC Basic to Transl Sci. 2016 Apr 1;1(3):170–9.

71. Hait WN. Anticancer drug development: the grand challenges. Nat Rev Drug Discov 2010 94. 2010 Apr;9(4):253–4.

72. Alteri E, Guizzaro L. Be open about drug failures to speed up research. Nat 2021 5637731. 2018 Nov 13;563(7731):317–9.

73. Smith C. Drug target validation: Hitting the target. Nat 2003 4226929. 2003 Mar 20;422(6929):342–5.

74. Cortés-Cros M, Schmelzle T, Stucke VM, Hofmann F. The Path to Oncology Drug Target Validation: An Industry Perspective. Methods Mol Biol. 2013;986:3–13.

75. Pushpakom S, Iorio F, Eyers PA, Escott KJ, Hopper S, Wells A, et al. Drug repurposing: progress, challenges and recommendations. Nat Rev Drug Discov 2018 181. 2018 Oct 12;18(1):41–58.

76. Cha Y, Erez T, Reynolds IJ, Kumar D, Ross J, Koytiger G, et al. Drug repurposing from the perspective of pharmaceutical companies. Br J Pharmacol. 2018 Jan 1;175(2):168–80.

77. De Chaffoy De Courcelles D, Roevens P, Van Belle H, Kennis L, Somers Y, De Clerck F. The Role of Endogenously Formed Diacylglycerol in the Propagation and Termination of Platelet Activation: A biochemical and functional analysis using the novel diacylglycerol kinase inhibitor, R 59 949. J Biol Chem. 1989 Feb 25;264(6):3274–85.

78. Liu K, Kunii N, Sakuma M, Yamaki A, Mizuno S, Sato M, et al. A novel diacylglycerol kinase α -selective inhibitor, CU-3, induces cancer cell apoptosis and enhances immune response. J Lipid Res. 2016 Mar 1;57(3):368–79.

79. Yamaki A, Akiyama R, Murakami C, Takao S, Murakami Y, Mizuno S, et al. Diacylglycerol kinase α-selective inhibitors induce apoptosis and reduce viability of melanoma and several other cancer cell lines. J Cell Biochem. 2019;120(6):10043–56.

80. Ugedo L, Grenhoff J, Svensson TH. Ritanserin, a 5-HT2 receptor antagonist, activates midbrain dopamine neurons by blocking serotonergic inhibition. Psychopharmacol 1989 981. 1989 May;98(1):45–50.

81. Wiesel FA, Nordström AL, Farde L, Eriksson B. An open clinical and biochemical study of ritanserin in acute patients with schizophrenia. Psychopharmacology. 1994 Feb;114(1):31–8.

82. Leysen JE, Gommeren W, Van Gompel P, Wynants J, Janssen PF, Laduron PM. Receptor-binding properties in vitro and in vivo of ritanserin: A very potent and long acting serotonin-S2 antagonist. Mol Pharmacol. 1985;27(6).

83. Hsu K-L. Targeting diacylglycerol kinases for immuno-oncology. Cancer Res. 2018 Jul 1;78(13 Supplement):681–681.

84. Fu L, Li S, Xiao WW, Yu K, Li S, Yuan S, et al. DGKA mediates resistance to PD-1 blockade. Cancer Immunol Res. 2021;9(4):OF1–15.

85. Griner EM, Kazanietz MG. Protein kinase C and other diacylglycerol effectors in cancer. Nat Rev Cancer. 2007;7(4):281–94.

86. Garg R, Benedetti LG, Abera MB, Wang H, Abba M, Kazanietz MG. Protein kinase C and cancer: what we know and what we do not. Oncogene. 2014;33:5225–37.

87. Tanguy E, Wang Q, Moine H, Vitale N. Phosphatidic Acid: From Pleiotropic Functions to Neuronal Pathology. Front Cell Neurosci. 2019 Jan 23;13:2.

88. Wang X, Devaiah SP, Zhang W, Welti R. Signaling functions of phosphatidic acid. Progress in lipid research. 2006 May 1;45(3):250-78.

89. Topham MK. Signaling roles of diacylglycerol kinases. Vol. 97, Journal of Cellular Biochemistry. 2006. p. 474–84.

90. Mueller DL. Linking diacylglycerol kinase to T cell anergy. Nat Immunol. 2006 Nov;7(11):1132–4.

91. Zha Y, Marks R, Ho AW, Peterson AC, Janardhan S, Brown I, et al. T cell anergy is reversed by active Ras and is regulated by diacylglycerol kinase-α. Nat Immunol. 2006 Nov 8;7(11):1166–73.

92. Jung I-Y, Kim Y-Y, Yu H-S, Lee M, Kim S, Lee J. Tumor Biology and Immunology CRISPR/Cas9-Mediated Knockout of DGK Improves Antitumor Activities of Human T Cells. Cancer Research. 2018 Aug 15;78(16):4692-703.

93. Murray PJ, Allen JE, Biswas SK, Fisher EA, Gilroy DW, Goerdt S, et al. Macrophage Activation and Polarization: Nomenclature and Experimental Guidelines. Immunity. 2014 Jul 17;41(1):14–20.

94. He L, Marneros AG. Macrophages are essential for the early wound healing response and the formation of a fibrovascular scar. Am J Pathol. 2013 Jun 1;182(6):2407–17.

95. Wang X, Seed B. A PCR primer bank for quantitative gene expression analysis. Nucleic Acids Res. 2003 Dec 15;31(24):e154–e154.

96. Spandidos A, Wang X, Wang H, Dragnev S, Thurber T, Seed B. A comprehensive collection of experimentally validated primers for Polymerase Chain Reaction quantitation of murine transcript abundance. BMC Genomics. 2008 Dec 24;9(1):1–17.

97. Spandidos A, Wang X, Wang H, Seed B. PrimerBank: A resource of human and mouse PCR primer pairs for gene expression detection and quantification. Nucleic Acids Res. 2009 Nov 10;38(SUPPL.1):D792–9.

98. Olenchock BA, Guo R, Carpenter JH, Jordan M, Topham MK, Koretzky GA, et al. Disruption of diacylglycerol metabolism impairs the induction of T cell anergy. Nat Immunol. 2006;7(11).

99. Bankhead P, Loughrey MB, Fernández JA, Dombrowski Y, McArt DG, Dunne PD, et al. QuPath: Open source software for digital pathology image analysis. Sci Rep. 2017 Dec 1;7(1):1–7.

100. Wilson HM, Lenz LL. SOCS proteins in macrophage polarization and function. Frontiers in Immunology. 2014 Jul 28;5:357.

101. Whyte CS, Bishop ET, Rückerl D, Gaspar-Pereira S, Barker RN, Allen JE, et al. Suppressor of cytokine signaling (SOCS)1 is a key determinant of differential macrophage activation and function. J Leukoc Biol. 2011 Nov;90(5):845–54.

102. Arnold CE, Whyte CS, Gordon P, Barker RN, Rees AJ, Wilson HM. A critical role for suppressor of cytokine signalling 3 in promoting M1 macrophage activation and function in vitro and in vivo. Immunology. 2014 Jan;141(1):96–110.

103. Jenkins SJ, Ruckerl D, Cook PC, Jones LH, Finkelman FD, Van Rooijen N, et al. Local macrophage proliferation, rather than recruitment from the blood, is a signature of T H2 inflammation. Science (80- ). 2011 Jun 10;332(6035):1284–8.

104. Yang N, Isbel NM, Nikolic-Paterson DJ, Li Y, Ye R, Atkins RC, et al. Local macrophage proliferation in human glomerulonephritis. Kidney Int. 1998 Jul 1;54(1):143–51.

105. Brizova H, Kalinova M, Krskova L, Mrhalova M, Kodet R. A novel quantitative PCR of proliferation markers (Ki-67, topoisomerase IIα, and TPX2): an immunohistochemical correlation, testing, and optimizing for mantle cell

lymphoma. Virchows Arch. 2010 Jun;456(6):671–9.

106. Prihantono P, Hatta M, Binekada C, Sampepajung D, Haryasena H, Nelwan B, et al. Ki-67 expression by immunohistochemistry and quantitative real-time polymerase chain reaction as predictor of clinical response to neoadjuvant chemotherapy in locally advanced breast cancer. J Oncol. 2017 Oct 31;2017.

107. Wu NC, Wong W, Kenneth ·, Ho E, Chu VC, Rizo A, et al. Comparison of central laboratory assessments of ER, PR, HER2, and Ki67 by IHC/FISH and the corresponding mRNAs (ESR1, PGR, ERBB2, and MKi67) by RT-qPCR on an automated, broadly deployed diagnostic platform. Breast Cancer Res Treat. 2018;172:327–38.

108. Ralph P, Nakoinz I. Direct Toxic Effects of Immunopotentiators on Monocytic, Myelomonocytic, and Histiocytic or Macrophage Tumor Cells in Culture. Cancer Res. 1977;37(2).

109. Kai F. Regulatory effects of lipopolysaccharide in murine macrophage proliferation. WJG. 1998;4(2):137–9.

110. Wang C, Yu X, Cao Q, Wang Y, Zheng G, Tan TK, et al. Characterization of murine macrophages from bone marrow, spleen and peritoneum. BMC Immunol 2013 141. 2013 Feb 5;14(1):1–10.

111. Braiman-Wiksman L, Solomonik I, Spira R, Tennenbaum T. Novel Insights into Wound Healing Sequence of Events. Toxicol Pathol. 2007 Jun 25;35(6):767–79.

112. Kim BS, Rongisch R, Hager S, Grieb G, Nourbakhsh M, Rennekampff HO, et al. Macrophage Migration Inhibitory Factor in Acute Adipose Tissue Inflammation. PLoS One. 2015 Sep 8;10(9):e0137366.

113. Rossi AG, Haslett C, Hirani N, Greening AP, Rahman I, Metz CN, et al. Human circulating eosinophils secrete macrophage migration inhibitory factor (MIF). Potential role in asthma. J Clin Invest. 1998 Jun 15;101(12):2869–74.

114. Ghigo A, Franco I, Morello F, Hirsch E. Myocyte signalling in leucocyte recruitment to the heart. Cardiovasc Res. 2014 May 1;102(2):270–80.

115. Waddell LA, Lefevre L, Bush SJ, Raper A, Young R, Lisowski ZM, et al. ADGRE1 (EMR1, F4/80) is a rapidly-evolving gene expressed in mammalian monocyte-macrophages. Front Immunol. 2018 Oct 1;9(OCT):2246.

116. West MA, LeMieur T, Clair L, Bellingham J, Rodriguez JL. Protein kinase C regulates macrophage tumor necrosis factor secretion: Direct protein kinase C activation restores tumor necrosis factor production in endotoxin tolerance. Surgery. 1997 Aug 1;122(2):204–12.

117. J C, K U, J S. PKC-zeta is essential for endotoxin-induced macrophage activation. J Surg Res. 2004 Sep;121(1):76–83.

118. Brantley DM, Chen CL, Muraoka RS, Bushdid PB, Bradberry JL, Kittrell F, et al. Nuclear factor-kappaB (NF-kappaB) regulates proliferation and branching in mouse mammary epithelium. Mol Biol Cell. 2001;12(5):1445–55.

119. Park MH, Hong JT. Roles of NF-κB in Cancer and Inflammatory Diseases and Their Therapeutic Approaches. Cells. 2016 Mar 29;5(2):15.

120. Liu T, Zhang L, Joo D, Sun SC. NF-κB signaling in inflammation. Signal Transduct Target Ther 2017 21. 2017 Jul 14;2(1):1–9.

121. Kanazawa H, Ohsawa K, Sasaki Y, Kohsaka S, Imai Y. Macrophage/Microglia-specific Protein Iba1 Enhances Membrane Ruffling and Rac Activation via Phospholipase C-γ-dependent Pathway. J Biol Chem. 2002 May 31;277(22):20026–32.

122. Ohsawa K, Imai Y, Kanazawa H, Sasaki Y, Kohsaka S. Involvement of Iba1 in membrane ruffling and phagocytosis of macrophages/microglia. J Cell Sci. 2000 Sep 1;113(17):3073–84.

123. Ito D, Imai Y, Ohsawa K, Nakajima K, Fukuuchi Y, Kohsaka S. Microglia-specific localisation of a novel calcium binding protein, Iba1. Mol Brain Res. 1998 Jun 1;57(1):1–9.

124. Okano T, Nakagawa T, Kita T, Kada S, Yoshimoto M, Nakahata T, et al. Bone marrow-derived cells expressing Iba1 are constitutively present as resident tissue macrophages in the mouse cochlea. J Neurosci Res. 2008 Jun 1;86(8):1758–67.

125. Sellers RS. Translating Mouse Models: Immune Variation and Efficacy Testing. Toxicol Pathol. 2017 Jan 1;45(1):134–45.

126. Erny D, De Angelis ALH, Jaitin D, Wieghofer P, Staszewski O, David E, et al. Host microbiota constantly control maturation and function of microglia in the CNS. Nat Neurosci. 2015 Jun 25;18(7):965.

127. Hasan Mohajeri M, La Fata G, Steinert RE, Weber P. Relationship between the gut microbiome and brain function. Nutr Rev. 2018 Jul 1;76(7):481–96.

128. Noy R, Pollard JW. Tumor-Associated Macrophages: From Mechanisms to Therapy. Vol. 41, Immunity. Cell Press; 2014. p. 49–61.

129. Mantovani A, Schioppa T, Porta C, Allavena P, Sica A. Role of tumor-associated macrophages in tumor progression and invasion. Vol. 25, Cancer and Metastasis Reviews. Springer; 2006. p. 315–22.

130. Holmdahl R, Malissen B. The need for littermate controls. Eur J Immunol. 2012 Jan 1;42(1):45–7.

131. Mahajan S, Mellins ED, Faccio R. Diacylglycerol Kinase ζ Regulates Macrophage Responses in Juvenile Arthritis and Cytokine Storm Syndrome Mouse Models. J Immunol. 2020 Jan 1;204(1):137–46.

132. Luo B, Regier DS, Prescott SM, Topham MK. Diacylglycerol kinases. Cell Signal. 2004;16(9):983–9.

133. Krishna S, Zhong XP. Regulation of lipid signaling by diacylglycerol kinases during T cell development and function. Front Immunol. 2013;4(JUL):1–14.

134. Lim HK, Choi YA, Park W, Lee T, Ryu SH, Kim SY, et al. Phosphatidic Acid Regulates Systemic Inflammatory Responses by Modulating the Akt-Mammalian Target of Rapamycin-p70 S6 Kinase 1 Pathway. J Biol Chem. 2003;278(46):45117–27.

135. Purow B. Molecular pathways: Targeting diacylglycerol kinase alpha in cancer. Clin Cancer Res. 2015 Nov 15;21(22):5008–12.

136. Sanjuán MA, Jones DR, Izquierdo M, Mérida I. Role of diacylglycerol kinase α in the attenuation of receptor signaling. J Cell Biol. 2001;153(1):207–19.

137. Prinz PU, Mendler AN, Masouris I, Durner L, Oberneder R, Noessner E. High DGK-α and Disabled MAPK Pathways Cause Dysfunction of Human Tumor-Infiltrating CD8 + T Cells That Is Reversible by Pharmacologic Intervention. J Immunol. 2012;188(12):5990–6000.

138. Moon EK, Wang L-C, Dolfi D V., Wilson CB, Ranganathan R, Sun J, et al. Multifactorial T cell hypofunction that is reversible can limit the efficacy of chimeric antibody receptor-transduced human T cells in solid tumors. Clin Cancer Res. 2014;20(16):4262–73.

139. Joshi RP, Schmidt AM, Das J, Pytel D, Riese MJ, Lester M, et al. The zeta isoform of diacylglycerol kinase plays a predominant role in regulatory T cell development and TCR-mediated Ras signaling. Sci Signal. 2014;6(303):1–34.

140. Tsuchiya R, Tanaka T, Hozumi Y, Nakano T, Okada M, Topham MK, et al. Downregulation of diacylglycerol kinase ζ enhances activation of cytokine-induced NF-κB signaling pathway. Biochim Biophys Acta. 2015;1853(2):361–9.

141. Faris M, Kokot N, Lee L, Nel AE. Regulation of interleukin-2 transcription by inducible stable expression of dominant negative and dominant active mitogen-activated protein kinase kinase kinase in jurkat T cells: Evidence for the importance of Ras in a pathway that is controlled by dual . J Biol Chem. 1996;271(44):27366–73.

142. Takeishi K, Taketomi A, Shirabe K, Toshima T, Motomura T, Ikegami T, et al. Diacylglycerol kinase alpha enhances hepatocellular carcinoma progression by activation of Ras-Raf-MEK-ERK pathway. J Hepatol. 2012;57(1):77–83.

143. Bozelli JC, Yune J, Takahashi D, Sakane F, Epand RM. Membrane morphology determines diacylglycerol kinase α substrate acyl chain specificity. FASEB J. 2021;35(6):1–11.

144. Sakane F, Mizuno S, Takahashi D, Sakai H. Where do substrates of diacylglycerol

kinases come from? Diacylglycerol kinases utilize diacylglycerol species supplied from phosphatidylinositol turnover-independent pathways. Adv Biol Regul. 2018;

145. Sakai H, Kado S, Taketomi A, Sakane F. Diacylglycerol kinase δ phosphorylates phosphatidylcholinespecific phospholipase C-dependent, palmitic acidcontaining diacylglycerol species in response to high glucose levels. J Biol Chem. 2014;289(38):26607–17.

146. Mizuno S, Kado S, Goto K, Takahashi D, Sakane F. Diacylglycerol kinase ζ generates dipalmitoyl-phosphatidic acid species during neuroblastoma cell differentiation. Biochem Biophys Reports. 2016;8(September):352–9.

147. Arranz-Nicolás J, Ogando J, Soutar D, Arcos-Pérez R, Meraviglia-Crivelli D, Mañes S, et al. Diacylglycerol kinase α inactivation is an integral component of the costimulatory pathway that amplifies TCR signals. Cancer Immunol Immunother. 2018;67(6):965–80.

148. Velnati S, Massarotti A, Antona A, Talmon M, Fresu LG, Galetto AS, et al. Structure activity relationship studies on Amb639752: toward the identification of a common pharmacophoric structure for DGKα inhibitors. J Enzyme Inhib Med Chem. 2020;35(1):96–108.

149. Franks CE, Campbell ST, Purow BW, Harris TE, Hsu KL. The Ligand Binding Landscape of Diacylglycerol Kinases. Cell Chem Biol. 2017;24(7):870-880.e5.

150. McCloud RL, Franks CE, Campbell ST, Purow BW, Harris TE, Hsu K-L. Deconstructing lipid kinase inhibitors by chemical proteomics. Biochemistry. 2018;57(2):231–6.

151. Goto K, Watanabe M, Kondo H, Yuasa H, Sakane F, Kanoh H. Gene cloning, sequence, expression and in situ localization of 80 kDa diacylglycerol kinase specific to oligodendrocyte of rat brain. Mol Brain Res. 1992;16(1–2):75–87.

152. Goto K, Kondo H. Molecular cloning and expression of a 90-kDa diacylglycerol kinase that predominantly localizes in neurons. Proc Natl Acad Sci U S A. 1993;90(16):7598–602.

153. Granade ME, Harris TE. Purification of Lipin and Measurement of Phosphatidic Acid Phosphatase Activity from Liposomes. 1st ed. Vol. 607, Methods in Enzymology. Elsevier Inc.; 2018. 373–388 p.

154. Campbell ST, Franks CE, Borne AL, Shin M, Zhang L, Hsu KL. Chemoproteomic discovery of a ritanserin-targeted kinase network mediating apoptotic cell death of lung tumor cells. Mol Pharmacol. 2018;94(5):1246–55.

155. Joshi RP, Koretzky GA. Diacylglycerol kinases: Regulated controllers of T cell activation, function, and development. Int J Mol Sci. 2013;14(4):6649–73.

156. Cibrián D, Sánchez-Madrid F. CD69: from activation marker to metabolic gatekeeper. Eur J Immunol. 2017 Jun 1;47(6):946.

157. Cerami E, Demir E, Schultz N, Taylor BS, Sander C. Automated network analysis identifies core pathways in glioblastoma. PLoS One. 2010;5(2).

158. Koshy M, Villano JL, Dolecek TA, Howard A, Mahmood U, Chmura SJ, et al. Improved survival time trends for glioblastoma using the SEER 17 population-based registries. J Neurooncol. 2012;107(1):207–12.

159. Eckford PDW, Sharom FJ. ABC Efflux Pump-Based Resistance to Chemotherapy Drugs. Chem Rev. 2009 Jul 8;109(7):2989–3011.

160. Ughachukwu P, Unekwe P. Efflux pump-mediated resistance in chemotherapy. Ann Med Health Sci Res. 2012;2(2):191.

161. Espinoza-Jiménez A, Peón AN, Terrazas LI. Alternatively activated macrophages in types 1 and 2 diabetes. Mediators Inflamm. 2012;2012.

162. Tesch GH. Role of macrophages in complications of type 2 diabetes. Clin Exp Pharmacol Physiol. 2007 Oct 1;34(10):1016–9.

163. Kanter JE, Hsu CC, Bornfeldt KE. Monocytes and Macrophages as Protagonists in Vascular Complications of Diabetes. Front Cardiovasc Med. 2020 Feb 14;7:10.

164. Riss J, Khanna C, Koo S, Chandramouli GVR, Yang HH, Hu Y, et al. Cancers as Wounds that Do Not Heal: Differences and Similarities between Renal Regeneration/Repair and Renal Cell Carcinoma. Cancer Res. 2006 Jul 15;66(14):7216–24.

165. Dvorak HF. Tumors: Wounds that do not heal--Redux. Cancer Immunol Res. 2015 Jan 1;3(1):1.

166. Deyell M, Garris CS, Laughney AM. Cancer metastasis as a non-healing wound. Br J Cancer 2021 1249. 2021 Mar 17;124(9):1491–502.

167. Laviron M, Boissonnas A. Ontogeny of Tumor-Associated Macrophages. Front Immunol. 2019;10:1799.

168. Lin Y, Xu J, Lan H. Tumor-associated macrophages in tumor metastasis: biological roles and clinical therapeutic applications. J Hematol Oncol 2019 121. 2019 Jul 12;12(1):1–16.

169. Chen Y, Song Y, Du W, Gong L, Chang H, Zou Z. Tumor-associated macrophages: an accomplice in solid tumor progression. J Biomed Sci 2019 261. 2019 Oct 20;26(1):1–13.

170. Sharma P, Hu-Lieskovan S, Wargo JA, Ribas A. Primary, Adaptive and Acquired Resistance to Cancer Immunotherapy. Cell. 2017 Feb 9;168(4):707.

171. Bai R, Chen N, Li L, Du N, Bai L, Lv Z, et al. Mechanisms of Cancer Resistance to Immunotherapy. Front Oncol. 2020 Aug 6;10:1290.

172. Bu X, Mahoney KM, Freeman GJ. Learning from PD-1 Resistance: New

Combination Strategies. Trends Mol Med. 2016 Jun 1;22(6):448–51.

173. Gu J, Wang C, Cao C, Huang J, Holzhauer S, Desilva H, et al. DGKζ exerts greater control than DGKα over CD8+ T cell activity and tumor inhibition. Oncoimmunology. 2021;10(1).

174. Aminin D, Wang YM. Macrophages as a "weapon" in anticancer cellular immunotherapy. Kaohsiung J Med Sci. 2021 Sep 1;37(9):749–58.

175. Kim D, Wang J, Willingham SB, Martin R, Wernig G, Weissman IL. Anti-CD47 antibodies promote phagocytosis and inhibit the growth of human myeloma cells. Leuk 2012 2612. 2012 May 30;26(12):2538–45.

176. Willingham SB, Volkmer JP, Gentles AJ, Sahoo D, Dalerba P, Mitra SS, et al. The CD47-signal regulatory protein alpha (SIRPa) interaction is a therapeutic target for human solid tumors. Proc Natl Acad Sci U S A. 2012 Apr 24;109(17):6662–7.

177. Oldenborg PA, Zheleznyak A, Fang YF, Lagenaur CF, Gresham HD, Lindberg FP. Role of CD47 as a marker of self on red blood cells. Science (80- ). 2000 Jun 16;288(5473):2051–4.

178. Weiskopf K. Cancer immunotherapy targeting the CD47/SIRPα axis. Eur J Cancer. 2017 May 1;76:100–9.

179. Zhang M, Hutter G, Kahn SA, Azad TD, Gholamin S, Xu CY, et al. Anti-CD47 Treatment Stimulates Phagocytosis of Glioblastoma by M1 and M2 Polarized Macrophages and Promotes M1 Polarized Macrophages In Vivo. PLoS One. 2016 Apr 1;11(4):e0153550.

180. Montserrat- de la Paz S, Naranjo MC, Lopez S, Abia R, Muriana FJG, Bermudez B. Niacin and its metabolites as master regulators of macrophage activation. J Nutr Biochem. 2017 Jan 1;39:40–7.

181. Yang X, Mei S, Niu H, Li J. Nicotinic acid impairs assembly of leading edge in glioma cells. Oncol Rep. 2017 Aug 1;38(2):829–36.

182. Li J, Qu J, Shi Y, Perfetto M, Ping Z, Christian L, et al. Nicotinic acid inhibits glioma invasion by facilitating Snail1 degradation. Sci Reports 2017 71. 2017 Mar 3;7(1):1–12.

183. Sarkar S, Yang R, Mirzaei R, Rawji K, Poon C, Mishra MK, et al. Control of brain tumor growth by reactivating myeloid cells with niacin. Sci Transl Med. 2020 Apr 1;12(537).

184. Offermanns S. The nicotinic acid receptor GPR109A (HM74A or PUMA-G) as a new therapeutic target. Trends Pharmacol Sci. 2006 Jul 1;27(7):384–90.

185. Sarkar S, Döring A, Zemp FJ, Silva C, Lun X, Wang X, et al. Therapeutic activation of macrophages and microglia to suppress brain tumor-initiating cells. Nat Neurosci 2013 171. 2013 Dec 8;17(1):46–55.

186. Achkova D, Maher J. Role of the colony-stimulating factor (CSF)/CSF-1 receptor axis in cancer. Biochem Soc Trans. 2016 Apr 15;44(2):333–41.

187. Ries CH, Hoves S, Cannarile MA, Rüttinger D. CSF-1/CSF-1R targeting agents in clinical development for cancer therapy. Curr Opin Pharmacol. 2015 Aug 1;23:45–51.

188. Xu J, Escamilla J, Mok S, David J, Priceman S, West B, et al. CSF1R Signaling Blockade Stanches Tumor-Infiltrating Myeloid Cells and Improves the Efficacy of Radiotherapy in Prostate Cancer. Cancer Res. 2013 May 1;73(9):2782–94.

189. Swierczak A, Cook AD, Lenzo JC, Restall CM, Doherty JP, Anderson RL, et al. The Promotion of Breast Cancer Metastasis Caused by Inhibition of CSF-1R/CSF-1 Signaling Is Blocked by Targeting the G-CSF Receptor. Cancer Immunol Res. 2014 Aug 1;2(8):765–76.

190. Patel S, Player MR. Colony-Stimulating Factor-1 Receptor Inhibitors for the Treatment of Cancer and Inflammatory Disease. Curr Top Med Chem. 2009 Aug 13;9(7):599–610.

191. Pyonteck SM, Akkari L, Schuhmacher AJ, Bowman RL, Sevenich L, Quail DF, et al. CSF-1R inhibition alters macrophage polarization and blocks glioma progression. Nat Med. 2013 Oct;19(10):1264–72.

192. Khan OM, Ibrahim MX, Jonsson IM, Karlsson C, Liu M, Sjogren AKM, et al. Geranylgeranyltransferase type I (GGTase-I) deficiency hyperactivates macrophages and induces erosive arthritis in mice. J Clin Invest. 2011 Feb 1;121(2):628–39.

193. Khan OM, Akula MK, Skålen K, Karlsson C, Ståhlman M, Young SG, et al. Targeting GGTase-I activates RHOA, increases macrophage reverse cholesterol transport, and reduces atherosclerosis in mice. Circulation. 2013 Feb 19;127(7):782–90.